4th Annual Jackson School Research Symposium

February 7th, 2015

Sponsored by ConocoPhillips

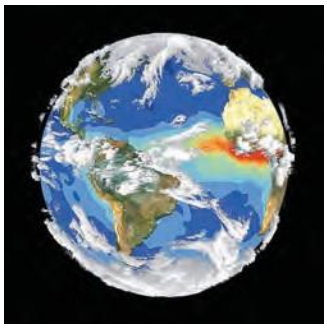

Climate, Carbon & Geobiology

Energy Geosciences

Marine Geosciences

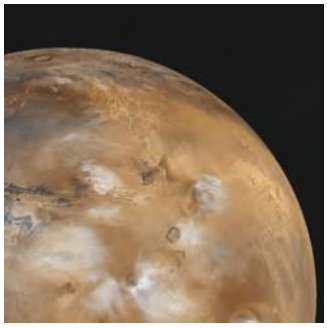

Planetary Geosciences

Solid Earth & Tectonic Processes

Surface & Hydrologic Processes

ConocoPhillips

GSEC
Graduate Student Executive Committee
Jackson School of Geosciences

THE UNIVERSITY OF TEXAS AT AUSTIN
JACKSON
SCHOOL OF GEOSCIENCES

Welcome to the 4th Annual Jackson School Research Symposium

It is with great pleasure we welcome you all to the 4th Annual Jackson School Research Symposium at UT-Austin! This symposium would not have been possible without the hard work of student volunteers, the support of faculty/research scientists, and generous support from ConocoPhillips. Thank you for taking part in supporting our students and growing research program within the Jackson School. Enjoy the posters!

Schedule of Presentations and Events

Breakfast, A.M. session poster set-up.....8:30 a.m.

Early Career Graduate (ECG) posters.....9:00-11:30 a.m.

Late Career Masters (LCM) posters.....9:00-11:30 a.m.

Lunch, A.M. session poster take-down.....11:30 a.m.

P.M. session poster set-up.....12:30 p.m.

Undergraduate (U) posters….....1:00-3:30 p.m.

Late Career PhD (LCPhD) posters.....1:00-3:30 p.m.

Happy hour/judging.....3:30 p.m.

Awards/closing.....4:00 p.m

Table of Contents

The abstracts are organized alphabetically by first author's last name in the booklet. The following is a list of abstracts organized alphabetically and by their judging categories.

EARLY-CAREER GRADUATE STUDENTS

LATE-CAREER MASTER STUDENTS

LATE-CAREER PHD STUDENTS

UNDERGRADUATE STUDENTS

A.M. POSTER LAYOUT

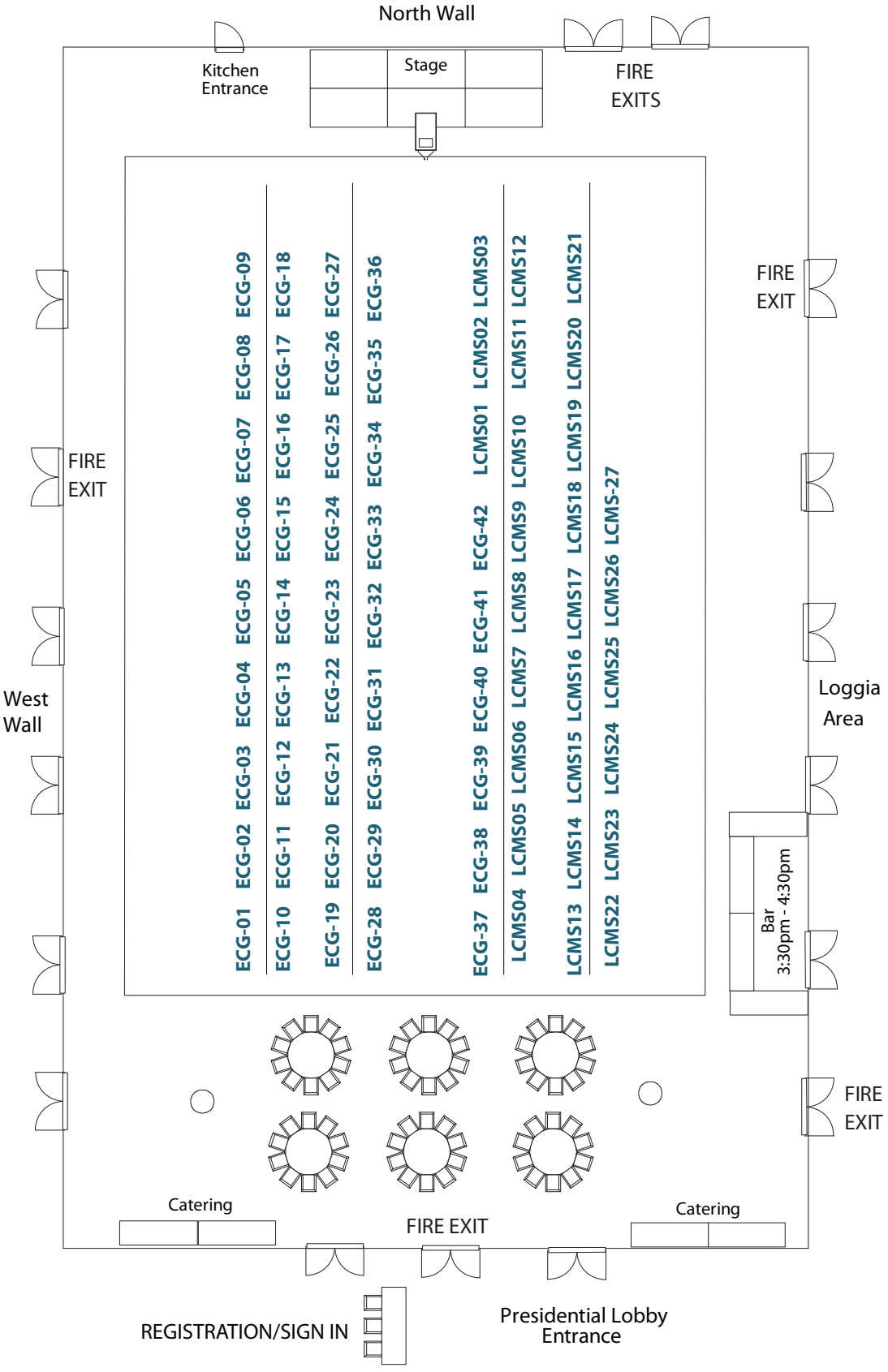

P.M. POSTER LAYOUT

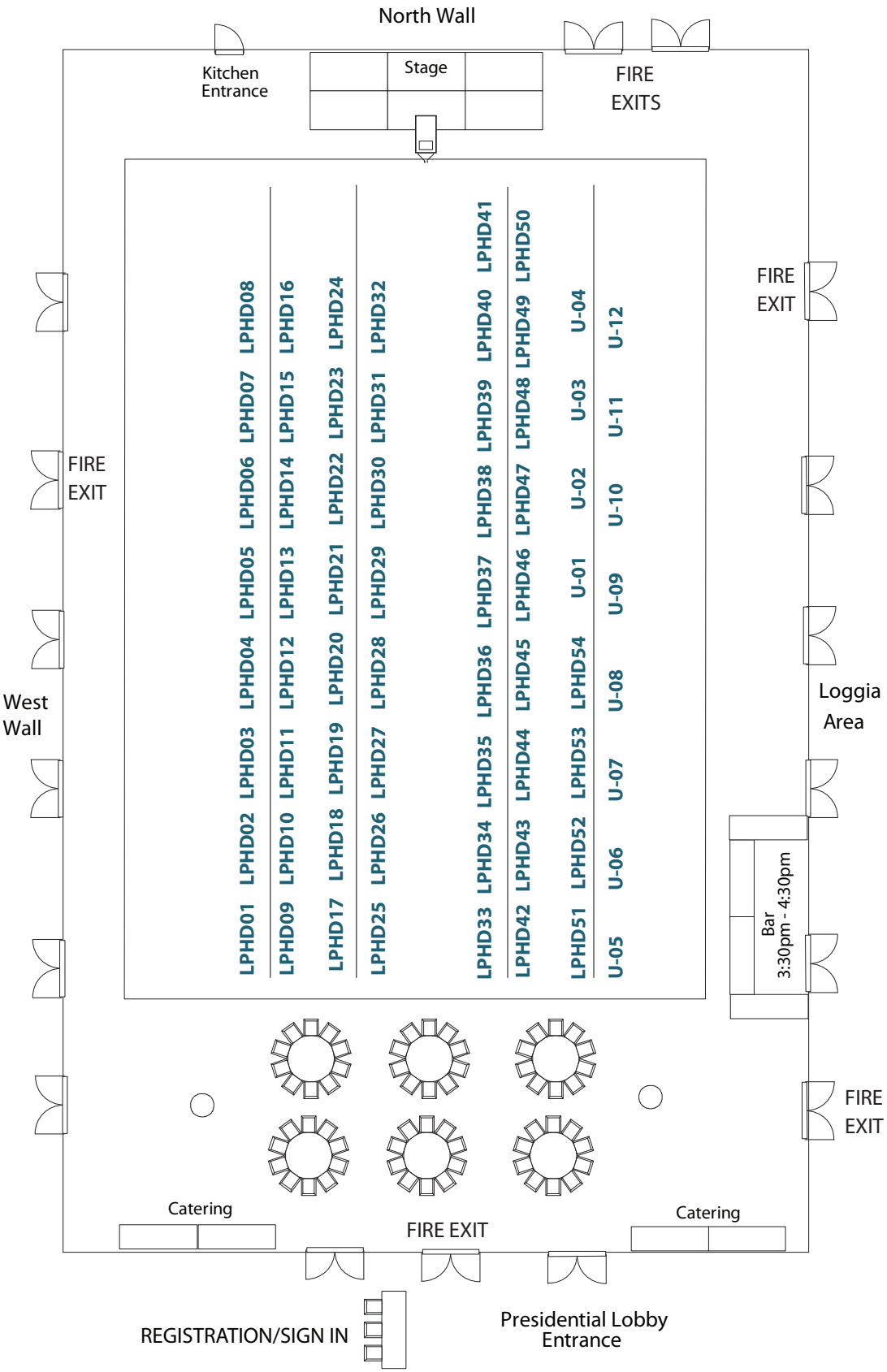

SHP
LCMS

A simple numerical model of ice-wedge polygon geomorphic evolution

chuck.abolt@gmail.com
Abolt, C., Department of Geological Sciences, The University of Texas at Austin, Austin, TX
Young, M., Bureau of Economic Geology, The University of Texas at Austin, Austin, TX

Ice-wedge polygons cover a large area of the global permafrost zone and are often found in carbon-rich peat soils. It has been hypothesized that low-centered polygons evolve into high-centered polygons through erosive processes driven by increased soil temperatures. Here we present a numerical model based on an established geomorphic paradigm, linear hillslope diffusion, to simulate the process of polygon thermo-erosion. The model is calibrated using high-resolution LiDAR data from the Alaska North Slope. In addition to demonstrating feasibility of the conceptual model of polygon transition from low-centered to high-centered form, the model tracks soil material fluxes from eroding polygons into water-filled trough spaces. Results suggest that a consistent ratio of soil volume to polygon area is shed into troughs during transition, approximately 0.15 m^3/m^2. Decreases in depressional storage capacity as polygons erode, also evaluated by the model, may have implications for catchment-scale hydrology in the Arctic.

Keywords: permafrost, soil, patterned ground, hillslope diffusion, LiDAR

SHP
LCPHD

Causes of abnormally low-pressure in natural CO2 reservoirs and implications for the safety of Geological CO2 Storage

daria.akhbari@gmail.com
Akhbari, D., Jackson School of Geosciences, University of Texas at Austin
Hesse, M., Jackson School of Geosciences, Institute for Computational Engineering and Sciences, University of Texas at Austin

The Bravo Dome field in northeast New Mexico is one of the largest gas accumulations worldwide and the largest natural CO2 accumulation in North America. The field is only 580-900 m deep and located in the Permian Tubb sandstone that unconformably overlies the granitic basement. Sathaye et al. (2014) estimated that 1.3 Gt of CO2 is stored at the reservoir. A major increase in the pore pressure relative to the hydrostatic pressure is expected due to the large amount of CO2 injected into the reservoir. However, the pre-production gas pressures indicate that most parts of the reservoir are approximately 5 MPa below hydrostatic pressure. Three processes could explain the under pressure in the Bravo Dome reservoir; 1) erosional unloading, 2) CO2 dissolution into the ambient brine, 3) cooling of CO2after injection.
Analytical solutions suggest that an erosion rate of 180 m/Ma is required to reduce the pore pressures to the values observed at Bravo Dome. Given that the current erosion rate is only 5 m/Ma (Nereson et al. 2013); the sub-hydrostatic pressures at Bravo Dome are likely due to CO2dissolution and cooling.
To investigate the impact of CO2 dissolution on the pore pressure we have developed new analytical solutions and conducted laboratory experiments. We assume that gaseous CO2 was confined to sandstones during emplacement due to the high entry pressure of the siltstones. After emplacement the CO2 dissolves in to the brine contained in the siltstones and the pressure in the sandstones declines. Assuming the sandstone-siltstone system is closed, the pressure decline due to CO2 dissolution is controlled by a single dimensionless number, $\eta = KHRTVw /Vg$. Herein, KH is Henry's constant, R is ideal gas constant, T is temperature, Vw is water volume, and Vg is CO2 volume. The pressure drop is controlled by the ratio of water volume to CO2 volume and η varies between 0.1 to 8 at Bravo Dome. This corresponds to pressure drops between 0.8-7.5 MPa and can therefore account for the observed 5 MPa drop in pore pressures at Bravo Dome. This is consistent with geochemical observation suggesting significant dissolution of CO2 at Bravo Dome (Gilfillan 2009). The observation of sub-hydrostatic pressures in CO2 reservoirs is important because they illustrate that CO2 dissolution may mitigate problems due to injection induced overpressure in the long-term.

Keywords: abnormal pressure, carbon capture and storage, Bravo Dome,

SETP
LCMS

IMPACT OF METEORIC FLUID FLOW ON THE THERMAL EVOLUTION OF THE GOTTHARD MASSIF

danielarnost@utexas.edu
Arnost, D., The University of Texas at Austin, Austin, TX
Stockli, D., The University of Texas at Austin, Austin, TX
Antognini, M., Museo Cantonale di storia naturale, Lugano, Switzerland

The 57 km Gotthard Base Tunnel provides an orogen-perpendicular cross section through the central Swiss Alps and a window into the subsurface thermal structure of the Gotthard Massif. The modeled temperature profile in the tunnel mimics topography; increasing from 11°C at the north entrance to 42°C in the middle where overburden exceeds 2300 meters. A 15°C negative temperature anomaly exists 35 km south of the Erstfeld portal at the intersection of the Piora zone syncline; a structure comprised of heavily deformed and kartsified Triassic dolomite that overlies the gneissic basement of the Gotthard Massif. This aquifer is a conduit that funnels cold Alpine meteoric water deep into the massif where it absorbs heat from the adjacent bedrock, creating an advective thermal regime and a local negative temperature anomaly.
The interplay of uplift and erosion, conductive heat loss, radiogenic heat production, along with the coupled effect of topography and meteoric fluids can influence near-surface geothermal gradients and therefore, apatite (U-Th)/He cooling histories. 1D thermal calculations and 2D thermal modeling in COMSOL show that the topology of the apatite (U-Th)/He partial retention zone is sufficiently deflected by surficial processes to be resolved within the precision of the apatite (U-Th)/He (AHe) technique.
Multiple thermochronometers (Apatite and zircon (U-Th)/He, apatite fission track) from Gotthard Base Tunnel samples and overlying surface transects allow for a comprehensive, high resolution, post-Alpine exhumation and cooling history over the last 12 million years. Rock temperatures in the tunnel are within the lower bounds of the AHe partial retention zone, allowing access to a recent, detailed thermal history that can potentially resolve transient thermal anomalies. The low closure temperature of the AHe system (T_c = 60-70 °C) is uniquely suited to track the fluid induced thermal anomaly and its effect on the background conductive cooling of the Gotthard Massif throughout its thermal evolution. Apatite (U-Th)/He ages from tunnel samples increase from ~2.5 Ma to ~5.0 Ma approaching the Piora zone. The anomalously old ages in the Piora zone are consistent with depressed AHe partial retention zone isotherms caused by cold meteoric fluids. The majority of both tunnel and surface zircon (U-Th)/He ages range from 8 Ma to 12 Ma and are unaffected by Piora zone cooling, showing that the geothermal gradient is unaltered at the depth of the ZHe partial retention zone. Time-temperature paths of vertical sample arrays generated by inverse modeling in HeMP yield rapid cooling from 10 Ma to 7 Ma followed by slow conductive cooling from 7 Ma to present. This method attempts to examine the interface between endogenic and exogenic tectono-thermal forcing; and the potential influence of climate variations on tectonics. The combination of apatite (U-Th)/He thermochronometer ages and thermal modeling can be used for detailed investigations of the causes and magnitudes of near surface isotherm perturbations and their significance regarding the interpretation of complex thermal histories.

Keywords: Apatite, Zircon, (U-Th)/He

SHP
LCPHD

Statistical Analysis of Small-Scale Bedforms Formed by Hurricane Sandy Offshore Fire Island, New York

khushbooarora@utexas.edu
Goff, J., Institute for Geophysics, Jackson School of Geosciences, University of Texas at Austin, Austin, TX
Wood, L., Bureau of Economic Geology, Jackson School of Geosciences, University of Texas at Austin, Austin, TX

Multibeam bathymetry surveys acquired two months after hurricane Sandy offshore of Fire Island, NY, revealed broad areas of small-scale (<15 m) bedforms on top of large-scale (200–3000 m) sand ridges and sorted bedforms. The small-scale bedforms were absent prior to the hurricane, as evidenced by previous surveys in 2003 and 2011. Here we statistically analyze these bedforms in conjunction with seabed sedimentary properties and storm history to understand the correlation of sedimentary deposition with the storm history. The Fire Island shoreface/inner shelf has been the site of ongoing studies by the USGS. The western half is dominated by 1–3 km-wide sand ridges, with abundant finemedium sand. The eastern half, on the other hand, is largely starved of modern sand, and the bedform morphology is dominated by 0.2–1.0 km-wide sorted bedforms. We utilize two post-storm surveys, one along the western half of the island and the other to the east, providing an opportunity to compare these different nearshore settings. A Gaussian covariance model is used, with four parameters: rms height, orientation and characteristics length and width. An iterative, least-squares inversion is used to estimate these parameters and their uncertainties from selected sample areas. Bedforms with aspect ratio (length/width) > 1.5 are categorized as two-dimensional, and have rms heights ~3–7 cm and widths 4–6 m. Bedforms with aspect ratio < 1.5 are categorized as three-dimensional, and have smaller rms heights (~1.5–4 cm) and larger widths (~6–13 m). Parameters are correlatable with grain size and large-scale bedform topography. Three-dimensional bedforms tend to form in finer sands and have been interpreted as hummocky bedforms formed by long-period surface gravity waves generated during the storm. The two-dimensional bedforms are interpreted as large ripples that show consistent lineation oblique to the orientation of larger sand ridges. For this study we will compare bedform lineations to storm history in order to infer stage at which these bedforms originated with respect to the passage of the storm. These results should help to improve our understanding of storm processes and their impact on sediment transport and deposition, as well as deduce the magnitude and frequency of ancient storm processes based upon the preserved rock record.

Keywords: Superstorm Sandy, hummocky bedforms, storm processes, sediment transport and deposition

SETP
LCPHD

Understanding late-stage exhumation of inner Cottian Alps (Western Alps, Italy) using an integrated multidisciplinary method

marco.bacenetti@gmail.com
Bacenetti, M., Department of Earth Sciences, University of Torino, Italy
Stockli, D., Jackson School of Geosciences, The University of Texas at Austin, Austin, TX
Cadoppi, P., Department of Earth Sciences, University of Torino, Italy

Late-stage exhumation of the Western Alps is understood as the interlude of tectonics and erosion. While the former has been influenced by a decrease in plate convergence, the latter has been suggested to be affected by climatic variation.
This study focuses on the Inner sector of the Cottian Alps (Western Alps, Italy). This area is affected by a diffuse seismicity with low magnitude (> 3) although in the past there have been some events of greater magnitude, such as the one in 1980 (ML = 4, 8) with its epicenter in Cumiana, and that of 1808 (MS = 5.5), with its epicenter in Prarostino. From tectonic point of view the Western Alps is characterized by a widespread extensional regime located in the core of the belt and a dominant transcurrent tectonic regime at the outer borders of the chain, with some local compressive areas.
The present work aims to understanding the late-stage of exhumation in the Germanasca Valley (Western Alps, Italy), a sector of Cottian Alps poorly known through an integrated, multidisciplinary approach combining Structural analysis, Quaternary Geology, Geomorphology, PSInSAR™ data and Thermochronology.
Geomorphology and morphotectonic analyses have been performed using field mapping activities, digital orthophotos (AGEA Orthophoto 2009), aerial stereo couples and DEMs (LiDAR5x5 meters, Regione Piemonte 2009). All collected data have been included in a GIS project, and then elaborated in a morphotectonic map. Preliminary interpretation shows strong geomorphological anomalies affecting hydrographic network, slope morphology and distribution of Quaternary deposits.
A lineament geometry analysis has been conducted by using TerraExplorer® Software. Statistical analysis of lineament trend individualized three sets of tectonic features: Ln1 (N0° - N30°E), Ln2 (N50° - N70°E), Ln3 (N80° - N100°E)
Application of Permanent Scatterers Synthetic Aperture Radar Interferometry (PSInSAR™) provided high-resolution assessment of surface deformations over a wide region of weak uplift. We resolved vertical and horizontal motion in the area.
The Hot Spot maps were compared with geological, geomorphological, and lineament geometry data in order to analyze the current tectonics and the crustal mobility of the studied sector. The preliminary results suggests that the Cottian Alps are in general uplift. The current crustal mobility could be governed by the three system of discontinuities (see lineaments analysis). Field mapping data and results of morphotectonic analysis confirmed this trend. Moreover the local high density of landslides, compared to adjacent sectors, could be directly connected to the enhanced uplift of this sector.
The cooling history has been investigated by using apatite and zircon (U-Th-Sm)/He thermochronometers along a pseudo-vertical bedrock profile (elevation between 650 and 2850 m) resulting in a total elevation difference of nearly 2,2 km.. In situ and detrital thermochronological apatite fission track data indicate slow rates (<0.2 km m. y.-1) of erosional exhumation across this region during Oligocene-Miocene times (~29–10 Ma). The available thermo-chronological data in this area suggest that the post-metamorphic evolution, characterized by two main stages, began since the late(?) Oligocene, but this hypothesis is not supported by adequate geological data.

Keywords: Tectonic Geomorphology, (U-Th-Sm)/He data, PSInSAR™, Italian Western Alps

SETP
ECG

Detrital zircon U-Pb and trace-element depth-profiling analysis and (U-Th)/He double-dating of Lower Cretaceous-Cenozoic strata in Duhok, Iraqi Kurdistan

douglasbarber@utexas.edu
Barber, D., Department of Geological Sciences, Jackson School of Geosciences, The University of Texas at Austin, Austin, TX
Stockli, D., Department of Geological Sciences, Jackson School of Geosciences, The University of Texas at Austin, Austin, TX
Koshnaw, R., Department of Geological Sciences, Jackson School of Geosciences, The University of Texas at Austin, Austin, TX
Horton, B., Department of Geological Sciences, Jackson School of Geosciences, The University of Texas at Austin, Austin, TX
Tamar-Agha, M., Department of Earth Sciences, College of Science, University of Baghdad, Baghdad, Iraq

Detrital zircon (DZ) U-Pb geochronology has been recognized as a powerful tool for reconstructing sedimentary provenance, tracing orogenic unroofing, and inferring areas of paleorelief in a diverse array of tectonic environments. However, the utility of DZ U-Pb dating alone is often complicated in complex orogenic settings due to the prevalence of sediment recycling and homogenized U-Pb age signatures among multiple source areas. With recent technological breakthroughs in laser-ablation split-stream (LASS)-ICP-MS depth-profiling, we are now able to access powerful new dimensions of provenance data by simultaneously collecting comprehensive age information and geochemical signatures across multiple growth domains (rim/core) of single zircon grains. Integration of these criteria with (U-Th)/He double-dating of single grains provides us with a broader spectrum of criteria to ultimately allow for more robust discrimination of source terranes and detection of sediment recycling. This method also provides a potential means of source-terrane characterization with respect to cooling history, petrologic growth environment, and geodynamic setting.

The NW Zagros orogen is the result of the multistage collisional history associated with Late Cretaceous-Cenozoic convergence of the Arabian and Eurasian continents and final closure of Neotethys. Siliciclastic strata preserved within the NW Zagros fold-thrust belt of Duhok, Iraqi Kurdistan (DIK), provide a widespread record of passive-margin to foreland basin sedimentation along the northern margin of ancestral Arabia. As a means of assessing basin evolution and provenance, we present results from combined DZ U-Pb and trace-element depth-profiling analysis and (U-Th)/He dating of these deposits. The basin fill in DIK was dominantly derived from Pan-African/Arabian-Nubian, Peri-Gondwandan, Eurasian, and Cretaceous to Cenozoic volcanic arc terrenes. However, the sediment source regions of these strata varies systematically through time with an overall increase in complexity upsection. Combined DZ data record distinct shifts in provenance signals associated with multiple phases of collision during convergence of Arabia and Eurasia. Results suggest (1) Lower Cretaceous passive margin basin deposits were shed from uplifted Pan-African sources to the west, (2) Paleogene foreland basin strata were derived from accreted Abian-Cenomanian island arc complexes during the proto-Zagros orogeny; (3) early-mid Miocene strata record the first influx of sediment from the Bitlis Zone in SE Turkey during the initial stage of final Arabia-Eurasia collision; (4) mid-late Miocene fluvial sandstones record the initial arrival of Eurasian (Pontide) sediments in Arabia associated with terminal Arabia-Eurasia collision, and (5) Late Miocene-Pliocene sandstones and conglomerates indicate the onset of sediment recycling from proto-Zagros basin associated with propagation of the Zagros thrusting. Lastly, we use detrital apatite and zircon (U-Th)/He dating to better constrain depositional ages. Overall, combined U-Pb and trace-element LASS-ICP-MS depth-profiling with (U-Th)/He double-dating of a single detrital zircon grain can be used to pinpoint the provenance of a single zircon with much higher resolution than conventional methods, thus allowing us to more effectively delineate the tectonic and paleodispersal evolution of geologically complex terranes.

Keywords: detrital zircon, Zagros, provenance, geochronology, thermochronology, geochemistry, tectonics, sedimentology

SHP
LCMS

Pre-Existent Topography Influence on Turbidity Deposits in an Active Basin; Lycium Member of the Latrania Formation in Fish Creek-Vallecito Basin, Southern California

sarahbateman@utexas.edu
Bateman, S., Department of Geosciences, The University of Texas at Austin
Steel, R., Department of Geosciences, The University of Texas at Austin
Olariu, C., Department of Geosciences, The University of Texas at Austin

This study documents the influence of the pre-existent topography on the deposition of turbidite deposits in the Fish Creek-Vallecito Basin, a tectonically subsiding basin. The Fish Creek-Vallecito Basin of southern California contains a continuous record of sedimentation into the Mio-Pliocene Gulf of California. Initial sedimentation into the basin began at 8.0 Ma and primarily consisted of locally derived alluvial conglomerates. Subsequent deepening of the basin created conditions for deposition of subaqueous gravity flow deposits. Sedimentation into the basin can be divided into two main phases: 1) Pre-Colorado River deposition in alluvial fan facies and later turbidite deposition after marine incursion and 2) capture and progradation by the Colorado River system.

The deposition of the initial marine sediments by subaqueous sediment gravity flows known lithostratigraphically as the ~6.2 to 5.2 Ma Lycium Member of the Latrania Formation is about 90 m thick. The Lycium Mbr. is thought to have been derived from a coeval alluvial system sourced from nearby local basement. This study used 12 sedimentological logs taken laterally throughout the 5 km outcrop belt and integrated thin-section petrography on samples taken from logged outcrops.

Correlation of high-resolution sections and photopanel interpretation allow for lithofacies associations to be interpreted as well as architectural elements to be diagrammed. Thick, sandy intervals (10s meters) consisting of lenticular, amalgamating, fining upward sandstones are interpreted to be channels while more laterally extensive sheet like sandstones are interpreted to be lobes. This channel to lobe transition occurs from NW to SE in a similar orientation to paleoflow which likely supplied sediment from the NW.

Keywords: turbidite,

SHP
U

The Progradation of a Delta on a Mobile Substrate: Experiment

carolina.baumanis@gmail.com
Baumanis, C., The University of Texas at Austin, Austin, TX
Kim, W., The University of Texas at Austin, Austin, TX

Understanding the two way interaction between sedimentation and substrate deformation is imperative for unraveling stratigraphic signatures. Previous experimental studies have explored the progression of deltas with external controls of changes in sea level, tectonic movement, and/or sediment supply rates. These external controls are independently controlled and do not change in response to delta progradation. What still remains to be explored and what we emphasize here are the differences between subsurface architecture developed on a rigid basement and a mobile basement, which deforms as a delta advances. Understanding these differences is key for improving stratigraphic interpretation. We conducted a series of experiments at the University of Texas at Austin to discover the effect of a mobile substrate on an evolving delta. All of the runs had constant sediment supply, water supply, and base level, but the mobile substrate thickness varied from 0 cm to 3 cm. The substrate used was a low viscosity polymer that has the ability to deform in a matter of just a couple of hours. The experiments including the polymer produced dynamic changes in the surface topography of the mobile substrate. In fact, the polymer lying underneath the delta deformed into an undulatory surface that resembled a sinusoidal curve. These undulations also increased in amplitude, but decreased in frequency with increased distance from the upstream sediment source. Furthermore, with the addition of polymer the overall progradational rate of the delta decreased with the addition of polymer due to further subsidence into the mobile basement.

Keywords: stratigraphy, progradation, mobile substrate, experiment, delta

SHP
LCPHD

Calculating the amount of renewable groundwater using age distributions

kevinbefus@utexas.edu
Gleeson, T., University of Victoria
Jasechko, S., University of Calgary
Luijendijk, E., Gottingen University

Time-scales of groundwater dynamics can control how groundwater interacts with many Earth system processes, including weathering, the transport of solutes or contaminants, and hydrologic responses to climate change. In this study, we quantified the global volume and distribution of groundwater that has been recharged over the past 50 years, a time-scale relevant to current policy planning and intimately tied to human generations. We modelled groundwater residence time distributions with several thousand two-dimensional flow and age-as-mass transport simulations guided by global datasets of basin geometric and hydraulic properties. The models suggest that less than 15% of the groundwater on Earth to 2 km depth was recharged in the past 50 years. For most watersheds on Earth, this young groundwater is restricted to the upper 100 m of the Earth's crust. Uncertainty in our estimate stems from the simplification of two-dimensional flow and uncertainty in permeability and porosity.

Keywords: groundwater, sustainability, renewability

SETP
U

GPS Measurements of Interseismic, Coseismic, and Postseismic Deformation in Puysegur Subduction Zone, New Zealand

nick.j.benz@gmail.com
Benz, N., Institute for Geophysics, The University of Texas at Austin
Wallace, L., Institute for Geophysics, The University of Texas at Austin
Hreinsdottir, S., GNS Science- Institute for Geological and Nuclear Sciences Ltd., New Zealand
Denys, P., University of Otago, New Zealand
Pearson, C., University of Otago, New Zealand

A combination of continuous and campaign style geodetic measurements from sites on the South Island of New Zealand help us constrain long-term and short-term deformation adjacent to the Puysegur subduction zone, offshore Fiordland, New Zealand. We update an elastic block model for the region that consists of an array of microplates bounded by active faults. We invert GPS velocities, and long-term fault slip rates and earthquake slip vectors for tectonic block rotations, fault coupling coefficients, and permanent block strain. Three large subduction interface earthquakes, 2003 Secretary Island (Mw 7.2), 2007 George Sound (Mw 6.7), and 2009 Dusky Sound (Mw 7.8) complicate interpretation of the GPS time series over the last decade in the Fiordland region. To deal with this, we also conduct time-dependent inversions for coseismic and postseismic slip in those earthquakes using TDefnode (McCaffrey, 2009), fitting the campaign and continuous GPS timeseries with the best-fitting coseismic and postseis- mic slip models for those events. We evaluate the interseismic coupling model for the Puysegur subduction zone in the context of the recent earthquakes, and in particular find that the source region of the Mw 7.8 Dusky Sound earth- quake was interseismically coupled prior to 2009. Overall, the campaign and continuous GPS are well-fit by a par- tially locked subduction interface undergoing seismic and aseismic slip as well as distributed (likely permanent) de- formation east of the main plate boundary fault.

Keywords: slow slip, locking, subduction, deformation, geodetics

SETP
ECG

Fabrics and Rheology of the Mojave Lower Crust and Lithospheric Mantle

rachelbernard@utexas.edu
Bernard, R., Department of Geological Sciences, The University of Texas at Austin, Austin, TX
Behr, W., Department of Geological Sciences, The University of Texas at Austin, Austin, TX

We use xenoliths from young (3 Ma to present) cinder cones in the tectonically active Mojave desert region of southern California to characterize the rheological properties of the lower crust and upper mantle. The xenoliths were collected from two localities ~90 km apart: the Cima and Dish Hill volcanic fields. The xenolith suites represent a depth range of ~25-60 km and include spinel and plagioclase facies peridotites and lower crustal gabbros. We document how stress, temperature, water content, deformation mechanism, lattice preferred orientation, and style of localization vary with increasing depth in both xenolith suites.

Key findings thus far include the following:

(1) Both xenolith suites exhibit a wide range of deformation textures, ranging from granular, to protogranular, to porphyroclastic and mylonitic. The higher strain fabrics show no evidence for static annealing, thus are likely reflecting youthful deformation and strain gradients at depth.

(2) Both xenolith suites show abundant dynamic recrystallization and other evidence for dislocation creep as the dominant deformation mechanism. This is consistent with recent models of upper mantle post-seismic relaxation following the Landers and Hector Mine earthquakes, which require a component of power-law creep in order to fit the post-seismic surface response.

(3) A- and E-type olivine LPOs occur in both xenolith suites. Further work will determine whether these fabrics are related to changes in water content as inferred from experimental studies.

(4) Deformation in most lower crustal gabbros is weak, but some show strong fabrics associated with plagioclase-rich zones.

(5) Measurements of olivine subgrain sizes in Dish Hill samples are similar to previously published measurements from Cima, suggesting similar stress magnitudes at depth in both locations. Paleopiezometers for olivine and plagioclase indicate stress magnitudes of 11-20 MPa for the uppermost mantle, and 0.1 MPa for the lowermost crust.

Keywords: mantle, rheology, xenoliths, Mojave, lithosphere

EG
LCMS

Comparing Facies Variation in the Upper and Lower Bakken Intervals via Integrated Geochemical Analysis

jesseberney@utexas.edu
Berney, J., Bureau of Economic Geology, The University of Texas at Austin, Austin, TX
Rowe, H., Bureau of Economic Geology, The University of Texas at Austin, Austin, TX
Ruppel, S., Bureau of Economic Geology, The University of Texas at Austin, Austin, TX

The Bakken Formation is a mid-Carboniferous mudstone-siltstone succession which is a major source rock and oil producer in the Williston intracratonic basin. During the Devonian the Williston Basin was just south of the equator, connected to the open ocean via the Alberta Basin. The Bakken was deposited from late Devonian to early Mississippian and overlies the Three Forks Formation; it transitions gradationally up into the Scallion member of the Lodgepole limestone. The Bakken interval encompasses the globally recognizable Hangenberg mass extinction event, and was deposited during a great deal of tectonic activity. Some cores show surfaces of erosion between and within the Three Forks and Bakken formations.

The Bakken is commonly divided into three members: a lower black mudrock, a middle light gray siltstone, and an upper black mudrock. In some places a fourth, silty to sandy member known as the Pronghorn is present at the base of the Bakken formation.The Middle and Pronghorn members have been thoroughly described in previous work, but the Lower and Upper mudrocks are visually cryptic and have not been studied with the same level of detail. Geochemical analysis makes it possible to uncover enormous variation in the Lower and Upper mudrocks and offer insight into the environment in which they were deposited. The Upper and Lower Bakken look very similar: flat laminated to structureless, black mudrock with frequent pyrite laminations and very rare fossils. A handheld Bruker X-ray fluorescence (XRF) instrument was used to collect elemental data on the Charlie Sorenson 17-8 core at 1-inch intervals within the Lower and Upper members, with two- to six-inch resolution in the Middle Bakken, Lodgepole, and Three Forks. The major elemental data (Mg-Fe) helps define mineralogy while trace elements (V-U) reflect oceanographic conditions at the time of deposition. Taken in concert, these data illuminate chemostratigraphic intervals within the Bakken.

The Upper and Lower Bakken are highly silicic, with hardly any carbonate content. Aluminum values make a good proxy for clay content; in this core they range from 0-9% by weight, indicating that clays are not a major component and that much of the silicon is in biogenic or detrital quartz. Titanium concentrations hover around 0.2% in the middle part of the Lower Bakken and around 2.5% in the upper part of the Lower Bakken; Ti is anti-correlated with Si in much of the Upper and Lower Bakken, suggesting that much of the quartz is biogenic in origin. Using Ti as a proxy for detrital input, this slight enrichment in Ti suggests an increase in detrital sediment in the upper part of the Lower Bakken. The Upper Bakken shows a much more distinct upward increase in Ti concentration, with a corresponding decrease in Si.

Both the Upper and Lower Bakken show enrichment in redox-sensitive elements like nickel, vanadium, and molybdenum, suggesting a restricted and oxygen-depleted environment of deposition. All three elements become increasingly enriched from the bottom to the top of the Lower Bakken interval, signaling a gradual decrease in oxygenation or circulation; that trend is less visible in the Upper Bakken, which is also a much shorter interval in this core. The presence of abundant pyrite and other sulfidic minerals in both the Upper and Lower Bakken suggests that the waters may have been euxinic at least part of the time.

Taken together, it appears that the Bakken system was deposited in an overall oxygen-poor, restricted-basin environment. The contact from Lower to Middle Bakken in this core is transitional; unfortunately the contact between Upper Bakken and Middle is missing. The Middle Bakken is enormously different from the mudrocks it lies between, in everything from grain size to signs of life to chemical and mineralogical makeup. However, the similarities between the Upper and Lower Bakken suggest that the Middle member represents a punctuated deviation from the background equilibrium that produced the black mudrocks of the Bakken succession.

Keywords: geochemistry, bakken, mudrocks, devonian

SHP
LCPHD

Abbé Paramelle, 19th Century Karst Hydrogeologist

pbobeck@utexas.edu
Bobeck, P., The University of Texas at Austin, Austin, TX

Jean-Baptiste Paramelle (1790-1875) developed a scientific method for finding groundwater. Between 1827 and 1854, he found groundwater at 10,275 locations throughout France. In 1856, he published a book entitled "L'Art de découvrir les sources" [The Art of Finding Springs] that describes his method. As a result of his success in 39 departments of France, Paramelle was more famous than Henry Darcy, the father of quantitative hydrogeology, whose book on Dijon's public fountains was also published in 1856. Paramelle's methods remained central to French hydrogeology well into the 20th century.

Abbé Paramelle, a country priest, began his research in 1818 when a parishioner asked for help in finding water. Finding little guidance in the literature of the day, Paramelle began to explore on foot the limestone plateaux (the "causses") of the surrounding region (Lot). The causses lack surface drainage but are covered with sinkholes; this was obviously karst terrain but the word "karst" would not be introduced until 1893. By 1827, Paramelle had developed a theory based on his observations that sinkholes were often aligned in dry valleys and were associated with underground conduits where water flowed. He had observed water flowing into sinkholes and water spouting from sinkholes during rainstorms, and the sound of running water in sinkholes during non-rainy periods.

Subsidized by the local government, Paramelle began finding water for residents of the Department of Lot. His fame spread to neighboring departments and by the time he retired, he had "indicated" groundwater over about half the surface of France. Most of his discoveries provided water for a rural residence, a few residences, or a village.

Paramelle played an important role in popularizing groundwater in France and his observations have been reviewed and confirmed by contemporary and later scientists. Henry Darcy sent a geologist into the field with Paramelle to evaluate his method and favorably reviewed Paramelle's book in his 1856 publication. O.E. Meinzer translated and published Paramelle's discussion of the use of plants as groundwater indicators and cites Paramelle as a leader of 19th century groundwater research in France.

Keywords: karst, hydrogeology, causses, sinkholes, springs, dry valleys, groundwater, Darcy

CCG
LCMS

New ornithischian dinosaur material from the Lower Jurassic Kayenta Formation of northern Arizona

bbreeden@utexas.edu
Breeden, B., Jackson School of Geosciences, The University of Texas at Austin, Austin, TX

Ornithischia is one of two major clades within Dinosauria, and as such, it is a group comparatively popular and well studied among fossil taxa. While once thought to be fairly well represented by fossil teeth and jaw fragments throughout the Late Triassic, recent taxonomic revisions have reduced the number of verifiable Triassic ornithischian taxa to three: *Eocursor parvus* Butler, Smith, & Norman 2007 from South Africa, *Pisanosaurus mertii* Casamiquela 1967 from Argentina, and an unnamed heterodontosaurid from Argentina. Ornithischian fossils are thus rare and fragmentary from the Late Triassic, and they remain relatively so until the Late Jurassic. Nevertheless, the group had diversified and achieved a global distribution by the Early Jurassic, with members of Heterodontosauridae, Neornithischia, and Thyreophora present in Lower Jurassic strata worldwide.

The oldest ornithischian fossils from North America have been found in the silty facies of the Lower Jurassic Kayenta Formation in northeastern Arizona. These include the thyreophoran *Scutellosaurus lawleri* Colbert 1981, an unnamed heterodontosaurid, and osteoderms tentatively attributed to the English thyreophoran genus *Scelidosaurus* Owen 1859.

I report here new ornithischian dinosaur material collected from the Kayenta Formation along the Adeii Eechii Cliffs of northern Arizona between 1997 and 2000 by field parties directed by Dr. Timothy Rowe for the Texas Memorial Museum at The University of Texas at Austin. Among this new material are two associated skeletons of *Scutellosaurus lawleri,* each preserving cranial anatomy not previously known for the taxon. Traditional techniques of fossil preparation have been augmented with high-resolution X-ray computed tomography to safely extract these specimens from their plaster field jackets. In addition to these associated skeletons, several dozen other fragmentary specimens of *Scutellosaurus lawleri* have been identified, drastically increasing the known sample size for the taxon. Several relatively large isolated indeterminate ornithischian fossils have also been recovered, which may indicate that ornithischian diversity in the Kayenta Formation is greater than is currently understood.

Keywords: Thyreophora, Ornithischia, Dinosauria, Lower Jurassic, Kayenta Formation, computed tomography

CCG
LCMS

An Assessment of Natural History Collections Database Practices

lbrensk@utexas.edu
Brenskelle, L., Jackson School of Geosciences, The University of Texas at Austin, Austin, TX

Harnessing digital technology in order to store scientific specimen data in perpetuity is a complex obstacle facing natural history museums today. As research and collections staff apply more advanced analytical and imaging techniques to specimens housed in scientific collections, the question of how to store and manage new specimen-derived data formats, such as computed tomography scans, surface scans, histological sections, isotopic analyses, and frozen tissues, often arises. The evolution of collections database management systems has resulted in a variety of options for natural history collections to store specimen data and to connect all data to the objects from which they are derived. This study surveys the database practices of different types of natural history collections (paleontological, geological, zoological, and botanical). Collections managers from different natural history disciplines were observed performing routine database tasks, and interviewed about their opinions regarding the database management software their institution utilizes. The aim is to assess the collection staff's knowledge-base of the databases they work with on a daily basis, to determine what additional database training should be made available to employees, and to evaluate how the usability of database schemas could be improved to more accurately represent the information natural history collections need to preserve about their specimens.

Keywords: museum collections, paleontology, scientific data, databases, data management

PS
LCPHD

A new model for the stratigraphic and morphologic evolution of Mars' north pole basal unit

tcbrothers@utexas.edu
Brothers, T., University of Texas Institute for Geophysics
Holt, J., University of Texas Institute for Geophysics

Reconstructing climate and hypothesizing habitable regimes is fundamental to Mars' science. The preserved martian polar ice layering has been hypothesized to contain a regional record of modern climate [*Cutts and Lewis*, 1982; *Laskar et al.*, 2002]. While the uppermost pure water ice deposits on Mars' north pole may represent only the past four million years [*Laskar et al.*, 2002; *Greve et al.*, 2010], an older mixture of sand and ice is present. This older mixture of sand and ice theoretically provides climatic data for a more ancient Mars. The two geologic units that compose this mixture of sand and ice are the rupes and cavi unit [*Tanaka et al.*, 2008]. The older unit, rupes, is hypothesized to be nearly one billion years old [*Tanaka et al.*, 2008]. Together these two members comprise the basal unit of Mars' north pole and contain stratigraphy deposited during a past climate regime.

Radar sounding instruments such as Shallow Radar (SHARAD) have enabled extensive subsurface mapping of ice stratigraphy on Mars' north pole [*Phillips et al.*, 2008; *Putzig et al.*, 2009; *Holt et al.*, 2010]. Mapping studies using SHARAD data have revealed that the oldest icy deposits on the north pole, the rupes and cavi members, do not form a smooth interface with overlying deposits [*Putzig et al.*, 2009; *Brothers et al.*, 2010]. This finding emphasized the need to better understand the causes for irregular basal unit topography in order to make inferences about their depositional regime.

Here we analyze and offer explanation for two of the most enigmatic basal unit attributes revealed by radar mapping, an asymmetric ridge at the unit's point of maximum thickness and a morphologic disparity between eastern and western portions of the deposit. Our hypothesis explains the basal unit's morphology, composition, and expression using known processes currently operating in the north polar region. In addition, this work is able to offer evidence suggesting that the origin of the spiral troughs on Mars' north pole may have initiated as a result of basal unit topography, making them younger than previously hypothesized [*Smith and Holt*, 2010]. These findings indicate that the basal unit does not necessitate a different climate regime for deposition and alteration. Instead, we posit that the climatic conditions both during and following basal unit emplacement were very similar to the modern.

Bibliography

Brothers, T. C., J. W. Holt, S. R. Christian, and P. Choudhary (2010), Investigating subsurface geomorphology of the basal unit of Planum Boreum Mars with SHARAD to constrain early erosional processes, *41st Lunar Planet. Sci. Conf*.

Cutts, J. A., and B. H. Lewis (1982), Models of climate cycles recorded in Martian polar layered deposits, *Icarus*, *50*(2–3), 216 – 244, doi:http://dx.doi.org/10.1016/0019-1035(82)90124-5.

Greve, R., B. Grieger, and O. J. Stenzel (2010), MAIC-2, a latitudinal model for the Martian surface temperature, atmospheric water transport and surface glaciation, *Planet. Space Sci.*, *58*(6), 931–940, doi:10.1016/j.pss.2010.03.002.

Holt, J. W., K. E. Fishbaugh, S. Byrne, S. Christian, K. Tanaka, P. S. Russell, K. E. Herkenhoff, A. Safaeinili, N. E. Putzig, and R. J. Phillips (2010), The construction of Chasma Boreale on Mars, *Nature*, *465*(7297), 446–449, doi:10.1038/nature09050.

Laskar, J., B. Levrard, and J. F. Mustard (2002), Orbital forcing of the martian polar layered deposits, *Nature*, *419*(6905), 375–377, doi:10.1038/nature01066.

Phillips, R. J. et al. (2008), Mars North Polar Deposits: Stratigraphy, Age, and Geodynamical Response, *Science*, *320*(5880), 1182–1185, doi:10.1126/science.1157546.

Putzig, N. E., R. J. Phillips, B. A. Campbell, J. W. Holt, J. J. Plaut, L. M. Carter, A. F. Egan, F. Bernardini, A. Safaeinili, and R. Seu (2009), Subsurface structure of Planum Boreum from Mars Reconnaissance Orbiter shallow radar soundings, *Icarus*, *204*(2), 443–457.

Smith, I. B., and J. W. Holt (2010), Onset and migration of spiral troughs on Mars revealed by orbital radar, *Nature*, *465*(7297), 450–453, doi:10.1038/nature09049.

Tanaka, K., J. Rodriguez, J. Skinnerjr, M. Bourke, C. Fortezzo, K. Herkenhoff, E. Kolb, and C. Okubo (2008), North polar region of Mars: Advances in stratigraphy, structure, and erosional modification, *Icarus*, *196*(2), 318–358, doi:10.1016/j.icarus.2008.01.021.

Keywords: Mars, Ice, Stratigraphy, Basal Unit, SHARAD, Radar

CCG
LCPHD

Incorporating the Role of Nitrogen in the Noah-MP Land Surface Model for Climate and Environmental Studies

xitian.cai@utexas.edu
Cai, X., Department of Geological Sciences, The University of Texas at Austin, Austin, TX
Yang, Z., Department of Geological Sciences, The University of Texas at Austin, Austin, TX
Fisher, J., Jet Propulsion Laboratory, California Institute of Technology, Pasadena, CA

Noah-MP (Niu et al., 2011; Yang et al., 2011) is the next generation land surface model for the Weather Research and Forecasting (WRF) meteorological model and the Climate Forecast Systems in the National Centers for Environmental Prediction. While Noah-MP does not currently contain a dynamic nitrogen cycle, this can readily be updated with the interactive vegetation canopy option. In this study, Noah-MP is coupled with the Fixation & Uptake of Nitrogen (FUN) model (Fisher et al., 2010) for the above ground processes and the soil nitrogen model from the Soil and Water Assessment Tool (SWAT) for the below ground processes. This combines FUN's state-of-the-art concept of the carbon cost theory and SWAT's strength in representing the anthropogenic effects on the nitrogen cycle. The processes employed from FUN are the nitrogen uptake and fixation of plants, both of which are directly linked to the plant productivity. If passive nitrogen uptake cannot meet the nitrogen demand, plants have to spend part of the photosynthesized carbon production on nitrogen acquisition. The processes employed from SWAT are nitrogen mineralization, nitrification, immobilization, volatilization, atmospheric deposition, and leaching. In addition, the modified universal soil loss equation is used to more accurately account for the nitrogen removal in sediment caused by surface runoff. Because human input of nitrogen greatly changes the nitrogen cycle, a simple nitrogen fertilization approach is also applied to crops. Preliminary results show that Noah-MP is capable of simulating the dynamics of the major nitrogen pools. Further comprehensive evaluation of the new model will be conducted at one or more experimental sites.

Keywords: Noah, land surface model, nitrogen cycle, carbon cycle

SETP
LCPHD

Interactions between chemical alteration, brittle deformation, and epithermal mineralization at the Dixie Comstock Mine, Dixie Valley, NV

owen.callahan@gmail.com
Callahan, O., Bureau of Economic Geology, The University of Texas at Austin, Austin, TX
Eichhubl, P., Bureau of Economic Geology, The University of Texas at Austin, Austin, TX

The location and longevity of hydrothermal flow arises from competing mechanical and chemical processes – mechanical fracture opening versus chemical cementation. The interaction between these two mechanisms is complicated by chemical alteration potentially modifying the mechanical properties of the rock. The goal of this study is to characterize the mechanical properties of rocks that have undergone different degrees of hydrothermal alteration, to assess the impact that these changes may have on fracture network evolution, and describe the role these spatially and temporally variable properties may have on the lifecycle of hydrothermal systems.

The Dixie Comstock Mine is a fault controlled, epithermal gold deposit located at the base of the Stillwater Range in central Nevada. Exhumed silicified gabbro and quartz breccia are preserved as triangular facets along the moderately east dipping, range-bounding fault. Gold occurs as electrum in quartz breccia and in crushed and altered gabbro. Gabbro in the footwall and in clasts in quartz-cemented breccia is altered to quartz, chlorite, sericite, montmorillonite, and sulfides.

We measured fracture attributes in outcrop from several locations around this deposit, including one scan line through silicified breccia and two scan lines through less altered footwall rock north and south of the main mineralized zone. Quartz-cemented fractures in all three scan lines are dominantly steeply ENE to ESE dipping, however, fracture intensity (number of fractures per meter) in the silicified breccia is 10 times the background population. Hand sample and thin section observations of cross cutting relationships show that fracture intensity in the breccia arises from repeated brittle failure and cementation. Silicified breccia includes clasts of previously silicified material, including altered gabbro and chalcedony, both of which contain, and are cut by, quartz filled microfractures (<1 mm). Fractures in the less silicified background material include thick (2-3 cm) cloudy quartz and euhedral quartz±calcite cemented fractures that have dilated in left lateral and oblique shear, and sheared fractures which sole into fault-parallel shear zones.

We hypothesize that mechanical changes caused by hydrothermal alteration have modified the response of the rock so that repeated failure in silicified material is dominated by opening mode fractures, while chlorite and clay alteration in the background material favors shear failure and more widely spaced veins. Rock and fracture mechanics tests of the silicified breccia and background assemblages in this system are currently underway to evaluate this hypothesis. If supported, the mechanical contrast between these units may serve as a mechanism for focusing hydrothermal flow and help concentrate mineralizing fluids required to achieve economic ore grades.

Keywords: Dixie Valley, epithermal, hydrothermal, alteration, fracture, rock mechanics

SETP
ECG

Mesozoic-Cenozoic Sedimentation, Provenance, and Basin Evolution along the Eastern Margin of the Central Andes (19°-22°S)

azcallep@utexas.edu
Calle, A., Department of Geological Sciences, The University of Texas at Austin, Austin, TX; Institute for Geophysics, The University of Texas at Austin, Austin, TX
Horton, B., Department of Geological Sciences, The University of Texas at Austin, Austin, TX; Institute for Geophysics, The University of Texas at Austin, Austin, TX
Stockli, D., Department of Geological Sciences, The University of Texas at Austin, Austin, TX

New insights on Mesozoic-Cenozoic sedimentation and fold-thrust deformation are critical to improved assessment of established petroleum systems and potential new plays in the central Andes. We provide a progress report on the regional distribution and long-term evolution of Andean and pre-Andean basins in southern Bolivia (19°-22°S). The spatial-temporal responses to tectonic, climatic, and drainage-network modifications are evaluated for a protracted record involving pre-Andean (Mesozoic) extension and post-rift thermal subsidence followed by Andean (Cenozoic) shortening and cratonward advance of a retroarc foreland basin system. Sediment dispersal trends are derived from new and published facies analyses, paleocurrents, detrital zircon U-Pb age distributions, sandstone petrography, and conglomerate clast compositions. Detailed surface and subsurface stratigraphic analyses combined with sediment provenance data along the Eastern Cordillera and Subandean belt reveal clastic deposition of distal to proximal facies (fluviolacustrine, fluvial megafan, alluvial fan) in different depozones characteristic of a progressively compartmentalized foreland basin. Depositional age constraints and sediment accumulation rates for Cenozoic basin fill are refined through newly dated tuffs and maximum depositional age constraints defined by the youngest detrital zircon populations.

A >4 km-thick clastic succession exposed in the Eastern Cordillera records the transition from a Cretaceous post-rift sag basin to a Paleocene–Miocene eastward-advancing foreland basin. Similarly, deposition of up to 6 km-thick upward-coarsening and thickening succession in both the Subandes and modern Chaco basin records the cratonward propagation of the fold-thrust belt and resulting deposition in different foreland depozones. Analyses of new growth stratal relationships preserved in the western Subandean zone (El Rosal syncline) provide clear evidence for syndeformational deposition and elucidate the exhumation history of the older components of the advancing basin. Regional-scale analyses of stratigraphic signatures (depositional facies, sediment composition, dispersal pathways) shed light on the propagation of the Andean thrust belt and associated basin compartmentalization, which progressed eastward from the Eastern Cordillera (Middle Eocene) to Interandean zone (Early Miocene), and finally into the Subandean zone (Late Miocene).

Keywords: Mesozoic sedimentation, central Andes, growth strata, foreland basins

SETP
U

Application of the TitaniQ geothermobarometer to metamorphic rocks of the Santa Rosa Mylonite Zone in southern California

taylorcanada@utexas.edu
Canada, T., Jackson School of Geosciences, The University of Texas at Austin, Austin, TX
Behr, W., Jackson School of Geosciences, The University of Texas at Austin, Austin, TX
Stockli, D., Jackson School of Geosciences, The University of Texas at Austin, Austin, TX
Stockli, L., Jackson School of Geosciences, The University of Texas at Austin, Austin, TX

In order to study the behavior of the crust in different regions and over time, it remains important to be able to quantify the pressure (P) and temperature (T) conditions of metamorphism in exhumed rocks. The recently developed technique, known as “Titanium-in-quartz” (TitaniQ) shows particular promise as both a geothermometer and geobarometer, because it focuses on one of the most abundant minerals on Earth—quartz—and it can thus be applied to a very wide range of rock types. Despite the potential of TitaniQ, two aspects of the technique remain poorly understood. Firstly, the two most recently developed calibrations predict Ti concentrations that differ by close to a factor of three at the same temperature. Secondly, the effect of deformation on Ti re-equilibration at temperatures where static diffusion is sluggish is debated. We address these aspects of the TitaniQ thermobarometer by applying the technique to a suite of rocks in the Santa Rosa mylonite zone of eastern California that were deformed and metamorphosed at known P-T conditions.

The Santa Rosa mylonite zone is a 100-km-long Cretaceous ductile thrust system that juxtaposes deformed metasedimentary rocks (P = 3-5 kbar, T = 600-800 C) known as the Palm Canyon Series in the hanging wall against mylonitized granodiorites (P 4-5 kbar, T = 400-550) of the Peninsular Ranges Batholith in the footwall. The Palm Canyon series includes quartzites, amphibolites and garnet-mica schists, most of which contain titanite as the primary Ti-bearing phase. We measure Ti concentrations in several samples from this unit to see whether they are consistent among different rock types and whether calibrations of the TitaniQ thermobarometer match the P-T conditions constrained by mineral assemblages. The granodiorites show a distinct strain gradient developed over approximately one kilometer as they are incorporated into the Santa Rosa mylonite zone; they range from weakly deformed at the shear zone margin to ultramylonitic in the shear zone core. We examine Ti concentrations in rocks collected across this strain gradient to determine the degree to which progressive strain (accommodated by pervasive dynamic recrystallization) can redistribute Ti in quartz.

Keywords: Geothermobarometer, quartz, titanium, temperature

SETP
ECG

Neogene synorogenic sedimentation and structural evolution of the Bermejo foreland basin, southern central Andes, Argentina

tcapaldi@utexas.edu
Capaldi, T., Jackson School of Geosciences, The University of Texas at Austin, Austin, TX
Horton, B., Jackson School of Geosciences, The University of Texas at Austin, Austin, TX
McKenzie, R., Department of Geology and Geophysics, Yale University, New Haven, CT
Mackaman-Lofland, C., Jackson School of Geosciences, The University of Texas at Austin, Austin, TX

In the Andes of Argentina (27-33°S), the major cities of Mendoza and San Juan have been repeatedly damaged or leveled by large-magnitude earthquakes (e.g., M 7-8 events in 1977, 1952, 1944, 1927, 1894, 1861, 1782) generated by stresses related to flat-slab subduction and associated crustal shortening expressed along the Eastern Precordillera (EPC) thrust system. The EPC is a 175 km-long, N-S trending, west-directed backthrust system, forming a frontal triangle zone with respect to the oppositely verging, east-directed Central Precordilleran (CPC) ramp-flat thrust system in the orogenic hinterland to the west. The EPC has been structurally linked to west-directed, basement-involved reverse faults of the Sierras Pampeanas (SP) to the east that have broken the once-contiguous foreland basin. Reconstructions of the EPC tectonic history show large uncertainties in terms of when deformation initiated and how it was spatiotemporally distributed along strike. Cenozoic shortening broadly advanced from the High Andes to the CPC, recycling large segments of the retroarc foreland basin. The timing and style of this thrust propagation and associated progressive uplift of the modern Andean deformation front remain debated. Previous studies interpreted initial shortening at 5-2 Ma in the CPC-EPC and 2.6 Ma in the SP, largely on the basis of inferred links with Cenozoic volcanic arc migration. Previous studies also suggest that uplift swept from north to south with subduction of the Juan Fernandez ridge and flattening of the subducting oceanic Nazca plate. However, recent geo- and thermo-chronologic studies indicate wholesale deformation of CPC at 12-9 Ma with no evidence of major along-strike (N-S) variations. New structural, stratigraphic, thermochronologic, and provenance data from the EPC are required to resolve these competing kinematic models and evaluate the structural relationships between the CPC and SP. Reconstructing the structural and temporal evolution of the EPC is critical for evaluating not only the long-term interactions of frontal thrust structures with foreland-basin sedimentation but also assessing Andean earthquake hazards that will impact human populations and infrastructure in western South America.

Keywords: tectonics, basin analysis, detrital geochronology, thermochronolgy,

PS
LCMS

Evidence for changes in coastline-controlled base level from fluvial stratigraphy at Aeolis Dorsa, Mars

benjamin.cardenas@utexas.edu
Cardenas, B., Jackson School of Geosciences, The University of Texas at Austin, Austin, TX
Mohrig, D., Jackson School of Geosciences, The University of Texas at Austin, Austin, TX

There is evidence that a subset of fluvial deposits at Aeolis Dorsa, a basin on Mars, preserve incised valleys carved and filled during changes in base level, which was likely controlled by water surface elevation of a large lake or sea. Three low-albedo, channelized corridors, each several tens of kilometers long, contain relict point bars and scooped boundaries at their bases, indicating that the base and lateral extent of each corridor was defined by a migrating, net-erosional river. Above the basal deposits are stacks several tens of meters thick of "inverted sinuous ridges", which are channel-filling deposits that have been exhumed and topographically inverted. Indicators of avulsions, channel re-occupations, an overall flattening of basal topography, and confinement of inverted sinuous ridges to the dark corridors are evidence of the gradual filling of a valley cut by the basal migrating river. Valley incision and fill are common responses to sea level change on Earth. Aeolis Dorsa is currently open to the northern lowlands of Mars, where an ocean has been hypothesized to have once existed, although a large lake could have also controlled base level. Cross-cutting valleys require at least two episodes of base level fall and rise. The magnitudes of the base level changes are estimated at about 80 meters, based on the thickness of the valley-filling stratigraphy. Meander asymmetry is consistent with a southeastern flow direction, and is supported by a set of branching fluvial deposits 40 km to the southeast which, qualitatively, appear to be deltaic in origin.

Keywords: Mars, incised valleys, martian ocean, fluvial processes, sedimentary geology

CCG
LCPHD

ASSESSING THE ROLE OF THE CARBONIC ANHYDRASE ENZYME IN CONTROLLING H2O-CO2 OXYGEN ISOTOPE EXCHANGE RATES DURING SPELEOTHEM GROWTH

petercarlson@utexas.edu
Carlson, P., Department of Geological Sciences, The University of Texas at Austin, Austin, TX
Breecker, D., Department of Geological Sciences, The University of Texas at Austin, Austin, TX
Banner, J., Department of Geological Sciences, The University of Texas at Austin, Austin, TX

The cave at Westcave Preserve in central Texas is a unique location to study speleothem growth due to the consistently low CO_2 concentrations and seasonally-variable temperature in the cave. Average calcite growth rates in the cave are high, ranging seasonally from 8-40 mg/day, as opposed to the 0-15 mg/day rates observed in other central Texas caves. Despite the rapid growth rates and low ambient CO_2, the calcite is growing at or near isotopic equilibrium with its drip water (Feng *et al.*, 2014). We hypothesize that this unexpected equilibrium is caused by the activity of the enzyme carbonic anhydrase (CA) in the drip water. CA catalyzes the hydroxylation of CO_2 to bicarbonate. It is produced by many organisms, especially photosynthesizers, and is found in soil pore waters. CA has not been previously shown to play a role in speleothem formation, but this may be due to a sampling preference for speleothems from dark zones.

The speleothems in Westcave are in entrance or twilight zones, which may allow *in situ* production of CA on the speleothem by photosynthetic microorganisms, altering the kinetic controls of the carbonate system and allowing for the rapid growth of calcite near isotopic equilibrium with its drip water. We allowed CO_2 to equilibrate with cave and deionized water for 0-22 hours at 25 °C. We duplicated this test with drip water from a dark site in Inner Space Cavern. Initial tests indicated that CO_2 reaches oxygen isotope equilibrium with drip water in Westcave significantly faster than with deionized water at 25 °C (~9 hours versus ~14 hours), but drip water from Inner Space Cavern showed no significant difference from deionized water. Further tests did not reproduce these results. Both caves showed faster oxygen-isotopic equilibration rates than deionized water, but with similar first-order reaction rates. These apparent reaction rates may be influenced by different rate-limiting steps at different stages of the experiment. Our current methods are unable to resolve reaction rates early in the experiment, and therefore are insufficient to determine the activity of carbonic anhydrase in cave drip waters. Further examination, using different methods, is required to determine whether or not CA is responsible for the fast oxygen-isotopic equilibration observed at Westcave and Inner Space. If further testing confirms our initial hypotheses, near-entrance, twilight zone speleothems should not be treated as purely inorganic carbonate systems, but may still be important sources of stable-isotope climate proxies.

Keywords: Speleothems, Carbonic anhydrase, oxygen isotopes

CCG
LCPHD

Changes in Deep Convective Ice and Rainrate due to Pollution as Observed from Satellites.

sudipm09@gmail.com
Chakraborty, S., Jackson School of Geosciences, The University of Texas at Austin, Austin, TX
Fu, R., Jackson School of Geosciences, The University of Texas at Austin, Austin, TX

The influence of aerosols on ice water content (IWC) and rainrate has been suggested by some numerical simulations and observational studies. This is often complicated by a lack of contextual information regarding the dynamic structure and life cycle of the cloud systems. We investigate IWC and rainrate from deep convections (DC) using datasets from AURA Microwave Limb Sounder, CloudSat, Aqua Moderate Resolution Imaging Spectroradiometer, and International Satellite Cloud Climatology Project over the Congo, the Amazon, and South Asia during three different stages of lifecycle. We use measurements from AURA MLS to investigate the change in water content associated with the smaller sized ice crystals at anvil level and CloudSat to derive the relation between the amounts of larger sized ice crystals and rainrate with ambient aerosol loadings. We integrate reflectivity above freezing level (IZ) to calculate the amount of ice and differentiate reflectivity (DZ) with respect to altitude below the freeing level to estimate the attenuated rainfall under the cloud. Our analysis using the reflectivity data shows that IZ and DZ don't change with aerosols loadings during the growing stage. However, IZ increases and DZ decreases, suggesting a delayed precipitation and increase of ice formation, during the matured stage. During the decaying stage, DZ increases, leading to a loss in larger ice particles or as shown by a decrease of the IZ above freezing level. IWC within the anvils of the DCs during their growing stage shows no significant relations with the ambient aerosol concentration over the Congo and South Asia. However, anvil IWC decreases during the matured stage over the South Asia and increase over the Congo as aerosol optical depth surrounding the DCs increases. Aerosol's concentration plays an important role during the decaying stage and is significantly and positively correlated with the IWC of the anvils, suggesting an increase of smaller ice particles in convective anvils with aerosols.

Together with the result of CloudSat, our results supports the hypothesis that an increase of aerosols tend to invigorate large mesoscale deep convection by delaying precipitation and increasing both large and smaller ice particles in convective anvils during the mature phase, and increase precipitation during the decay phase.

Keywords: Dynamic structure of deep convective clouds, aerosols, satellite.

SHP
ECG

Evolution of Terminal Fans over Salt Substrate

echatmas@utexas.edu
Chatmas, E., Department of Geological Sciences, The University of Texas at Austin, Austin, TX

Evolution of Terminal Fans over Salt Substrate

In the Appotomox-Vicksburg area in the Gulf of Mexico there have been several studies involving the interactions of the Louann salt layer and the deposited Norphlet sandstone on top of it. Under geologic conditions, salt behaves as a viscous fluid and causes deformation, which therefore effects the current location of the deposited brittle layers. Over time there has been a significant amount of deformation in this region, so the location of the Norphlet sandstone is less well known, especially since it is located near the salt which produces difficulties in seismic images. In this region there is evidence of large terminal fans prograding onto the salt and terminating into the large dune field that was also present during this time.

This research focuses on studying physical experiments to understand how a fan's behavior changes when placed on top of a salt substrate. A three-dimensional basin was created that is 120 cm in length, 60 cm in width and 32 cm in height. A layer of viscous polymer (PDMS) is put down as an analog for natural salt, and 100-micron quartz sediment and water is fed into the system from the top of the basin at constant rates for 60 minutes. The basin is slightly sloped, allowing the water to flow downwards and to prevent ponding around the fan. The sediment slowly progrades onto the salt, causing deformation to occur within the salt and therefore changing the behavior of the fan.

In this system, the water leaves the fan and forms channels within the salt substrate. With an increased slope the amount of subsidence in the fan increases and more sediment is moved into the channels, creating relatively deep, narrow channels. With a lower slope, channels are still established but the amount of subsidence in the system is less overall, so the amount of sediment in the channels is noticeably less. The fan goes through periods of increased growth and periods of lesser growth, which shows periods of dominated fan growth or fan subsidence in response to the salt moving.

Keywords: surface processes

SETP
LCPHD

186Os/188Os isotopic compositions of peridotites: Constraints on Pt/Os evolution of the upper mantle and implications for the late veneer hypothesis

rudra025@gmail.com
Chatterjee, R., Department of Geological Sciences, The University of Texas at Austin, Austin, TX
Lassiter, J., Department of Geological Sciences, The University of Texas at Austin, Austin, TX

Global correlations between Al_2O_3 and Pt/Os in mantle peridotites suggest that Pt behaves incompatibly relative to Os during partial melting [c.f., 1]. Because ^{190}Pt decays to ^{186}Os ($t_{1/2}$ = 468 Ga), correlations between $^{186}Os/^{188}Os$ and peridotite fertility can be used to constrain the long-term Pt/Os evolution of the depleted mantle and the initial Pt/Os ratio of the primitive upper mantle (PUM). We examined $^{186}Os/^{188}Os$ in mantle peridotites from continental (Rio Grande Rift/Colorado Plateau) and oceanic (Lena Trough, Hawaiian Islands) settings that span a wide range in fertility (Al_2O_3 ~0.67-4.42 %) and $^{187}Os/^{188}Os$ ratios (0.1138-0.1305). The new data define a narrow range in $^{186}Os/^{188}Os$ (0.1198338 to 0.1198393, 2 SD~24 ppm), placing constraints on long-term Pt/Os variability in the DMM. $^{186}Os/^{188}Os$ is broadly correlated with indices of melt depletion including spinel Cr#, clinopyroxene Cr#, and clinopyroxene Yb content, consistent with the inferred relative compatibility of Pt and Os during partial melting. Extrapolation of the alumina-$^{186}Os/^{188}Os$ trend to PUM alumina content (~4.5 wt% Al_2O_3; [2]) suggests a PUM $^{186}Os/^{188}Os$ of ~0.1198380±15, similar to the $^{186}Os/^{188}Os$ of H chondrites (~0.1198398±16; [3]). This $^{186}Os/^{188}Os$ value is consistent with a PUM Pt/Os of 1.8±0.3, similar to Pt/Os values measured in several classes of chondrites (Carbonaceous ~1.9±0.2, Ordinary ~2.0±0.3 and Enstatite ~1.9±0.2; [3]). Whereas ~84% of peridotites worldwide [excluding low-[Os] samples (<1 ppb Os) that may have been compromised by melt-rock reaction and/or weathering and alteration] with measured Pt/Os ratios have Pt/Os between 0.3 and 3.1 (the range permissible from $^{186}Os/^{188}Os$ variations for melt extraction from PUM at ~1.5 Ga), only ~36% fall between 1.3 and 2.2 (a narrower range consistent with an older ~4.5 Ga melt depletion age). This suggests that much of the observed Pt/Os variability in mantle peridotites is relatively recent. Close agreement between our inferred Pt/Os_{PUM} with previous estimates inferred from chondrites [3] is consistent with the addition of a chondritic late veneer to explain the HSE abundances in the upper mantle. [1] Becker et al., GCA 2006; [2] McDonough et al., Chem Geo 1995; [3] Brandon et al., GCA 2006

Keywords: melt depletion, late veneer hypothesis, Os isotopes, Pt/Os

EG
LCPHD

Time-frequency analysis for tracking horizons, detecting karstification and low-frequency anomalies, using synchrosqueezeing wavelet transform: a case study applied to Boonsville field

chenyk1990@gmail.com
Chen, Y., Texas Consortium for Computational Seismology, Bureau of Economic Geology, The University of Texas at Austin, Austin, TX
Xie, Q., China University of Petroleum - Beijing
Wang, E., PetroChina Changqing Oilfield Company

The synchrosqueezing wavelet transform (SSWT) can capture the local frequency variation in the seismic data with high time and frequency resolutions. In this paper, we proposed two novel applications of TF analysis using the SSWT. First, we propose to use SSWT to aid in tracking horizons due to the super-high resolution of SSWT in temporal direction. Secondly, we proposed to use SSWT to detect karstification, which is also closely related with oil & gas traps. We also provide examples showing better performance for detecting low-frequency anomalies using SSWT. All the studies in this paper is based on the 3D migrated data from the Boonsville field.

Keywords: tracking horizons, karstification, low-frequecy anomaly, synchrosqueezing wavelet transform

SETP
LCPHD

Assessing the impact of orogenic inheritance on the architecture, timing and magmatic budget of hyperextended rift systems: a mapping approach

pauline.chenin@gmail.com
Chenin, P., The University of Texas at Austin & Université de Strasbourg
Manatschal, G., Université de Strasbourg
Lavier, L., The University of Texas at Austin

In order to investigate the impact of orogenic inheritance on the characteristics of hyperextended rift systems, we develop large-scale observation-driven mapping methods highlighting (1) the distribution of major heterogeneities inherited from previous orogenies; (2) the first-order architecture of hyperextended rifts; and (3) the timing of the main rifting events.
1) Mapping orogenic inheritance
We map the structures and heterogeneities inherited from previous orogenies that may have significantly influenced subsequent rifting, limiting our selection to features that: (i) are important enough to have had a potential impact on subsequent deformation; (ii) are preserved through time; and (iii) bear the potential to be reactivated. Using these criteria, we map oceanic sutures, deformation fronts, foreland basins, magmatic arcs and majors magmatic additions.
2) Mapping rift architecture:
In order to highlight the first-order architecture of rift systems, we map rifted margins distinguish between three domains as a function of their architecture and lithology: (i) the *proximal domain* made of un- or barely thinned continental crust; (ii) the *oceanic domain* characterized by steady-state oceanic crust; and (iii) the transitional *hyperextended domain* concentrating most of the deformation between them. We use seismic sections as well as gravity and magnetic data to identify and correlate the limits of these domains through space.
3) Age of major rift events:
To constrain the timing of rifting, we determine the age of *necking* and *lithospheric breakup*, which correspond to the formation of the continentward and oceanward limit of the hyperextended domain, respectively. These events are recorded as two major uncomformities within the sediment deposits that can be identified seismic sections.
Applying this approach in the North Atlantic region highlights the different behaviour of the rift with respect to the Caledonian and Variscan orogenic lithospheres, the Variscan front appearing to be a major limit. Indeed, the rift cuts through the Caledonian orogen and parallels its structural grain, while it circumvents the core of the Variscides. In addition, rifting is protracted and polyphase, and breakup is magma-rich North to the Variscan front, as opposed to the South where a single, apparently continuous extensional event lead to magma-poor breakup in less than 50 Myrs. These observations point to a major influence of orogenic inheritance on the characteristics of hyperextended rift systems. On the other hand, our study supports that rifts reactivate sutures corresponding to former large (> 2 000 km) oceans, while leaving sutures of small (< 500 - 1 000 km) oceanic basins little affected, suggesting a significant impact of the pre-orogenic histories on subsequent extensional processes as well.

Keywords: North Atlantic, Orogenic inheritance, Hyperextended rift architecture, Rift timing, Map

CCG
ECG

Impacts of enhanced soil-hydrology-vegetation interactions on soil moisture using Noah-MP

swchung@utexas.edu
Chung, S., Jackson School of Geosciences, The University of Texas at Austin, Austin, TX
Yang, Z., Jackson School of Geosciences, The University of Texas at Austin, Austin, TX

The precipitation forecasts have been limited in intraseasonal and seasonal scales. Simulation of land surface states, slowly responding to the atmosphere, plays an important role to improve precipitation forecasts, especially in midlatitude and the interior of large continents. Many studies have addressed the importance of feedback between soil moisture and precipitation. Soil moisture simulation can rely on vegetation phenology, soil moisture heterogeneity and water table depth, with influencing surface energy fluxes, atmospherics boundary processes and runoff production. The objective of this study is to investigate to what degree the Noah land surface model with multiple physics (Noah-MP) can improve soil moisture simulation skill with using various soil-hydrology-vegetation interactions. Noah-MP has been implemented multiple parameterization options, and each physics combination can act as an individual model (Version 1.6 is currently published). In this study, the physics combinations apply the various processes of vegetation, canopy stomatal resistance, soil moisture factor for stomatal resistance, and runoff and groundwater. Soil moisture and those soil moisture-related variables such as evaporation, runoff, and groundwater are simulated with each physics combination in global scale for the period from 1980 to 2007.

Keywords: Land Surface Model, Noah-MP, Soil Moisture

SETP
ECG

Exhumation of the Lesser Himalaya of Northwest India: (U-Th)/He thermochronometric constraints and implications for the Neogene isotopic composition of seawater

ccolleps@utexas.edu
Colleps, C., Jackson School of Geosciences, The University of Texas at Austin, Austin, TX
Stockli, D., Jackson School of Geosciences, The University of Texas at Austin, Austin, TX
McKenzie, R., Department of Geology and Geophysics, Yale University, New Haven, CT

The proposed timing of Lesser Himalayan (LH) uplift in the Uttarakhand-Himachal region of Northwest India remains a topic of debate, the resolution of which may provide insight into the relationship between the weathering of Himalayan source rock and the secular changes in isotopic composition of osmium in Neogene seawater. The weathering of black shale enriched in radiogenic ^{187}Os in the LH has been suggested as a potential source for the steady rise in the $^{187}Os/^{188}Os$ ratio starting at ~16 Ma from the osmium seawater record. Here we use zircon (U-Th)/He (ZHe) thermochronology to constrain the timing of emplacement and exhumation of distinct Himalayan thrust sheets and test two contrasting models on the origin of the Tons Thrust, which divides the LH into inner (iLH) and outer (oLH) zones. The iLH consists mostly of late Paleo-Mesoproterozoic rocks whereas the oLH primarily contains Cryogenian to Cambrian sedimentary rocks. One model suggests that the Tons Thrust shared an original decollement with the South Tibetan Fault System and that the oLH is a far-traveled klippe emplaced against the iLH during the Eocene-Oligocene. In contrast, a second model suggests that the oLH is a short travelled, in sequence thrust sheet emplaced in the Late Miocene. Our current data yield average ZHe cooling ages of 7.2 ± 1.8 Ma (n=6) for the lowermost oLH, 16.2 ± 1.5 Ma (n=15) for the middle oLH, and 10.5 ± 3.6 Ma (n=12) for the iLH. These data support at a first-order the short travelled kinematic model for the emplacement of the oLH and are consistent with predicted ZHe ages of the LH in respect to the seawater geochemical record. With a higher spatial resolution of cooling ages along strike from the hinterland coupled with detrital zircon U-Pb-He double dating of foreland basin deposits, we can further constrain LH exhumation and more confidently link the weathering of the LH to the observed shifts in osmium seawater compositions.

Keywords: Himalaya, India, Thermochronology, Geochronology, (U-Th)/He

SHP
LCMS

Paleogeography evolution during the Eocene Upper Wilcox in the Houston embayment with consideration of the Yoakum Canyon fill

david.conwell@utexas.edu
Conwell, D., Jackson School of Geoscience, The University of Austin, Austin, TX
Steel, R., Jackson School of Geoscience, The University of Austin, Austin, TX
Olariu, C., Jackson School of Geoscience, The University of Austin, Austin, TX

The Eocene Upper Wilcox sequence represents the second major pulse of clastic sedimentation into the Gulf of Mexico basin. The clastic deposition began with the progradational Lower Wilcox (Upper Paleocene) which was followed by the Middle Wilcox (Eocene-Paleocene) and was capped by the Upper Wilcox (Lower Eocene). Conventional Wilcox fields have produced gas over the last 80 years, these resources have largely been exhausted. Recently interest in the Wilcox has been reinvigorated with the drilling of the Baha prospect in 2001 and the associated discovery of 2.5 billion barrels of producible oil in deepwater turbidite deposits. To better characterize and understand the deepwater deposits, research in the delivery systems that transported sediments from the Laramide uplift to the deep Gulf of Mexico is required, especially on the Wilcox shelf margin.

This study incorporates over 300 well logs, outcrop, and cores to analyze the Upper Wilcox shelf deposits in the Houston embayment. The area of the study extends from outcrop belt in the north-northwest down into the subsurface to the limit of well control, around 150 km south. In From east to west it extends for about 170 km between Lavaca county in the west to Grimes county in the east.

The thickest Upper Wilcox deposits have been described in the south Texas Rio Grande embayment. In the Houston embayment, the Upper Wilcox was interpreted previously as mainly fluvial deposits that prograded out across the relatively stable substrate provided by the underlying delta complexes of the Lower Wilcox. In the western part of the study area the underlying Yoakum Canyon influenced the Upper Wilcox deposition. Previous authors have asserted that the Yoakum Canyon had its entire 3,000' filled with prodelta muds prior to the progradation of the Upper Wilcox. The paleogrography maps generated by differentiating between marine and terrestrial log signatures for the four distinct units of the Upper Wilcox identify the topographic low area of the Yoakum Canyon that is then filled in sequentially by the sandy units of the Upper Wilcox.

The shoreline locations of each unit help define the topography at their time of deposition. Over the Yoakum Canyon region, the first shoreline is roughly 50km updip from the shoreline further to the northeast. The subsequent shorelines over the Yokaum region prograde down dip, until the last unit, whose the shoreline is roughly in line with the shorelines to the northeast that are relatively constant throughout the roughly four million year episode. In this fashion the shoreline of the Upper Wilcox is stable in the northeast but swings down the region of the Yoakum Canyon through time.

Keywords: Wilcox, Upper Wilcox, Yoakum Canyon, Shorelines, Houston Embayment

SETP
U

Detrital-Zircon U-Pb Geochronologic Constraints on Provenance of Adriatic turbidites (Alps-Apennines system)

lauradafov@gmail.com
Dafov, L., The University of Texas at Austin, Jackson School of Geosciences, Austin, TX, 78712
Anfinson, O., The University of Texas at Austin, Jackson School of Geosciences, Austin, TX, 78712
Malusá, M., University of Milano-Bicocca, Department of Earth and Environmental Sciences, Milano, Italy
Stockli, D., The University of Texas at Austin, Jackson School of Geosciences, Austin, TX, 78712

U-Pb geochronology of detrital zircon is an effective method for evaluating exhumation history, provenance, and depositional age constraints of sedimentary deposits. Over 1400 grains evaluated from thirteen samples collected from distal and proximal Oligo-Miocene strata of Adriatic turbidites are consistent with modern characterization of the proposed source region. Studies indicate that the principal source area of Oligo-Miocene strata from Adriatic deposits is the Lepontine Dome of the Central Alps. Our data reveals a significant shift in detrital zircon U-Pb age populations during the Oligocene-Miocene boundary which, when compared with data from modern sands, closely correlates to the westward shift of the erosional foci within the Lepontine Dome, from the Ticino to the Toce subdome, due to progressive indentation of Adria. This is coeval with progressive unroofing of Periadriatic magmatic rocks of Tertiary age along the Insubric Fault. The lowermost Upper Oligocene proximal samples collected from the Como and Villa Olmo Conglomerates are dominated by Caledonian and Cadomian detrital zircon U-Pb age populations. The uppermost Oligocene and lower Miocene proximal samples collected from the Como Conglomerate are dominated instead by Periadriatic detrital zircon.
Distal samples collected from the Lower Oligocene Aveto Formation have a dominant Periadriatic age peak with lesser amounts of late Cretaceous, Variscan, Caledonian and Cadomian detrital zircon. The lowermost Upper Oligocene distal samples collected from the Macigno Formation contain populations of Periadriatic, Variscan, Caledonian, and Cadomian detrital zircon, with major shifts in relative abundance from the lower to upper strata. The most dramatic shift in provenance in the distal units is between two samples located relatively proximally to one another in the Modino unit: Upper Oligocene marls contains primarily Variscan and Caledonian zircon grains with no individuals yielding Periadriatic ages, whereas the Upper Oligocene – Lower Miocene sandstones of the same unit include dominant Periadriatic and Variscan age populations. The youngest distal sample, from the Lower Miocene Bobbio Formation, primarily contains Variscan detrital zircon ages

Keywords: Detrital Zircon, Apennines, Lepontine Dome, Alps, Italy

PS
LCPHD

Sand transport in Martian craters

mdday@utexas.edu
Day, M., The University of Texas at Austin, Austin, TX
Kocurek, G., The University of Texas at Austin, Austin, TX
Anderson, W., The University of Texas at Dallas, Dallas, TX
Mohrig, D., The University of Texas at Austin, Austin, TX

Aeolian erosion and deposition control the modern Martian landscape. Saltating sands erode bedrock into yardangs, and form extensive dune fields across the planet. These features often occur in craters, the planet's dominant sedimentary basins. Sediment transport in ten representative crater topographies is modeled using large eddy simulation. Comparison between model results and observed Martian craters indicates that craters are temporary depo-centers from which sand is excavated only during high wind events. Sediments accumulate in the crater's downwind interior, often forming dune fields, and are only infrequently removed when wind speeds greatly exceed those required for deposition. Results demonstrate how aeolian sand transport could form a variety of intra-crater morphologies observed on Mars.

Keywords: Mars, aeolian, transport, craters, large eddy simulation,

EG
ECG

An integrated structural and geochemical study of fracture propagation in the Campito Formation of eastern California

natchd@utexas.edu
Doungkaew, N., Bureau of Economic Geology, The University of Texas at Austin, Austin, TX
Eichhubl, P., Bureau of Economic Geology, The University of Texas at Austin, Austin, TX

Fractures control fluid flow, heat transport, and the mechanical properties of the brittle crust. However, mechanisms and rates of fracture growth under subsurface conditions are not well understood. I investigate processes of fracture growth in the Campito Formation in eastern California by combining field structural observations, thin section petrography, fluid inclusion microthermometry, Scanning electron cathodoluminescence imaging, and isotope geochemistry. The lower Cambrian Campito Formation is exposed in a gently south-plunging, asymmetrical anticlinorium in the White Mountains east of Westgard Pass. Opening-mode fractures occur primarily perpendicular to bedding and are partially or completely cemented with quartz. Fractures are either bed-bound, terminating against bed interfaces, or cross multiple layers. First petrographic results suggest that the formation experienced low-grade metamorphic alteration as indicated by the presence of chlorite and sericite. Pressure solution is abundant. Quartz fracture cement forms cement bridges that span both fracture walls and that are interpreted to have formed concurrently with fracture opening. Scanning electron cathodoluminescence imaging is in progress to provide texture maps of the fracture cements. Fluid inclusion and oxygen isotope analysis of the quartz cement in the center and tip regions of fractures will provide information about the temperature at the time of fracture growth and the composition and origin of fluids leading to fracture cement precipitation. In combination with cement texture maps, maps of the fracture cement isotopic composition along the fracture obtained by ion microprobe analysis will allow us to discern changes in temperature or fluid composition during fracture growth and possible provide constraints on the duration and rate of fracture propagation. These results will be compared for bed-bound and through going fractures to determine controls of bedding interfaces on fracture propagation and arrest.

Keywords: fracture, fracture propagation, SEM, CL, Petrology, Stable Isotope, Ion microprobe,

CCG
LCPHD

RESOLUTION AND ACCURACY OF 3 DIMENSIONAL MODELS OF SPECIMENS USING PHOTOGRAMMETRY AND IMAGE STACKING SOFTWARE

englishl@utexas.edu
English, L., Jackson School of Geosciences, The University of Texas at Austin, Austin, TX
Brown, M., Vertebrate Paleontology Laboratory, The University of Texas at Austin, Austin, TX

Photogrammetry is a relatively inexpensive and more portable method of digitizing the three dimensional surface morphology of specimens through the use of digital images from a camera instead of a laser surface scanner. However, when photographing specimens that have considerable depth it can be difficult or impossible to keep the entire specimen in focus in each image, which has the potential to influence how photogrammetry software pieces together the images to build the 3D model. This is particularly challenging in the case of very small specimens, because in order to capture more detail, the specimen must fill the frame of the camera, which requires the camera to be relatively close to the specimen and the closer an object is to the camera, the more narrow the region in focus will be.

Image stacking is a technique whereby multiple images of the same view, but different distances in focus are digitally combined to create a single image with most or all of the object of interest in focus. This technique in conjunction with traditional photogrammetry has the potential to generate three dimensional models with high levels of detail without sacrificing accuracy or requiring large numbers of photographs taken at slightly different angles. However, there is also potential for details to be lost or image misalignments to occur and be amplified when processing images through more steps.

To determine how combining image stacking with photogrammetry influences model reconstruction, models of several objects of known dimensions and varying surface complexity were generated using the same sets of images from the same camera. Models were created of each object first by using photogrammetry software alone and then processing the original images with image stacking software before imputing the files into the photogrammetry software. Models were also constructed using half the number of photographs to compare the differences made by taking more photos from different views vs. the same view from different focal points.

Keywords: photogrammetry, image stacking, methods, 3D data

SHP
LCPHD

Clinoform Growth in a Miocene, Para-Tethyan Deep Lake Basin: Thin Topsets, Irregular Foresets, and Thick Bottomsets

rattanapornf@utexas.edu
Fongngern, R., Department of Geological Sciences, The University of Texas at Austin, TX
Olariu, C., Department of Geological Sciences, The University of Texas at Austin, TX
Steel, R., Department of Geological Sciences, The University of Texas at Austin, TX
Krezsek, C., OMV Petrom S.A. Exploration and Production, Bucharest, Romania

Late Miocene lacustrine clinoforms of up to 400 m thick are mapped using a 1,700 km^2 3-D seismic dataset in the Dacian foreland basin, Romania. Seven Meotian (late-Miocene) clinoforms, constructed by sediment from the South Carpathians, prograded to SW for over 25 km. The individual clinothems show meager, if any, topsets, greatly disrupted foresets and highly aggradational bottomsets. Basin margin accretion occurred in three stages with changing of clinoform heights and foreset gradients. The deltaic system prograded into an *early-stage* deep depocenter with high gradient clinoforms whose foresets were dominated by closely (100-200 m) spaced 1.5-2 km wide V-shaped sub-lacustrine canyons. During *intermediate-stage* growth, 2-4 km wide canyons were dominant on the clinoform foresets. From early to intermediate stages the lacustrine shelf edges were consistently indented. The *late-stage* outbuilding was characterized by smaller clinoforms with smoother foresets and less indentation along the shelf-edge. Truncated and thin topsets persisted through all three stages of clinoform evolution. Nevertheless, the resulting long-term flat trajectory shows alternating segments of forced and low-amplitude normal regressions. The relatively flat trajectory implies a constant base level over time and was due to the presence of the Dacian-Black Sea barrier that limited water level rise by spilling to the Black Sea. Besides the characteristic shelf-edge incision of the thin clinoform topsets and the resultant sediment bypass at the shelf edge, the prolonged regressions of the shelf margin promoted steady sediment supply to the basin and generated long-lived slope sediment conduits that provided sustained sediment transport to the basin floor. Isochrons of the clinothems show that large volumes of sediment were partitioned into the clinoform foresets, and especially the bottomsets. Very thick bottomsets are to be expected due to frequent hyperpycnal flow delivery. Decreasing subsidence over time out from the foredeep resulted in diminishing accommodation and clinoform height, reduced slope channelization and smoother slope morphology.

Keywords: Clinoforms, Lacustrine, Sub-lacustrine canyons

CCG
U

Centennial-scale winter climate variability over the last two millennia in the northern Gulf of Mexico based on paired ?18O and Mg/Ca in Globorotalia truncatulinoides

vfortiz@utexas.edu
Fortiz, V., Department of Geological Sciences, Jackson School of Geosciences, UT Austin
Thirumalai, K., Department of Geological Sciences, Jackson School of Geosciences, UT Austin;Institute for Geophysics, Jackson School of Geosciences, UT Austin
Richey, J., United States Geological Survey, St. Petersburg Coastal and Marine Science Center
Quinn, T., Department of Geological Sciences, Jackson School of Geosciences, UT Austin;Institute for Geophysics, Jackson School of Geosciences, UT Austin

We present a replicated record of paired foraminiferal $\delta^{18}O$ and Mg/Ca variations in multi-cores collected from the Garrison Basin (26º43'N, 93º55'W) in the northern Gulf of Mexico (GOM). Using $\delta^{18}O$ (sea surface temperature, SST; sea surface salinity, SSS proxy) and Mg/Ca (SST proxy) variations in non-encrusted planktic foraminifer Globorotalia truncatulinoides we produce time series spanning the last two millennia that is characterized by centennial-scale climate variability. We interpret geochemical variations in G. truncatulinoides to reflect winter climate variability because data from a sediment trap, located ~350 km east of the core site, reveal that annual flux of G. truncatulinoides is heavily weighted towards winter (peak production in January-February; Spear et al.,2011). Similar centennial-scale variability is also observed in the foraminiferal geochemistry of Globigerinoides ruber in the same multi-cores, which likely reflect mean annual climate variations. Our replicated results and comparisons to other SST reconstructions from the region lend confidence that the northern GOM surface ocean underwent large, centennial-scale variability, most likely dominated by changes in winter climate. This variability occurred in a time period where climate forcing is small and background conditions are similar to pre-industrial times.

Keywords: Globorotalia truncatulinoides, last two millenia, centennial-scale climate variability

MG
LCPHD

Seismic Stratigraphy of Ice Sheet Advance-Retreat Cycles on the Sabrina Coast Continental Shelf, East Antarctica

bruce.c.frederick@gmail.com
Frederick, B., Institute for Geophysics, The University of Texas at Austin, Austin, Tx
Gulick, S., Institute for Geophysics, The University of Texas at Austin, Austin, Tx
Saustrup, S., Institute for Geophysics, The University of Texas at Austin, Austin, Tx
Fernandez-Vasquez, R., Institute for Geophysics, The University of Texas at Austin, Austin, Tx
Domack, E., University of South Florida, St Petersburg, Fl
Lavoie, C., University of Aveiro, Aveiro, Portugal
Blankenship, D., Institute for Geophysics, The University of Texas at Austin, Austin, Tx
Leventer, A., Colgate University, Hamilton, NY
Shevenell, A., University of South Florida, St Petersburg, Fl

2D multichannel seismic (MCS), multibeam and CHIRP data were collected as part of the recent R/V Nathaniel B. Palmer (NBP1402) cruise to investigate the marine record of cryosphere-ocean dynamics on the continental shelf between the Dalton Ice Tongue and Totten Glacier systems. Outlet glaciers and ice shelves along this coastline drain a catchment area extending across the Aurora Subglacial Basin (ASB) whose topography lies below sea level and contains an ice volume of approximately 6.9m of sea level rise equivalent. Analysis of over 750km of high-resolution MCS data has revealed the preservation of extensive tilted fluvial-deltaic shelf sedimentation and the first evidence of polythermal glacial advance in this region with well-preserved subglacial meltwater channels and tunnel valley systems. This expansive fluvial to glacial sedimentary section is separated by a regional unconformity from a series of irregular, localized unconformities preserved in an otherwise seismically transparent facies. We interpret these transparent facies as subglacial diamictites deposited over several glacial cycles. Detailed seismic stratigraphic analysis of the glacial sequences above the regional unconformity identified at least 4 glacial cycles illustrated by grounding zone wedge moraine deposits recorded in both MCS and multibeam bathymetric data. Distinct differences were evident in the stratigraphic architecture of polar versus polythermal glaciations including greater preservation of till deposits above the regional unconformity proximal to the exposed bedrock boundary and the present-day ice front. Sedimentary sequence preservation here appears dictated by the geometry of local ice advance and allied basement structure controls. Integration of marine geology, high resolution CHIRP and multibeam bathymetry data with MCS sequence geometry and acoustic facies mapping has led to improved constraints on rates, styles and patterns of glacial retreat. Such improvements to deformable sediment distribution and lithologic character constraints are critical to numerical ice sheet model flow velocities and potential instability assessments, and continue to advance our understanding of ice sheet dynamics and basal conditions across both heavily fjorded and uniform basement architectures.

Keywords: Antarctica, seismic stratigraphy, Totten Glacier, Sabrina Coast continental shelf

MG
LCPHD

What Controls Landward Vergence of the Accretionary Prism offshore Northern Sumatra?

marina.frederik@utexas.edu
Frederik, M., Institute for Geophysics, The University of Texas at Austin, Austin, TX
Gulick, S., Institute for Geophysics, The University of Texas at Austin, Austin, TX
Austin, J., Institute for Geophysics, The University of Texas at Austin, Austin, TX
Bangs, N., Institute for Geophysics, The University of Texas at Austin, Austin, TX
Udrekh, U., Badan Pengkajian dan Penerapan Teknologi
Duncan, D., Institute for Geophysics, The University of Texas at Austin, Austin, TX

Five 2D MCS seismic profiles transecting the prism from the Sunda Trench to the Aceh Basin along with multibeam data have been used to investigate the structure and wedge morphology offshore northern Sumatra. The study area, 1-7°N and 92-97°E, covers the entire forearc from northwest of Aceh to west of Simeulue Island. The accretionary prism consists of steep outer slopes (5-12°) and a plateau ~100-120 km wide comprised of anticlinal folds of 2-16 km wavelength seaward of a steep slope adjacent to the Aceh (forearc) Basin. The seafloor depths vary from ~ -5 km in the Sunda Trench to < -1 km on the plateau. Analysis of fold vergence along the profiles and areal classification of the predominant vergence reveal three structural zones: 1) predominantly landward-vergent folds near the Sunda Trench, 2) predominantly seaward-vergent folds near the Aceh Basin, and 3) mixed vergent folds between those two zones. Extensive landward vergence is uncommon in accretionary prisms worldwide. One explanation is the existence of a rigid backstop with a seaward dipping edge, such that overlying younger sediments accreted to the prism form landward-vergent folds. We propose a rigid backstop geometry that extends from under the Aceh Basin to under the mixed vergence zone, based on the observed structural zones and published velocity models of this margin. Furthermore, using bathymetric data of before and after the 2004/5 earthquakes, along dip of the prism from the Aceh Basin to the Sunda Trench, we observed two zones of amplitude of depth change. A lower amplitude of change occurs from the Aceh Basin until ~80 km landward of the Trench. A higher amplitude of change occurs ~ 80 km from the trench and continues seaward. Based on our observed structural zones, we observed that the position of amplitude change to coincide with the seaward edge of our proposed rigid backstop.

Keywords: subduction zone, bathymetry, seismic reflection, landward-vergence, Sumatra, backstop

SETP
LCMS

Chronology of Laramide Magmatism and Stockwork Veining in the Red Hills Porphyry Mo-Cu Deposit, Presidio County, Texas

sfreling11@gmail.com
Frelinger, S., The University of Texas at Austin, Austin, TX
Kyle, R., The University of Texas at Austin, Austin, TX
Elliott, B., Bureau of Economic Geology, The University of Texas at Austin, Austin, TX
Gilmer, A., University of Bristol, Bristol, UK
Stockli, D., The University of Texas at Austin, Austin, TX

The Red Hills porphyry Mo-Cu deposit is hosted within a calc-alkaline igneous complex consisting of quartz monzonite porphyry (QMP), quartz latite porphyry (QLP), latite porphyry (LP), and biotite porphyry (BP) which have intruded Permian sandstones, siltstones, and dolostones resulting in an extensive hornfels zone with local garnet skarn. U-Pb ages of zircon from the unaltered QMP and mineralized QMP yielded ages of 62.54 + 0.49 Ma and 66.08 + 0.31 Ma, respectively. Cross cutting relationships between igneous phases at the Red Hills indicate a compositional and intrusive evolution with multiple injections of intermediate magmas in the following order: BP to QMP to QLP to LP. Secondary, shreddy biotite characterizes the potassic alteration and is most prevalent in deep BP dike intercepts, whereas significant overprinting by phyllic alteration has masked the higher temperature alteration in the QMP, QLP, and LP. Biotite-stable assemblages in the QMP occur proximal with the contact of the BP. Chlorite-epidote propylitic alteration occurs above and lateral to the phyllic alteration zone which extends extensively east of the deposit. A specular hematite halo borders the eastern margin of the propylitic alteration zone where the least altered igneous unit crop out. Destruction of pyrite by highly acidic fluids formed a hematite-goethite-jarosite leached cap and supergene alunite and alunite-kaolinite veins. Beneath the leach caps exists a thin transitional copper oxide zone which overlies a weak chalcocite blanket that is developed in intrusive rocks, but local high grade (>10% Cu) intercepts are present in pyritic hornfels.

At least two episodes of molybdenite stockwork mineralization are evident at the Red Hills. Mineralized xenoliths of BP are found in QMP where the second episode of stockwork fractures cut through both units. Early veining began with randomly oriented, discontinuous A-type barren quartz veins cut by B-type quartz-molybdenite (qz-mo+py) veins. The introduction of copper occurred late in the system by the ingress of fluids which formed D-type veins. Hypogene copper sulfide phases such as chalcopyrite, bornite, and covellite occur as inclusions in pyrite within D-veins and are commonly replaced by chalcocite at near surface levels. The latest fluids were enriched in Pb, Zn, Ba, Bi, and Ag as evidence by galena, sphalerite, bismuthinite, and silver-rich inclusions within pyrite and isolated barite grains all within late stage fractures or cavities.

Complex textures of hydrothermal vein quartz revealed by scanning electron microscope–cathodoluminescence (SEM-CL) have been classified by each vein type and the multiple quartz generations therein. With each quartz generation, the CL intensities diminish from bright to dark which correspond to trends in trace element abundances measured by EPMA trace element maps and LA-ICP-MS transects. Bright CL zones correspond to elevated concentrations of Ti, which are quantitatively measured to calculate crystallization temperatures by applying the Titaniq geothermometer. Thus, the Red Hills is a multi-phase intermediate igneous complex in which molybdenite mineralization occurred in earlier, higher temperature B-vein stockwork fractures and copper mineralization occurred in late, lower temperature D-veins which is the reverse sequence of mineralization found in typical porphyry Mo and Cu systems worldwide.

Keywords: Porphyry Mo, stockwork veins, SEM-CL, trace elements

EG
ECG

High Resolution Chemostratigraphic Profile of Austin Area Late Cretaceous Strata

kcgabb@gmail.com
Gabb, K., Bureau of Economic Geology, The University of Texas at Austin, Austin, TX
Rowe, H., Bureau of Economic Geology, The University of Texas at Austin, Austin, TX
Fisher, W., The University of Texas at Austin, Austin, TX
Ruppel, S., Bureau of Economic Geology, The University of Texas at Austin, Austin, TX

Chemostratigraphic analysis of major and trace elements is an important indicator of paleoceanographic conditions, defining times of anoxia in the bottom waters of the greenhouse period Late Cretaceous. This study is focused on further developing the local and regional subsurface stratigraphy of the time equivalent formations located in central Texas, overlying the paleotopographic high of the San Marcos Arch. Twelve shallow drill cores were recovered from the construction site of the AT&T Executive Education and Conference Center located on The University of Texas main campus in Austin, Texas. The cores cover an approximate area of 71,584 ft^2 and preserve intervals initially identified as the Del Rio and Buda formations (early Cenomanian age), late Cenomanian-Turonian Eagle Ford formation, and overlying Austin Chalk formation (Turonian and younger). Four of the most well preserved cores were investigated in further detail using energy-dispersive x-ray fluorescence (ED-XRF) for bulk elemental geochemistry, and two of the four cores were investigated for their mineralogical composition using x-ray diffraction (XRD). A Bruker Tracer-IV-SD ED-XRF was employed to develop core chemostratigraphies at the 3-inch sampling scale, and an Olympus BTX XRD was used to develop mineralogical models at the scale of a few feet. After depth correction (due to topographical differences), a high degree of chemostratigraphic replication is observable between the four cores, permitting sub-foot-scale correlation throughout much of the record. A 174 foot composite chemostratigraphic record combining two of the cores is presented, and will be used to 1) assess spatial variability between the UT campus succession and nearby Austin successions 2) further refine the regional stratigraphy.

The lowest interval in the composite is the Del Rio Formation. This formation is predominately a bluish-gray claystone, mineralogically composed of aluminum (Al) and silica (Si). Two distinct chemofacies are observed, differentiated by the low and high percent content of Calcium (Ca). The redox-indicating element Molybdenum (Mo) is present in minor concentrations (~0.001 ppm) in the Ca low facie. Above the Del Rio is the Buda Formation, lithologically defined as a massive packstone/wackstone limestone consisting of mollusk fragments and green glauconitic spheres. The formation is minerologically dominated by Ca (~40%), but four intervals within the Buda show an increase of Al (~2%) and Si (~5%), which represents and increase in clay content (terrestrial and biogenic). The Buda Formation can thus be broken into two chemofacies. The Eagle Ford Formation unconformably overlies the Buda and is broken into four members locally: the Pepper Shale Member, the Waller Member, the Bouldin Member, and the Southern Bosque Member. The Pepper Shale is identified as one chemofacie (high Si and Al content) and lithologicaly as a massive argillaceous mudrock facie. The Pepper Shale grades upward into the Waller Member, containing two lithological facies termed massive argillaceous foraminiferal mudrocks and laminated argillaceous foraminiferal mudrocks. The chemostragraphic profile reflects these facies, as the Ca content increases in the laminated areas, and decreases in the massive areas. Mo (up to 129 ppm) is also drastically enriched in both these chemofacies. The Bouldin Member consists of three lithological facies, laminated foraminiferal wackestones, laminated foraminiferal packstones, and massive bentonitic claystones. These facies are to be replicated in the chemostratigraphic column. This member also has the highest average concentration of Mo, indicating the highest potential of redox sensitive preservation. The Southern Bosque Member is composed of the same two lithofacies as the Waller Member, and has similar chemostratigraphic facies, with reduced levels of Mo compared to the Bouldin Member. A thick section of Austin Chalk overlies the Eagle Ford-equivalent strata. This lime mudstone/wackestone varies in the amount of bioturbation and 5 intervals show increases Al (~3%) and Si (~9%) concentration. The Eagle Ford Formation is around 10 feet less than the chemostratigraphicaly defined ACC north well, indicating the formation thickens to the north. Hierarchal cluster analysis will be performed to determine elemental composition variations and how these compositions relate in all the

samples. Additional insights will hopefully be drawn from stable isotopic measurements of bulk carbonate and bulk organic matter.

Keywords: Eagleford, Cenomanian, Turonian, Austin Chalk, Buda, Chemostratigraphy

SETP
LCPHD

Stress and porosity in fold and thrust belts system

baiyuan@utexas.edu
Gao, B., Jackson School of Geosciences, The University of Texas at Austin, Austin, TX

We present a large-strain coupled poro-mechanical model to investigate the evolution of stress and pore pressure in fold and thrust belt systems. In the model, a 20 km long and 5km thick sediment layer overlies a frictional boundary ($\mu = 0.6$). We initialize the model with geostatic stress such that the beginning stress ratio of horizontal stress and vertical stress is 0.8. Then the left boundary of the material is subject to displacement at a constant rate (~1mm/yr). A tapered wedge develops as the model proceeds. Compaction is simulated by a Modified Cam Clay soil model to characterize stress and porosity behavior under various mean and differential stresses. As displacement proceeds, the horizontal stress increases until it is limited by the frictional strength of the material ($\mu = 0.43$, ?'=23^o). At final stage, the horizontal stress exceed 2 times of the vertical stress in the accretionary wedge region. The surface slope is about 7^0. We find sediment porosity decreases significantly within the wedge (e.g. from 0.24 to 0.18 at 4kmbsf) due to the increase in horizontal stress. At this condition, the material is in critical state, and any further deformation results in the growth of the tapered wedge at a constant angle. We will also conduct transient numerical model to couple both mechanical and fluid flow processes. We will run cases with different thrust rate and permeability, and then compare the results with drained cases to quantitatively understand the effect of fluids flow on stress and porosity in fold and thrust belt system.

Keywords: stress, porosity, fold and thrust belts

SETP
LCPHD

Origin of the Temporal-compositional Variations in Monogenetic Vent Eruptions: Insights from the Crystal Cargo in the Papoose Canyon Sequence, Big Pine Volcanic Field, CA

ruohan.gao@gmail.com
Gao, R., The University of Texas at Austin
Ramirez, G., The University of Texas at Austin
Lassiter, J., The University of Texas as Austin

Systematic temporal-compositional variations observed in many monogenetic vent eruption sequences (e.g. decreasing incompatible element concentrations, variation in major element and isotopic compositions) may reflect varying extents of crustal contamination (c.f., [1]), or melting and mixing of small-scale mantle heterogeneities (c.f., [2]). During eruption of the Papoose Canyon (PC) monogenetic vent incompatible trace element concentrations decreased a factor of 2, $^{87}Sr/^{86}Sr$ decreased (from ~0.7063 to 0.7055), and $^{143}Nd/^{144}$ Nd increased (from ~0.51246 to 0.51258) (c.f., [2]). Blondes et al. (2008) argued that the relatively primitive melt MgO content and apparent presence of mantle xenoliths in the sequence indicate limited melt storage and crustal contamination prior to eruption, and proposed melting and mixing of two distinct mantle components to explain the variations. However, PC olivine phenocryst compositions (Fo# ~76-89) span a wide range, extending to evolved (low-Fo) compositions, and the vast majority of phenocrysts are more evolved than olivines in equilibrium with the host scoria (Mg# ~87-89). In addition, olivine and clinopyroxene from xenoliths within the early sequence have Mg# (73-87) similar to the phenocrysts, and lower than typical mantle peridotites. Sr-Nd isotopic compositions of the xenoliths are also similar to the early PC lavas, but less enriched than the host melts. Therefore, the xenoliths are most likely cognate xenoliths derived from fractionated PC magmas. Finally, both phenocryst and xenolith olivines have $\delta^{18}O$ values (~5.5 to 5.7 ‰) higher than most mantle peridotites (~5.2 ±0.2 ‰), and clinopyroxene trace element abundances indicate derivation from melts with trace element abundances higher than the most enriched PC lavas. In conjunction, these features suggest that the phenocrysts and xenoliths derive from early PC melts that ponded and fractionated and assimilated continental crust, possibly in crustal sills. These melts were drained and mixed with more primitive melts as the eruption began, and the temporal-compositional trends in part reflect decreasing contaminated sill component over time. These results indicate that even “primitive” melts may contain a significant signature of crustal contamination.
[1] Erlund et al., 2010.
[2] Blondes et al., 2008.

Keywords: Monogenetic vent, geochemistry, crustal contamination

SETP
U

Pseudotachylites in the footwall of the Whipple detachment: implications of seismicity along low angle normal faults

gentrye93@gmail.com
Gentry, E., The University of Texas at Austin, Austin, TX
Behr, W., The University of Texas at Austin, Austin, TX
Wafforn, S., The University of Texas at Austin, Austin, TX

The Whipple detachment fault in E. California is a classic example of a large-displacement (~40 km), low-angle normal fault formed during Miocene Basin and Range extension. The footwall of this fault exhibits a range of mid-crustal rocks deformed near the brittle-ductile transition, including mylonites, cataclasites, and pseudotachylites, which provide insight into mid-crustal rheology from steady-state to seismic strain rates. Here we focus on a diverse array of pseudotachylites discovered in the Whipple footwall that have not been previously described. We examine the structural contexts, morphologies, and compositions of the pseudotachylites and discuss their implications for seismogenesis on continental low-angle normal faults.

Veins that we interpret to be pseudotachylites occur as planar, anastomosing, and reservoir-like injections found along the margins of dikes, along mini-detachments kinematically linked to the Whipple fault, and within a few tens of centimeters below the silicified, erosionally resistant “microbreccia ledge” of the main detachment. The orientations of the vein generation surfaces are dominantly shallowly E-dipping, subparallel to the detachment fault itself; some occur on higher angle normal faults that sole into low angle shear zones. Veins were not found cutting the microbreccia ledge itself, suggesting that comminution and silicification post-dates pseudotachylite formation.

In thin section, the veins exhibit a range in composition and degree of preservation. Some contain lath-shaped spherulites, others contain opaque, microcrystalline matrices with relict flow banding and embayed, primarily quartz clasts. Some pseudotachylite veins grade into cataclasites at their margins, suggesting cataclasis was precursory to vein formation, whereas others cut pristine mylonites with no evidence of earlier brittle deformation. Those that cut pristine mylonites contain clasts with dynamically recrystallized quartz grains with diameters of 5-7 um. This suggests a minimum shear stress for formation of the pseudotachylite veins of 60-80 MPa based on quartz paleopiezometry.

These data provide evidence that the low-angle Whipple fault and associated structures was seismically active at mid-crustal depths.

Keywords: pseudotahylite, Whipple, seismogenesis

SETP
LCPHD

Oxygen Isotope Zoning in Skarn Garnets: Evidence for Spatial and Temporal Fluid Source Variability in the Sierra Nevada and Mojave

mgevedon@utexas.edu
Gevedon, M., University of Texas at Austin
Ryan-Davis, J., Pomona College
Barnes, J., University of Texas at Austin
Lackey, J., Pomona College
Kitajima, K., University of Wisconsin Madison, WiscSIMS
Valley, J., University of Wisconsin Madison, WiscSIMS

Skarns provide insight to the depth, longevity, and dominant fluid regime associated with Sierra Nevada plutonism and Mesozoic magmatism in the Mojave National Preserve, which represent different spatial and temporal exposures of the Mesozoic arc. Skarns from these regions may serve as proxies for intricacies in the fluid source, and have the potential to resolve magmatic flare-ups and relative depths of emplacement.
Both laser fluorination (LF) and secondary ion mass spectrometry (SIMS) $\delta^{18}O$ analyses of garnet from multiple Mojave (Lucerne valley) skarns indicate a strong, early influence of meteoric fluid despite the presence of relatively deep plutonism. LF data from individual whole garnets and garnet chips broken during sample preparation reveal variation from +4.2‰ to -8.8‰ (n = 24), with an average of approximately -4.0‰. The large spread in these LF data suggest that (A) $\delta^{18}O$ reflects an average of varying $\delta^{18}O$ (fluid) compositions spanning multiple garnet growth oscillations; or (B) multiple generations of garnets exist within individual skarns, the growth of each coinciding with changes in the hydrothermal source and composition.
SIMS analysis of two individual Mojave skarn garnets with oscillatory zoning (seen in backscatter electron images) reveal cores with $\delta^{18}O$ values of -9.6‰, internal variations of -9.4‰ to -3.3‰, and crystal rims of -2.2‰ and -2.9‰ (precision ±0.3; 2σ). In general, $\delta^{18}O$ values negatively correlate with andradite compositions, with high andradite zones having lower $\delta^{18}O$ values ([AND + CaTi] compositions range from 100 to 73).
Similar analyses (both SIMS and LF) of garnets from Sierra Nevadan skarns (Tungsten Hills region) show variation in $\delta^{18}O$ values with LF data ranging from 5.4‰ to 6.2‰ (n = 8), with an average of 5.7‰, and an additional 2.7‰ value obtained from a garnet interior. SIMS data show $\delta^{18}O$ compositional variation from 4.0‰ to 5.9‰. Data across the two Tungsten Hills garnets analyzed via SIMS show the range of isotope compositions possible within a single crystal. All data from the Tungsten Hills skarns suggest meteoric water was less influential farther north in the arc, and that major skarn formation was likely the result of pluton-related magmatic fluids. Magmatic fluids would produce garnets with $\delta^{18}O > +6$‰.

Keywords: skarn, garnet, oxygen isotope, Sierra Nevada, meteoric fluid, decarbonation

SETP
LCPHD

Holocene geologic slip rate for the Banning strand of the southern San Andreas Fault near San Gorgonio Pass, southern California

peter.gold@utexas.edu
Gold, P., Dept. of Geological Sciences, University of Texas, Austin
Behr, W., Dept. of Geological Sciences, University of Texas, Austin
Rood, D., AMS Laboratory, Scottish Universities Environmental Research Center
Sharp, W., Berkeley Geochronology Center
Rockwell, T., Dept. of Geological Sciences, San Diego State University
Kendrick, K., Unites States Geological Survey, Pasadena

We present the first Holocene geologic slip rate for the Banning strand of the southern San Andreas Fault in southern California. The southern San Andreas Fault splays into the sub-parallel Banning and Mission Creek strands in the northwestern Coachella Valley, and although it has long been surmised that the Banning strand eventually accommodates the majority of displacement and transfers it into San Gorgonio Pass towards the densely populated Los Angeles Basin, until now it has been uncertain how slip is actually partitioned between these two fault strands. Our new slip rate measurement, critically located at the northwestern end of the Banning strand at the northwestern edge of the Coachella Valley, overlaps within errors with the published rate for the southern San Andreas Fault to the south, measured at Biskra Palms Oasis. This indicates that the majority of southern San Andreas Fault displacement transfers from the southeastern Mission Creek strand northwest to the Banning strand and into San Gorgonio Pass. Our result corroborates the UCERF3 hazard model, and is consistent with most previous interpretations of how slip is partitioned between the Banning and Mission Creek fault strands. To measure this slip rate, we used the B4 airborne LiDAR data to identify the apex of an alluvial fan offset laterally 25 ± 5 m from its source catchment. We calculated the depositional age of the fan using ^{10}Be in-situ cosmogenic exposure dating and U-Th dating of secondary pedogenic carbonate. Exposure dating of surface clasts indicates a fan age of 6.1 +3.0/-2.0 ka (95% C.I.), which is the same within error as the 5.1 ± 0.4 ka (95% C.I.) minimum age indicated by the carbonate dating. These ages are also consistent with the age suggested by the degree of soil development. Exposure dating of sedimentary material from within a soil pit indicated an age of 2.9 ± 0.7 ka (95 % C.I.). This significantly younger age is probably the result of higher nuclide concentrations in sand sized grains, and observation that is becoming commonplace in similar studies in this area. Combining the fan carbonate and clast exposure ages with the offset yields slip rates of <4.9 +1.0/-0.9 ka (95% C.I.) and 4.1 +2.2/-1.5 ka (95% C.I.), respectively. These slip rates are a minimum for the total slip entering San Gorgonio Pass since they do not capture slip transferred away from the Banning Fault to the Garnet Hill Fault. However, when combined with geomorphic observations, it seems likely that only around 20-40% of slip from the southern San Andreas Fault reaches San Gorgonio Pass, with the rest remaining on the Mission Creek Fault, and being transferred to the Eastern California Shear Zone. This result further emphasizes the need for additional measurements of slip rate and earthquake timing along faults in the NW Coachella Valley in order to inform current earthquake hazard models.

Keywords: San Andreas Fault, San Gorgonio Pass, slip rate, Be-10, pedogenic carbonate, exposure dating

SETP
LCPHD

Recovery of dynamic thermal histories recorded by highly damaged zircon with (U-Th)/He

atom.goldsmith@utexas.edu
Goldsmith, A., The University of Texas at Austin, Austin, TX
Stockli, D., The University of Texas at Austin, Austin, TX
Ketcham, R., The University of Texas at Austin, Austin, TX

Zircon (U-Th)/He (ZHe) thermochronometry is an increasingly popular technique for the interpretation of low-temperature thermal histories in a variety of geologic settings. As has also proved the case for apatite, however, accounting for the effect of radiation damage on helium diffusion kinetics is crucial for quantitative interpretation of ZHe data. Over geologic time, the crystal lattice of zircon becomes increasingly disordered due to energy released from the α-decay of U and Th, and the spontaneous fission of ^{238}U. With the growing number of ZHe analyses performed worldwide, many researchers have noted negative correlations between apparent ZHe age and effective uranium concentration (eU = [U] + 0.23[Th], in this context as a proxy for radiation dose) in the form of variations of up to hundreds of millions of years from different zircons separated from the same rock. Furthermore, in some cases these correlations appear to be systematic and to record actual thermal histories, in a similar but opposite fashion to the positive date-eU correlations observed for apatite (U-Th)/He thermochronometry. These data demonstrate that, in settings in which zircon populations have accumulated relatively high and/or highly variable radiation doses, ZHe thermochronometry is capable of recording thermal histories continuously over a range of temperatures and/or multiple thermal events. Unless the relationship between radiation dose and diffusion kinetics is quantitatively known, however, it is impossible to extract thermal history information from these data. It has long been recognized that radiation doses exceeding ~ 2 – 4 x 10^{18} α-decays/g cause sufficient damage to the crystalline structure to increase He diffusivity beyond the point at which the system is a reliable thermochronometer, however a fully quantitative understanding of the potential effects of lower radiation doses has remained elusive.

The ZRDAAM was intended to address this issue and others; these results, however, have only been tested in a limited number of settings. This study seeks to examine more closely the onset and progression of the increase in helium diffusivity associated with high radiation doses, by the characterization of a large number of zircons from different settings which display negative date-eU correlations with a multitude of techniques. To estimate α-radiation dose, we use Raman spectroscopy, which is a well-demonstrated non-destructive technique of measuring disorder in the crystal lattice. To detect and account for heterogeneous U and Th distributions, we use laser ablation ICP-MS pit profiling over the outer ~ 20 μm of each grain. Finally, to determine diffusion kinetics we perform step-heated, fractional loss diffusion experiments on grains selected based on size and relative consistency of parent nuclide distribution down the laser ablation pit. Analyses are performed on zircons from assorted crystalline basement rocks of the Sinai Peninsula, Egypt and from intrusive rocks along a transect from the Hall Peninsula of Baffin Island, Nunavut, Canada. Analyses from both settings yield differences in apparent ZHe age over hundreds of millions of years from single rock samples, and with a clear negative log-linear relationship to eU. Results from diffusion experiments so far have shown a positive correlation between diffusivity and Raman-estimated radiation dose, with doses at least one order of magnitude lower than previously associated with significant diffusivity increases. Furthermore we observe closure temperatures as low as 116 °C (dT/dt = 10 °C/m.y.), as well as significant changes in diffusive behavior occurring at temperatures 540 - 560 °C including decreases in D0/a2 over two orders of magnitude. We believe that the results from these and future experiments will be instrumental in quantitatively understanding the relationship between radiation damage and helium diffusion kinetics in zircon, and in improving our capability to extract complex thermal histories from the zircon (U-Th)/He thermochronometer at high radiation doses.

Keywords: zircon, (U-Th)/He, thermochronometry, radiation damage, Raman spectroscopy

EG
ECG

The Wettability of Shale and Its Relation to CO2 Sequestration

eric.guiltinan@utexas.edu
Guiltinan, E., Department of Geological Sciences, The University of Texas at Austin, Austin, TX
Cardenas, B., Department of Geological Sciences, The University of Texas at Austin, Austin, TX

The wettability of CO2/brine/shale systems is an important factor in quantifying the safe storage capacity of proposed CO2 reservoirs for geological CO2 sequestration. However, to date, direct measurements of CO2/brine/shale wettability have not been conducted. It is believed that muscovite mica, a component of clay, may represent the wettability of shale. In this poster, previous mica studies are compared with direct measurements made on two shale samples using XRCT in simulated capillaries. The shale samples show unique wettability characteristics believed to be the result of different mineralogical composition. This phenomenon cannot be represented by studies on one mineral alone. Further investigations into the wettability of shales with different mineralogical compositions are proposed.

Keywords: Wettability, Shale, CO2, sequestration, geologic sequestration

CCG
ECG

Solar-induced chlorophyll fluorescence climatology based on Global Ozone Monitoring Experiment-2 retrievals

m.halubok@gmail.com
Halubok, M., Jackson School of Geosciences, The University of Texas at Austin, Austin, TX
Yang, Z., Jackson School of Geosciences, The University of Texas at Austin, Austin, TX

Solar energy that is re-emitted at longer wavelengths after having been absorbed by chlorophyll molecules in plants is commonly referred to as solar-induced chlorophyll fluorescence (SIF). Quantum of light absorbed by a molecule of chlorophyll rises its electrons from ground to the excited state, from which the excitation energy can take different pathways. Intrinsically, there are three main de-excitation pathways: photosynthesis, heat dissipation (non-photochemical quenching) and re-emission as fluorescence. All these processes are occurring in competition, so fluorescence yield is higher when less energy is used for photosynthesis purposes or dissipated as heat. As such, SIF is an excellent indicator of photochemistry and non-photochemical quenching efficiency.

This study intends to investigate the patterns and characteristics of solar-induced chlorophyll fluorescence climatology by employing 7-year datasets of satellite observations from Global Ozone Monitoring Experiment-2 (GOME-2_F v25 level 3 data). Satellite-retrieved seasonal values averaged for 2007–2013 period show that high SIF values are found in the Amazon River and Congo River basins throughout the year. However, areas with maximum SIF are located in the eastern part of North America in summer. EOF analysis performed on weekly data suggests that regions with the largest fluorescence variability tend to be situated in central and eastern North America and Europe as well as northeastern China. Using GOME-2 and TRMM (Tropical Rainfall Measuring Mission) datasets we further show that there exists a moderate to strong correlation (r up to 0.61) and no lag period between precipitation and SIF for the majority of study domains. The results of this study may have implications for understanding the mechanism linking solar-induced chlorophyll fluorescence and precipitation.

Keywords: solar-induced chlorophyll fluorescence, precipitation, satellite-based retrievals, Global Ozone Monitoring Experiment

PS
LCPHD

Estimation of Pre-Deformation Bulk Microporosity Using 3D Measurement of Deformed Chondrules in CM2 Murchison

romy@jsg.utexas.edu
Hanna, R., Jackson School of Geosciences, University of Texas at Austin, Austin, TX
Ketcham, R., Jackson School of Geosciences, University of Texas at Austin, Austin, TX

Measurement of meteorite porosity and comparison with the estimated porosity of asteroids based on remote observations has shown that asteroids are significantly more porous than their meteorite analogs. Typically this difference is attributed to asteroid macroporosity, which in turn can influence the interpretation of the asteroid's structural coherency (i.e. "rubble-piles"). But there is also surely a sampling bias as highly porous, friable carbonaceous chondrites are likely not able to survive ejection from the parent asteroid or Earth entry and landing. Therefore, our chondrite collection may not provide an accurate representation of actual asteroid microporosities.

Deformation of chondrules to form foliation in chondrites is thought to occur due to matrix pore collapse and squeezing of chondrules into surrounding pore space. Assuming that deformation is accommodated completely by this pore loss, their departure from an initial sphere (a suitable assumption for chondrules) can be used to estimate the amount of uniaxial shortening. This degree of compaction combined with an estimate of current porosity permits calculation of pre-compaction microporosity.

High resolution X-ray computed tomography (HRXCT) has revealed a prominent foliation defined by the preferred alignment of deformed chondrules in a ~44 g Murchison stone USNM 5487. This HRXCT volume dataset was analyzed with Blob3D to measure the shape and orientation of deformed chondrules by approximating their shape with a best-fit ellipsoid. From these best-fit ellipsoid shapes an average aspect ratio (k) was calculated and the uniaxial shortening (a) estimated as: $a = 1 - k^{-2/3}$, where a=0 represents no shortening.

The average aspect ratio of best-fit ellipsoids to 165 deformed chondrules in USNM 5487 is 1.53, corresponding to a mean uniaxial shortening of 0.25. Using the average Murchison bulk porosity estimate of 22.1% this suggests a pre-compaction porosity of 41.3%. However, two assumptions inherent in this calculation are: 1) the chondrules are incompressible and their deformation is accommodated in two dimensions by squeezing into the surrounding pore space and 2) porosity loss due to chondrules filling pore space during deformation is negligible. Violation of either assumption would result in greater porosity loss; therefore the pre-compaction porosity estimate above represents a minimum.

Keywords: X-ray Computed Tomography, XCT, chondrite, chondrule, porosity

MG
ECG

A First Look at the Wide Angle Refraction Data from the Eastern North American Margin Community Seismic Experiment

jharding@utexas.edu
Harding, J., The University of Texas Institute of Geophysics, Austin, TX
Van Avendonk, H., The University of Texas Institute of Geophysics, Austin, TX
Hayman, N., The University of Texas Institute of Geophysics, Austin, TX

The Eastern North American Margin (ENAM) Community Seismic Experiment is an ongoing effort to seismically image the lithosphere across the margin using onshore and offshore, broadband and short-period seismic data. The offshore wide-angle reflection data was collected in September and October of 2014. The ENAM data has the potential to constrain the scale of lithospheric deformation and magmatism during early rifting and seafloor spreading history. The offshore short-period ocean bottom seismometers were deployed on four intersecting transects, each approximately 400 km long. A first inspection of wide-angle refractions in these data reveals that the seismic wave speeds in the mantle are higher parallel to the Blake Spur magnetic anomaly than perpendicular to this anomaly. This observation is consistent with the azimuthal anisotropy of continental rift zones. In contrast, the seismic anisotropy pattern produced at mid-ocean ridges is very different, as the highest seismic wave speeds are usually oriented in the spreading direction, perpendicular to the magnetic anomalies. This suggests that a margin-parallel mantle fabric formed beneath the Blake Spur Magnetic during continental rifting, and that it was not affected by later seafloor spreading in the early Atlantic Ocean. This preliminary observation is consistent with an eastward ridge jump during the Jurassic, causing the distal part of the West African rifted margin lithosphere to be left behind offshore the eastern U.S, where it forms the Blake Spur magnetic anomaly.

Keywords: marine seismology, tectonics and magmatism, Eastern North American Margin, rift jump

SETP
LCMS

Coupled bedrock and detrital thermochronometry of a hyper-extended continental margin, Mauléon Basin, Western Pyrenees

hartnic4@utexas.edu
Hart, N., Jackson School of Geosciences, The University of Texas at Austin, Austin, TX
Stockli, D., Jackson School of Geosciences, The University of Texas at Austin, Austin, TX, Institute for Geophysics, The University of Texas at Austin, Austin, TX
Lavier, L., Jackson School of Geosciences, The University of Texas at Austin, Austin, TX, Institute for Geophysics, The University of Texas at Austin, Austin, TX
Hayman, N., Jackson School of Geosciences, The University of Texas at Austin, Austin, TX, Institute for Geophysics, The University of Texas at Austin, Austin, TX

Continental rifting is a major plate-tectonic process resulting in ocean basins and most of the world's passive margins. Although McKenzie (1978) provided a time-tested model for the cooling and subsidence of rifted margins, discrepancies exist between observations and what the model predicts. It also does not account for spatial-temporal complexities in sedimentation, faulting, and heat flow that occur during the evolution of rifting from stretching to lithospheric necking, exhumation and continental break-up. In order to constrain the proximal to distal tectonic, stratigraphic and thermal evolution of rifted continental margins, bedrock and detrital zircon (U-Th)/He (ZHe) and zircon U-Pb dating techniques were applied to the Mauléon basin of the Western Pyrenees. This non-magmatic, asymmetric, hyper-extended rift basin formed during the Early Cretaceous. To accommodate crustal stretching, the South Mauléon Detachment (SMD) formed during the late Aptian, exhuming upper crustal material. Extreme thinning and hyper-extension in the mid-Albian allowed for the formation of the North Mauléon Detachment (NMD), which exhumed middle to lower crust and mantle. During Paleogene contraction Pyrenean thrusting lead to the inversion of the Mauléon basin as a tectonic pop-up block. The North Pyrenean Frontal thrust system and the Igountze-Mendibelza thrusts accommodated most of the shortening and allowed for preservation of pre-, syn- and post-rift structures in the minimally deformed Mauléon basin.

The proximal rift margin in the south is primarily composed of bedrock with Pan-African zircon U-Pb signatures with main age peaks at 550-700 Ma and 900-1,050 Ma. In contrast, the distal rift margin in the north is composed of exhumed lower crustal material, which has a similar Pan-African signature but with additional Variscan (Permian) overgrowths. Syn- to post-rift deposits were analyzed to determine how sedimentation varied during progressive rifting. Detrital zircon signatures of syn-rift deposits indicate compartmentalized, local sourcing from the bedrock in the south and the exhumed lower crust in the north. Late syn- to post-rift deposits indicate a shift to non-compartmentalized, regional sourcing from the proximal rift margin and hinterland.

ZHe data shows preservation of pre-rifting and rifting ages, 90-250 Ma, in structurally high bedrock and basin units of the proximal rift margin. The distal rift margin to the north records 30-80 Ma ages, which suggests the distal margin was in excess of 180°C from syn- to post-rift times until exhumation due to Pyrenean deformation. Thermal modeling of these ages reveals geothermal gradients as high as 80°C/km during syn-rift times.

Through this study we have shown that the evolution of the proximal margin during the progression of rifting has distinct differences from the evolution of the distal margin. Although the spatial-temporal variations occurring during rifting can be complex; with strategic sampling and analytical work these histories can be understood and put into the larger framework of increasing our understanding of rifting evolution and constraints.

Keywords: Pyrenees, Zircon, U-Pb, (U-Th)/He, Double-dating, Extensional tectonics

EG
LCPHD

Depositional and Diagenetic Controls on NMR Pore-Size Distribution in Grain-Dominated Carbonates from Lower Cretaceous Sligo Ooid Shoal Complex, Frio County, South-Central Texas

ahahassan@utexas.edu
Hassan, A., Jackson School of Geosciences, The University of Texas at Austin, Austin, TX
Loucks, R., Bureau of Economic Geology, The University of Texas at Austin, Austin, TX
Kerans, C., Jackson School of Geosciences, The University of Texas at Austin, Austin, TX

Despite their volumetric significance to hydrocarbon production globally, adequate characterization of carbonate pore networks remains a complex problem. A key factor contributing to this challenge is the intimate juxtaposition of pores varying considerably in size within the same geological facies. Understanding the effects of pore-size variations on production-governing properties (i.e., permeability) and linking that to geological processes of deposition and diagenesis are not well-understood. In this study, we aim to address this issue through two objectives (1) establishing pore-size classification based on Nuclear Magnetic Resonance NMR measurements and (2) investigating the depositional and diagenetic processes that cause the transformation of one pore-size class into another. Potential implications of our findings include the predictability of rock fabrics and their reservoir quality from NMR well-logs.

This study focuses on ooid-shoal complexes of Lower Cretaceous Sligo Formation in Frio County, South Texas. We use 20 core plug samples collected from two wells. To quantify pore-size distribution, we fully saturate the plugs with brine and then measure the NMR relaxation time T_2. T_2 is directly proportional to pore space; larger pores result in higher values of T_2.To study rock fabric, we use plain light and fluorescence microscopy on 20 polished thin-sections. On the basis of NMR, we establish a pore-size classification scheme. Each pore-size class is characterized by a dominant T_2 peak that varies at least by one order of magnitude from the other group. Further, the dominant T_2 peak characterizing each group must constitute at least 60% of the total measured porosity.

Our findings show that NMR T_2 measurements display three distinct pore-populations which we interpret as macropores (T_2 mode >100 ms), micropores (10 ms≤T_2 mode≤100 ms), and nanopores (T_2 mode<10 ms). We classify the studied samples into Group I: Strong bimodal porosity consisting of macro- and micropores, Group II: Micropore-dominated samples, and Group III: Nanopore-dominated samples. Group I display good reservoir quality having a porosity and permeability ranges of 6.0-17% and 0.1-10 md, respectively. The good reservoir quality of this group is produced by the presence of interparticle macropores forming between ooids and mollusk fragments and exhibiting minor to moderate cementation by blocky calcite spar. Reservoir quality shows a pronounced degradation in Group II samples with porosity and permeability ranges of 5.2-7.6% and 0.02-0.23 md, respectively. Using UV-light microscopy, we found that the distribution of micropores is associated with ooids, miliolids, and peloids. Further, micritic envelopes represent an important contributor to micropores. Highly microporous micritic envelopes exist around elongate fragments of bivalves and other mollusks. Group III displays the poorest reservoir quality with porosity and permeability ranges of 2.0-2.7% and 0.01-0.02 md, respectively. Group III samples are characterized by extensive chemical compaction in the form of stylolites as well as textures of mud-dominated packstones.

Keywords: Carbonates, Pore-Size Distribution, Nuclear Magnetic Resonance (NMR)

EG
ECG

Chemostratigraphy, lithofacies and depositional environment of the Upper Cretaceous Buda Formation, Dimmit County, Texas

chrishendrix@utexas.edu
Hendrix, C., Bureau of Economic Geology, The University of Texas at Austin, Austin, TX
Loucks, R., Bureau of Economic Geology, The University of Texas at Austin, Austin, TX
Rowe, H., Bureau of Economic Geology, The University of Texas at Austin, Austin, TX

The Buda Formation of South-Central Texas is a biomicritic lime wackestone that represents the drowned shelf environment of the Comanche platform before deepening in the Late Cenomanian. The Buda overlies the Early Cenomanian Del Rio Formation conformably and underlies the Late Cenomanian-Early Turonian Eagle Ford Formation unconformably. The latter boundary defines a major sea-level transgression. Geochemical data were collected from 164 ft of drill core containing the Eagle Ford, Buda and Del Rio formations from Dimmit County, Texas. A Bruker Tracer handheld XRF (x-ray fluorescence) unit was used to analyze the major (Mg-Fe) and trace (V-U) elemental composition of the core at two-inch intervals (976 samples). Powder samples were extracted from the core at 1 ft intervals and examined with an Olympus bench top XRD (x-ray diffraction) machine for their mineralogical composition. Unique samples showing high Mg values (up to 8%) were drilled and analyzed to determine dolomite composition (175 total XRD samples).

Quantitative geochemical data are integrated with lithological interpretation of the core to provide greater context for understanding the paleoceanographic conditions in which the Buda Formation and bounding strata formed. ?, which largely ranges from 30-40% in the Buda succession, is used as a calcite proxy. A stoichiometric conversion shows the Buda is comprised of 3-100% calcite with most samples in the 90-100% range. Preliminary elemental data show an intermittent disruption of the calcite-dominated matrix by Si- and Al-rich intervals that correspond to thin (0.25 – 3 in) mudflow layers in the core. Al/K ratios are used as a proxy for argillaceous input and these data support the contention that the drapes are dominated by clay minerals. An increase in Fe at the base of the core is consistent with visible pyritization in the Del Rio section. Above-average Mg values are observed at irregular depths likely due to dolomitization of the limestone matrix. Significant trace metal constituents representative of anoxic conditions at time of deposition are mostly confined to the lower Eagle Ford sediments. The presence of heavy bioturbation and absence of redox-sensitive metals suggest that the Buda Formation was deposited under oxygenated conditions.

Keywords: Buda, Cretaceous, Chemostratigraphy, Geochemistry, Comanche Platform

SETP
LCPHD

Timing and signatures of fluid alteration in magnetites, Syros, Greece

emilyhgoldstein@utexas.edu
Hernandez Goldstein, E., The University of Texas at Austin, Austin, TX
Stockli, D., The University of Texas at Austin, Austin, TX

Fluid alteration of the mantle is a ubiquitous process that occurs under a range of physical conditions that are closely linked with temperature, pressure, oxygen fugacity and silica activity. Furthermore, the hydration of ultramafic rocks has a fundamental influence on rheology by lowering the strength and density, and chemical recycling, especially at the interface between mantle and crustal material. Although the chemical and physical reactions of this alteration are well studied, the timing of different events remains challenging or impossible to ascertain. We provide a novel approach to unravel multiple fluid alteration events by coupling magnetite trace element analyses and (U-Th)/He dating. The Kampos Melange in Syros, Greece is a natural laboratory to test the competence of this method due to its multi-stage metamorphic history and sample quality. The high-pressure, low-temperature subduction complex is composed of sedimentary, mafic and ultramafic lithologies subducted and metamorphosed in the Eocene at high pressure, low temperature (HPLT) conditions, then exhumed to shallow crustal levels in the Miocene and most recently cut by Pliocene high angle normal faults. The mélange matrix is composed of serpentinite and chlorite schists, or "hybrid" rocks that form from the transfer of elements at the interface between subducting oceanic crust and mantle through fluid interaction. Trace elements reveal chemical differences that identify three populations of magnetite, associated with different alteration signatures: 1) blackwall alteration, 2) serpentinization and 3) talc-overprinting. Stage 1 occurs exclusively in the chlorite schist. Magnetites from these rocks record blackwall fluid alteration of crustal material, with trace amounts Cr or Ni indicating little-to-no mantle contribution. Magnetite He ages from this sample record regional exhumation from HPLT subduction in the Miocence (14 ± 5 Ma). In contrast, in the serpentinite-talc magnetites high Cr and Ni verify alteration of ultramafic material. Trace elements distinguish two magnetite populations within this sample, associated with two alteration stages. Stage one records magnetite growth during serpentinization, while stage two records talc alteration. Magnetite ages from this sample are interpreted to record high angle normal faulting in the Pliocene (4 ± 1 Ma). These results are the first to use magnetite to date alteration in ultramafic systems. The ability to fingerprint magnetite formation from serpentinization and subsequent overprinting has great potential to investigate the timing of talc or carbonate overprinting in geologic settings worldwide.

Keywords: magnetite, thermochronology, fluid alteration, subduction, Syros

CCG
LCMS

Physical and geochemical response in cave drip waters to recent drought, central Texas, USA: Implications for drought reconstruction using speleothems

hulewicz@utexas.edu
Hulewicz, M., The University of Texas at Austin, Austin, TX
Banner, J., The University of Texas at Austin, Austin, TX
Casteel, R., The University of Texas at Austin, Austin, TX

Present-day variations in climate, such as drought, influence the physical and geochemical characteristics of cave drip waters. These changes in water chemistry, water flux, and climate through time may be preserved in cave calcite formations (speleothems). In 2011, a record drought began in central Texas, presenting an opportunity to assess the physical and geochemical response of cave drip waters. As part of a long-term cave monitoring study, drip water samples from eight sites in a cave on the Edwards Plateau were collected every 3 to 6 weeks before, during, and after the peak of the 2011 drought and analyzed for major and trace element concentrations. Physical parameters such as calcite growth rate, drip rate, and cave-air CO2 were also monitored.

We compare time series of the Palmer Drought Severity Index (PDSI) with time series of drip rate, calcite growth rate, and water composition. The drip sites show a range of response to drought by these parameters and only some sites record drought via elemental ratios and growth rate. Both drip rate and drip water elemental ratios (Mg/Ca and Sr/Ca) provide insight into water residence time and flow paths within the vadose zone. All sites show some correspondence between drip rates and PDSI and three of the eight have a statistically significant relationship (r^2=0.29-0.58, $p<0.001$). Mg/Ca and Sr/Ca ratios for four out of eight drip sites were higher during drought than during wet periods, consistent with longer residence times and, as a result, more water-rock interaction during droughts. Calcite growth rates of fast dripping sites (mean drip rate greater than 4.5 mL/min) demonstrate a long-term decrease in response to drought. The complexity of drip site response is likely a consequence of the combined effects of prior calcite precipitation (PCP), water-rock interaction, seasonal ventilation of cave-air CO2, and water flux in the vadose zone. The results of this study improve our understanding of variations in the modern cave system due to drought and have implications for selecting speleothems as paleo-drought proxies.

Keywords: drought, cave drip water, trace elements

EG
LCMS

AVO Modeling of P-P, P-SV and SV-P Multi-component Seismic Wave Modes, Andrews, Tx

ileri_1@hotmail.com
Ileri, S., MS

The Wolfberry system of the Midland Basin is composed of Lower Permian rocks of Wolfcampian and Leonardian age. The Wolfberry play includes not only reservoir rocks but also source rocks in lower Permian successions. Lower Permian rocks, from the top to the bottom are Spraberry, Leonard, and Wolfcamp intervals. AVO modeling is examined on 3D multi-component seismic volumes (P-P, P-SV & Sv-P) at different depths to evaluate hydrocarbon potentials in Spraberry and Wolfcamp formation units. In contrast, Wolfcamp formations are dominated by calcareous rocks and has a few siliciclastic intervals. Specifically Wolfcamp formation reflectors have given more promising gas potentials according to P-P & P-SV wave mode analysis.

Keywords: AVO, P-P, P-SV, SV-P, multi-component seismic

SETP
ECG

Fine Resolution Analysis of Lake Malawi Sediment Record Shows No Significant Climatic Impacts from the Mount Toba Super-Eruption of ~75ky

lilyjackson@email.arizona.edu
Jackson, L., University of Texas at Austin
Stone, J., Indiana State University
Cohen, A., University of Arizona

Debate over long, and short-term climatic impacts of the Mt. Toba super-eruption circa 75ky is often focused on East Africa. A severe drop in anatomically modern human populations has been hypothesized to be synchronous with a volcanic winter caused by the Toba super-eruption. If the Toba eruption caused a volcanic winter in East Africa, climatologically-sensitive ecosystems, such as Lake Malawi and its immediate watershed should show a direct and observable response in the sediment record. Cooler temperatures would cause a reduction of density contrast between epilimnion and hypolimnion waters, allowing for increased mixing and oxygenation of normally anoxic bottom waters. Enhanced mixing would cause noticeable changes in lake fly and algal communities. Cooler temperatures might also affect precipitation and the fire regime in the surrounding watershed. We analyzed two Lake Malawi cores at the finest practical resolution. Core 2A-10H-2 was analyzed in less than 6-year intervals and core 1C-8H-1 in 7-year intervals surrounding the Youngest Toba Tephra (YTT) for microfaunal abundance and variability, sediment composition, and evidence of changes in the occurrence of fires or watershed precipitation. Our analysis included point counts of diatoms and other algae, lake flies, charcoal, and siliciclastics. Changes in microfossil assemblage, variability, and abundance, as well as sediment composition around the YTT in Core 2A and 1C do not indicate that increased mixing or cooler temperatures occurred in either the central or northern basins of Lake Malawi. Similarly, charcoal counts do not suggest a change in fire regime. Our results indicate that at a subdecadal scale there was no substantial response in Lake Malawi or its immediate watershed to the Mt. Toba super-eruption, in contrast to predictions from the volcanic winter hypothesis.

Keywords: Lake Malawi, Toba, volcanic winter, east Africa

CCG
LCPHD

Radiative impacts of Middle East dust on Indian summer monsoon

jinqj05@gmail.com
Jin, Q., Jackson School of Geosciences
Yang, Z., Jackson School of Geosciences
Wei, J., Jackson School of Geosciences

Using the Weather Research and Forecasting model with online chemistry, the radiative impacts of Middle East dust aerosols on the Indian summer monsoon rainfall was studied. Eight numerical experiments were conducted to take into account uncertainties related to dust-absorbing properties, various assumptions used in calculating aerosol optical depth (AOD), and various radiation schemes. In order to obtain reasonable dust emission, model-simulated AOD and radiation forcing at the top of the atmosphere were compared with multiple satellite- and surface-based observations. Consistent with observations, modeled results show heavy dust loadings in the Arabian Peninsula and Pakistan, which can be transported through long distance to the Arabian Sea and the Indian Peninsula. By heating the atmosphere in the lower troposphere centered over the Iranian Plateau, these dust aerosols result in strengthened Indian summer monsoon circulations, which in turn transport more water vapor to the Indian Peninsula. The model shows that northern India becomes wetter during the monsoon season in dust cases than non-dust cases. Further observational analyses show an increasing trend in AOD over the Arabian Peninsula, which corresponds to an increasing trend of rainfall in northern India during summer monsoon seasons from 2000 to 2013. These observed trends of AOD and rainfall are consistent with the model-simulated positive relationship between Middle East dust and Indian summer monsoon rainfall. Our results highlight long-term (decadal) impacts of Middle East dust aerosols on the Indian summer rainfall.

Keywords: dust aerosol, Middle East, Indian summer monsoon

SHP
ECG

Architecture of a Delta Prograding on a Mobile Substrate

eunsil.jung@utexas.edu
Jung, E., Department of Geological Sciences, The University of Texas at Austin, Austin, TX
Kim, W., Department of Geological Sciences, The University of Texas at Austin, Austin, TX

Deposition of deltas on mobile substrate shows difference subsurface architectures from the deposition on a rigid basement. Sediment deposition experiments on a mobile substrate are important to understand distinguished process and stratigraphic patterns of deposition. Previous experimental studies have revealed the overall qualitative changes in surface topography of mobile substrate and progradation rate of the delta. What still remains to be explored are the differences between fluvial internal processes and stratigraphy of delta developed on a rigid basement and a mobile substrate, and in-depth studies for the mobile substrate movement as a delta advances. We performed a series of experiment to understand the salt deformation and stratigraphy of delta evolving on a mobile substrate. All of the runs had constant sediment and water discharge, but the mobile substrate thickness and water depth varied from 0 cm to 2 cm and from 1 cm to 2 cm, respectively. The experimental results provided insight into understanding delta depositions with mobile substrate underneath. The existence of mobile substrate likely played roles in controlling surface morphology and stratigraphy of delta. During the delta progradation on rigid basement, channels on the delta plain showed radial distribution and typical progradation and aggradation internal structural pattern. On the other hand, repetitive scouring and deposition occurred on the delta, which is prograding on mobile subsidence, showing elongated entire feature to basinward while mobile substrate creates more room for sediment to accumulate. Moreover, the polymer lying underneath the delta deformed into an undulatory surface and influenced to the internal stratigraphy during syn- and post- deposition of deltas.

Keywords: Delta, Salt, Mobile substrate

EG
LCPHD

Structure-constrained acoustic impedance using stratigraphic coordinates

paryparsian@gmail.com
Karimi, P., Bureau of Economic Geology, The University of Texas at Austin, Austin, TX

Acoustic impedance is the result of conversion of seismic traces to a reflection coefficient time series, and then into acoustic impedance. Different methods exist for the transformation of post-stack seismic data into impedance , but the assumption behind all these methods is that seismic traces can be modeled using the simple convolutional model. According to the convolutional model, a seismic trace is a normal-incidence record, which is an assumption that is strictly true only if the earth structure is composed of horizontal layers. In the presence of dipping layers, such an assumption is violated, which introduce bias in the result of impedance inversion. I propose to implement impedance inversion in the stratigraphic coordinate system, where the vertical direction is normal to reflectors and seismic traces represent normal-incidence seismograms. Tests on field data produce more accurate and detailed impedance results from inversion in the stratigraphic coordinate system, compared to impedance results using the conventional Cartesian coordinate system.

Keywords: Impedance inversion, convolutional model

SHP
ECG

Transport of Solutes in Hyporheic Zones with Temperature-Dependent Reversible Sorption

mhkaufman@gmail.com
Cardenas, M., Department of Geosciences, The University of Texas at Austin, Austin, TX
Zheng, L., Department of Geosciences, The University of Texas at Austin, Austin, TX

One of the most important processes impacting the mobility of heavy metals in rivers and their hyporheic zones is reversible sorption to sediment. Reversible sorption has been shown to be a temperature dependent process, however the impact of this variability on heavy metal fate and transport, as well as environmental metal concentrations, has not received much attention. In this study we used zinc as an example heavy metal. Previous studies of the impact of temperature on the sorption of zinc on a goethite substrate show a change in partitioning coefficient and thus retardation factor of 10 to over 60 percent with a temperature change from 10 to 25*C, depending on concentration of dissolved zinc in the water. This relationship was extrapolated to estimate the change in reversible sorption of zinc on silicate sand. This change was then utilized within a finite-element model coupling hyporheic fluid flow in porous media with heat transfer and solute transport with reversible sorption to explore the ways in which variations in surface water temperature over varying timescales can drive changes in both zinc sorption and dissolved zinc fluxes at the bedform scale. These linked processes are of fundamental importance when considering the number of different ways in which surface water temperatures can be varied through both human and non-human activities.

Keywords: hyporheic, transport, porous, metal

SHP
LCMS

Architecture and Evolution of Submarine Fans Coupling With High Sediment-Supply Shelf-Margins: Maastrichtian Washakie Basin, Wyoming

woongmo.koo@utexas.edu
Koo, W., Jackson School of Geosciences, The University of Texas at Austin, Austin, TX
Steel, R., Jackson School of Geosciences, The University of Texas at Austin, Austin, TX
Olariu, C., Jackson School of Geosciences, The University of Texas at Austin, Austin, TX
Kim, W., Jackson School of Geosciences, The University of Texas at Austin, Austin, TX

The linkage between relative sea-level change, architecture, and spatio-temporal evolution of Maastrichtian basin-floor fans in Washakie Basin, Wyoming has been investigated at the scale of beds, lobes, lobe complexes, and submarine fans using 3 cores and 630 wireline logs. The bottomset deposits of basin-scale clinothems 9 and 10 form lobate shapes on toe-of-slope and basin floor. The fan lobe complex is about 28 km long, 15 km wide, and 21 m thick.
The lobe complex is weakly developed during the early period indicating minor sediment volumes delivered to deep-water. During the main depositional phase, the lobe complexes of Clinothem 9 aggraded without strong lateral migration via fixed slope-channels in concert with a highly aggradational shelf-edge during relative sea-level rise. In contrast, the deep-water lobe complexes of Clinothem 10 prograded continuously coeval with shelf-edge progradation and slight sea-level fall. The depocenters of lobe complexes were laterally switched by compensational stacking and slope-channel avulsions. During the late development of both clinothems, the deep-water lobe complexes became smaller or retreated concurrent with shelf flooding.
At lobe scale, amalgamated channels, channel-levees, and muddy deposits are recognized in the axis, fringe, and distal fringe of lobes respectively. The channels are identified from the gamma-ray motifs, channel-levees from the repetition of thin and thick beds, and the muddy distal fringe of lobes from the high gamma ray. The core study shows that channelized lobe axes have amalgamated structureless or weakly flat-laminated sandstone beds with erosional surfaces and mud clasts, whereas levees are composed of thin ripple cross-laminated sandstone beds, interlayered with silt and mud. Mud with silt laminae and hybrid beds with soft deformation are deposited in distal fringe of lobes.
Washakie Basin deep-water fan-lobe complexes 1) are composed of amalgamated channel-levee systems connected to slope-channels; 2) evolve through stages of initiation, aggradation, progradation, and retreat. The lobe complex stages and switching of deep-water depocenters are linked to coeval shelf-edge trajectory changes between successive maximum flooding events on the shelf. Linkage of lobe-complex stacking pattern with shelf-edge behavior was possible because Washakie Basin had constantly high sediment discharge to deep-water fans despite significant sediment reworking of shelf-edge deltas by waves and tides.

Keywords: shelf-edge trajectory, deep-water fan-lobe complex

CCG
LCPHD

Snow radiance assimilation over North America

yhkwon@utexas.edu
Kwon, Y., Jackson School of Geosciences, The University of Texas at Austin, Austin, TX
Zhao, L., Jackson School of Geosciences, The University of Texas at Austin, Austin, TX
Yang, Z., Jackson School of Geosciences, The University of Texas at Austin, Austin, TX
Hoar, T., The National Center for Atmospheric Research, Boulder, Colorado
Toure, A., Hydrological Sciences laboratory, Code 617, NASA GSFC, Greenbelt, MD; Universities Space Research Association (USRA), Columbia, MD
Rodell, M., Hydrological Sciences laboratory, Code 617, NASA GSFC, Greenbelt, MD
Picard, G., UJF – Grenoble 1/CNRS, UMR5183, Laboratoire de Glaciologie et Géophysique de l'Environnement (LGGE), Grenoble, France

Snow is a critical component of the global energy and water balances, in particular at middle to high latitudes, because of snow's high albedo, low thermal conductivity, and water holding capacity. Data assimilation has been an important tool to obtain the distribution of snow depth and snow water equivalent (SWE), which are critical for climate and water resource applications. In previous studies, passive microwave (PM) radiance assimilation (RA) has shown promise for improving SWE estimations at point, local, and basin scales. In this study, we aim to address the feasibility of RA to improve SWE estimates at the continental scale. We use the Community Land Model version 4 (CLM4) for snow dynamics and the Dense Media Radiative Transfer–Multi Layers model (DMRT-ML) for snowpack brightness temperature (T_B) estimations. Atmospheric and vegetation radiative transfer models (RTMs) are also incorporated to consider the effects of atmosphere and vegetation on T_B at the top of the atmosphere. We assimilate the Advanced Microwave Scanning Radiometer?Earth Observing System (AMSR-E) T_B observations at 18.7 and 36.5 GHz vertical and horizontal polarization channels into the coupled CLM4/DMRT-ML using the Data Assimilation Research Testbed (DART) developed by the National Center for Atmospheric Research (NCAR). The RA results over North America are compared with the Canadian Meteorological Centre (CMC) and Snowpack Telemetry (SNOTEL) SWE data.

Keywords: Snow water equivalent, Radiance assimilation, Brightness temperature, Community Land Model, Radiative transfer model, Data Assimilation Research Testbed

SETP
LCMS

Patterns in fold-related brittle deformation using quantiative field data from the San Rafael Swell, central Utah

peter.laciano@utexas.edu
Laciano, P., Jackson School of Geosciences, The University of Texas at Austin, Austin, TX
Marrett, R., Jackson School of Geosciences, The University of Texas at Austin, Austin, TX

The San Rafael Swell is a Laramide uplift located in central Utah. Unlike similar uplifts farther east in Colorado, the overlying sedimentary units have not been eroded away and thus they preserve a record of Laramide strain and, most importantly for this study, fold-related deformation. The Swell is bounded on the east by a 70 km long monocline, a fault-propagation fold best modeled by trishear (Erlsev, 1991). The fold is an ideal natural laboratory for studying brittle deformation associated with folding. A highly resistant limestone member of the Carmel Formation is exposed at the surface along the length of the monocline and records substantial brittle deformation. Because the lithology of this member does not change substantially where it outcrops in the Swell, changes in brittle structures observed should be due predominantly to changes in structure. Furthermore, this limestone member is exposed outside of the fold, so I can determine which structures are pre- and post-folding and which are related strictly to folding.

During my six weeks in the field, I collected quantitative scanline data for brittle structures in the Carmel at 19 locations, which I will use to analyze how brittle deformation changes relative to the fold. I will calculate structure intensity, strain, and other benchmarks for each structure set to perform this analysis. Brittle structures observed in the field include veins, tectonic stylolites, small displacement conjugate faults as well as much larger displacement reverse faults. I hypothesize that both magnitude of folding (using bedding dip as a proxy) and structural domain (i.e. forelimb, synclinal hinge, monoclinal limb, anticlinal hinge, and backlimb) will each have a unique influence on brittle deformation. Brittle structures have a significant influence on bedrock permeability and thus understanding their intensity and spatial arrangement has important implications for any application related to fluid flow such as hydro- and petroleum geology.

Keywords: folds, faults, Laramide, field, brittle, fractures, limestone, strain

PS
LCPHD

Heterogeneity of Radar Reflection Power: Implications for the NPLD Climate Record

dlalich90@gmail.com
Lalich, D., University of Texas Institute for Geophysics
Holt, J., University of Texas Institute for Geophysics

The Martian polar caps are thought to represent a detailed history of the planet's late Amazonian paleoclimate. In particular, the North Polar Layered Deposits (NPLD), which are comprised of many sub-parallel layers of water ice with varying dust content, are thought to contain a climate signal related to the hydrologic cycle of Mars. Many internal reflections are visible in radar sounding data from the Shallow Radar (SHARAD) instrument on the Mars Reconnaissance Orbiter (MRO), presumably resulting from variations in dust content with depth. Some have sought to use these reflectors in concert with other data sets to reconstruct Martian paleoclimate conditions, based on the assumption that they record a cyclical process of ice and dust deposition and ablation. In these reconstructions, it is assumed that reflectors are spatially homogeneous and their physical properties are dominated by a global climate signal. However, recent investigation indicates that NPLD surface and subsurface reflectors exhibit different reflective properties from one location to another. This heterogeneity calls into question the validity of the assumption that reflectivity is dominated by a global signal. If the NPLD is to be used as a global climate record, the local processes involved in reflector formation must be better understood.
In this work, we compare the reflective properties of multiple surface and subsurface reflectors in the so-called Saddle Region of the NPLD, where the surface geometry allows for easy identification of individual reflectors without the interference of surface clutter. Using a combination of these radar observations, surface imagery, and a statistical radar backscattering model we aim to determine the source of the observed reflection power heterogeneity as well as its implications for the use of the NPLD as a global climate record.

Keywords: Mars, Polar, Cryosphere, Radar

SETP
LCMS

Hydrothermal Fluid Pathways in the Ertsberg East Skarn System, Ertsberg-Grasberg District, Papua, Indonesia

ledvina@utexas.edu
Ledvina, M., Jackson School of Geosciences, The University of Texas at Austin, TX

The Ertsberg-Grasberg District consists of world class Cu-Au porphyry and skarn deposits clustered in a 50 km^2 region atop the 4884 m high Sudirman Range of Papua, Indonesia. A hybrid porphyry-skarn deposit, the Ertsberg East Skarn System (EESS), contains ~3 Gt of ore, grading 0.59 % Cu and 0.49 g/t Au over a vertical extent of ~2km (Leys et al., 2012). Hydrothermal fluids sourced from a deep magmatic source are believed to have mineralized the EESS around 3Ma, but the pathways of these mineralizing fluids within the ore body are poorly understood. This study is an ongoing effort to characterize fluid pathways during mineralization of the EESS by preparing time-slices of temperature and salinity variation within the EESS ore zone.

Quartz±sulfide veining typical of porphyry systems is present in the Ertsberg Diorite and the deepest portions of skarn mineralization in the EESS. Because it is difficult to obtain temperature and salinity data from sulfides and Au-grains directly, the closely associated vein quartz is studied as a near analog for mineralizing fluids during Cu-Au precipitation. Drill core was sampled along a NE-SW trending section that dissects the central portion of the NW-SE trending ore zone to capture variation in quartz precipitation conditions over the vertical extent of the ore zone and from the diorite-hosted stockwork zone to more distal skarn-hosted quartz veins. SEM-CL transects of quartz-sulfide veins are used to distinguish and describe the quartz generations present in each EESS sample to identify variation in these generations throughout the system. These paragenetic relationships establish a relative timeline of quartz precipitation. Fluid inclusion microanalyses of quartz generations in each sample are used to estimate the temperature and salinity conditions of the fluids from which they were deposited. This study will culminate in a plot of vertical and lateral temperature and salinity variation in the EESS for each quartz generation using Surpac 3-D modeling software. Fluid vectors defined by the temperature and salinity profiles will constrain how fluid pathways evolved during the duration of the hydrothermal system.

Keywords: porphyry, skarn, cathodoluminescence, fluid inclusion microthermometry

CCG
ECG

Flood Monitoring and Detection Using the Coupled WRF-Hydro/RAPID Framework: A Case Study for Hurricane Ike in 2008

prlin@utexas.edu
Lin, P., Jackson School of Geosciences, University of Texas at Austin
Yang, L., Jackson School of Geosciences, University of Texas at Austin

Abstract
As part of the on-going National Flood Interoperability Experiment (NFIE), a vector-based river routing scheme named RAPID is implemented into the community-based hydrometeorological modeling framework – the Weather Research and Forecasting (WRF) model with terrestrial hydrological extensions (hence WRF-Hydro). The resulting augmented modeling package greatly enhances the routing efficiency as compared with the default grid-based routing scheme. In addition, the use of high-quality GIS-based river network dataset (NHDPlus) allows the framework to be more applicable to fine-scale water resource management. To evaluate the newly developed modeling framework, we perform a case study for Hurricane Ike in 2008, which is blamed for a big flood in Texas, especially in the Houston metropolitan area. The model is set up at two types of land grids, namely 4.5 km and 12.5 km, to examine the sensitivity of the coupled hydrometeorology and vector-based river routing to land resolution. Two types of precipitation data, namely NLDAS-2 forcing and NEXRAD, are used to examine how the flood detection capability is influenced by the precipitation uncertainty. The insights gained from using different land resolutions, coupling algorithms, and forcing data, are important to facilitate the future implementation of the NFIE for continental-scale flood monitoring and forecasting.

Keywords: Flood modeling, WRF-Hydro, RAPID, Hurricane Ike, NFIE

CCG
LCPHD

Improving global leaf area index (LAI) estimation based on Data Assimilation Research Testbed (DART) and the Community Land Model version 4 (CLM4.0)

lingxl08@126.com
Ling, X., Jackson School of Geosciences, The University of Texas at Austin, Austin, TX
Yang, Z., Jackson School of Geosciences, The University of Texas at Austin, Austin, TX
Guo, W., Institute for Climate and Global Change Research, School of Atmospheric Sciences, Nanjing University, Nanjing 210093, People's Republic of China

The leaf area index (LAI) influences the exchanges of momentum, carbon, energy, and water between the terrestrial biosphere and the atmosphere. As such, it is a key variable in regulating the global carbon, energy, and water cycles. Modern land surface models have included prognostic carbon and nitrogen components to simulate the LAI, but these LAI simulations show biases in both amplitude and phase. Such biases can be corrected by assimilating satellite-derived LAI into land surface models, which is the focus of this study.

The land data assimilation system in this study is the Community Land Model version 4 (CLM4.0) with the prognostic carbon–nitrogen (CN) option (hence CLM4.0CN), which is linked with the Data Assimilation Research Testbed (DART) from the National Center for Atmospheric Research (NCAR). An ensemble of 40-member atmospheric forcing fields is generated by running the DART and the Community Atmosphere Model. This ensemble forcing is used to drive the CLM4.0CN with or without LAI data assimilation (i.e. open loop). In our LAI data assimilation, the Moderate Resolution Imaging Spectroradiometer (MODIS) LAI is assimilated into the CLM4.0CN at a frequency of every 8 days, and the total leaf area index, leaf carbon and leaf nitrogen are adjusted by using the ensemble-adjustment Kalman filter. Being lower than the open loop result, the assimilated LAI is much closer to observations. This improvement is most obvious at low latitudes.

Keywords: Community Land Model, leaf area index, Data Assimilation Research Testbed

CCG
ECG

The effects of varied geographic binning and temporal calibration on phylogenetic ancestral range reconstructions: examples from the Late Cretaceous of North America

joshuarlively@utexas.edu
Lively, J., Department of Geological Sciences, The University of Texas at Austin, Austin, TX

Ancestral range reconstructions have become an integral part of studying the evolutionary biogeography of various clades. Several methods have been devised to investigate geographic range evolution using parsimony, maximum likelihood, or a combination of both. Those methods use the distributions of terminal taxa to reconstruct ancestral ranges along interior branches of a phylogeny. Those reconstructions are powerful tools for understanding the evolutionary biogeography of a clade and how the resultant patterns may relate to broader dynamics within the earth system. However, the effects of using different resolutions of geographic bins have not been explored. The paleogeographic ranges of fossil taxa may be binned by the basin(s), region, or continent in which they inhabited. When investigating a clade's historical biogeography, are the reconstructed patterns different when the taxa are geographically binned at different resolutions? Using dispersal-extinction-cladogenesis analysis, I reconstructed the ancestral ranges of four Late Cretaceous terrestrial vertebrate clades (Baenidae, Tyrannosauroidea, Chasmosaurinae, and Centrosaurinae). Taxa found in Upper Cretaceous basins across western North America (Laramidia) offer an excellent study system because individual depocenters are distinguishable and there is a clear regional break between northern and southern Laramidian basins. I altered the resolution at which terminal taxa of these clades were geographically binned: first by sedimentary basin and then regionally. I found that three of the four phylogenies analyzed produced congruent results when regional and basin-scale areas were specified. The greatest amount of variation between analyses resulted from how the phylogenies were temporally calibrated (i.e. minimized branch lengths vs. averaged branch lengths). These findings indicate a need to vary branch lengths used for maximum likelihood analyses and subsample throughout the stratigraphic ranges of taxa to gain insights into multiple hypotheses of a clade's geographic range evolution. My analyses also show key similarities and differences in the paleobiogeography of these four clades that may be indicative of physical and/or biological processes impacting vertebrate distributions during the Cretaceous.

Keywords: paleobiogeography, Cretaceous, North America, geographic binning, temporal calibration

SETP
LCPHD

Constraining Mantle Heterogeneities with Joint Inversions of Seismic, Geodynamic, and Mineral Physics Data

lcer87@gmail.com
Lu, C., Department of Geological Sciences, The University of Texas at Austin, Austin, TX
Grand, S., Department of Geological Sciences, The University of Texas at Austin, Austin, TX
Forte, A., GEOTOP, University of Quebec at Montreal, Montreal, QC
Simmons, N., Atmospheric, Earth and Energy Division, Lawrence Livermore National Laboratory, Livermore, CA

Two outstanding goals of solid earth geophysics are to determine the chemical structure of the Earth and to understand the dynamics of its interior. The dynamics of the mantle are controlled by density variations and combined knowledge of density structure and seismic velocities provide the strongest constraints on chemical heterogeneity. Unfortunately, most of the traditional geophysical methods such as seismic tomography and geodynamic modeling alone cannot adequately resolve the density structure within the mantle. Thus, seismic, geodynamic and mineral physics joint inversion methods have been applied to better understand the dynamics of the mantle in recent years (e.g. Simmons et al. 2010). In these joint inversions, P wave and S wave travel times, as well as four convection-related geodynamic observations (free air gravity, tectonic plate motion, dynamic topography, and the excess ellipticity of the core-mantle boundary) can be used to produce 3-D models of density and seismic velocities simultaneously. The approach initially attempts to find a model that can be explained assuming temperature controls lateral variations in mantle properties and then to consider more complicated lateral variations that account for the presence of chemical heterogeneity to further fit data. Here we present new joint inversion results include 50% more new S wave travel time data than in previous work and geodynamic data that extend to larger spherical harmonic degrees. In addition, temperature derivatives of P and S velocity and density have been determined using an updated mineral physics dataset. For the first time we include non-linear anelastic temperature effects on velocities in the joint inversion. The anelastic effects decrease the required high density component within the lower mantle superplumes. The hypothesis that temperature variations explain most observed heterogeneity within the mantle is consistent with our data.

Keywords: joint inversion, deep mantle, anelasticity, superplume

SETP
LCMS

Thermochronometric investigation of fluid flow and geothermal systems in extensional settings, Dixie Valley, Nevada

amacnamee@utexas.edu
MacNamee, A., The University of Texas at Austin, Austin, TX
Stockli, D., The University of Texas at Austin, Austin, TX

We utilize (U-Th)/He analysis of apatite (AHe) and zircon (ZHe) to resolve cooling ages due to exhumation from those reset by geothermal fluids, and show that structural features play a role in the occurrence of geothermal anomalies. We also test the potential of $^{4}He/^{3}He$ thermochronometry to record fluid-induced reheating of recently exhumed samples. Dixie Valley is located within the Basin and Range province of Nevada where it forms a half graben east of the Stillwater Range normal fault. This region is characterized by extension, thinned crust, elevated heat flow, and high seismicity. Within Dixie Valley the complex interplay between the NE-trending Stillwater Range normal fault and NW-trending dextral faults produced several prominent dilational corners. These corners are hypothesized to result in increased fracture permeability, and often host blind geothermal prospects. Therefore, Dixie Valley is an ideal case study for applied thermochronometry. Samples (n=79) from the footwall of the normal fault yield AHe aliquots ranging from ~0.2-16 Ma and ZHe aliquots from ~1-163 Ma. Three elevation transects of AHe ages record advective cooling of the footwall due to exhumation onset at ~3-5 Ma. AHe data younger than this exhumation age (~0.2-4 Ma) show a strong correlation with previously identified geothermal anomalies and areas of increased strain, thus suggesting that ages are reset by fluids. Additionally, we use the $^{4}He/^{3}He$ method to measure the spatial distribution of ^{4}He and to determine continuous t-T paths for individual apatite grains from ~70-20°C. The low-temperature sensitivity of the $^{4}He/^{3}He$ method makes it uniquely suited to address transient reheating by geothermal fluids. Dixie Valley and the Stillwater Range present an ideal opportunity to obtain empirical data regarding the temperature evolution of geothermal systems and develop a novel application of $^{4}He/^{3}He$ thermochronometry.

Keywords: thermochronometry, (U-Th)/He, 4He/3He, geothermal, structure, extension

EG
LCPHD

Mudrock Fracture Mechanics and Seal Capacity in Chemically-Reactive Environments: Insights from a Natural CO2 System

jmajor@mail.utexas.edu
Major, J., Bureau of Economic Geology, The University of Texas at Austin, Austin, TX
Eichhubl, P., Bureau of Economic Geology, The University of Texas at Austin, Austin, TX
Dewers, T., Rock Mechanics, Sandia National Laboratories, Albuquerque, NM

Assessing the coupled chemical and mechanical properties and behavior of reservoir and seal rocks is critical for ensuring both the short and long term security of injected CO_2 in the subsurface. An approach utilizing observations from natural analogs has great advantages for understanding these properties on longer time scales than is possible using laboratory or numerical experiments. Well-characterized field studies of natural analogs such as the Crystal Geyser/Little Grand Wash field site in eastern Utah are essential for providing realistic input parameters, calibration, and testing of numerical models across a range of spatial and temporal scales. This study assesses the potential for leakage via fracturing or capillary failure of reservoir and seal rocks altered by CO_2-water-rock interactions.

Fracture mechanics testing using the double torsion method was performed on a suite of naturally altered and unaltered reservoir and seal rocks exposed at the Crystal Geyser field site. These samples represent end-products of CO_2-related alteration over geologic time scales. Fracture toughness, which measures the stress required to initiate new fractures, and subcritical index were both measured. Test data demonstrate that CO_2-related alteration has weakened one reservoir sandstone unit by approximately 50%, but the subcritical index is not significantly affected. Another weak, poorly cemented sandstone unit measured shows reduced fracture toughness in an intensely CO_2-altered sample but increased fracture toughness for a different sample with elevated calcite cement due to precipitation from CO_2-rich fluids. CO_2–related alteration has also significantly elevated calcite content in shale samples measured and increased fracture toughness over unaltered shale. Combined, these results across several lithologies demonstrate that CO_2-related chemical alteration can significantly alter rock geomechanical properties. In general, geochemical reactions that lead to net dissolution of cements and grains weakens rock to fracturing (i.e. lowers fracture toughness), whereas precipitation of cements may make rocks more resistant to fracturing.

Mercury intrusion capillary pressure (MICP) analyses on shale samples taken from a fault-perpendicular transect show relatively low capillary seal capacity nearest the fault where CO_2-alteration is most intense. Seal capacity increases by nearly an order of magnitude at around 15 meters from the fault, then gradually declines by a factor of 4 over 100 meters laterally. This trend, along with systematic shifts in pore aperture size distributions correlates with measured bulk calcite content. Enhanced calcite precipitation is likely closing sub-micron-scale pore networks in the shale and is being investigated using SEM imaging.

The natural system at Crystal Geyser demonstrates that CO_2-water-rock interaction driven by changes in the geochemical environment have significantly altered rock geomechanical and flow properties over long time scales. Reduced fracture toughness of reservoir and seal rocks due to long term exposure to CO_2-rich environments could make them prone to failure, ultimately leading to fracturing and leakage of subsurface reservoirs. CO_2-related alteration can either lower the seal capacity of shales or increase it in areas where CO_2-rich fluids drive significant precipitation of carbonate minerals. It is therefore critical to recognize these processes for enhanced oil recovery, wastewater, and CO_2 sequestration injection applications.

Keywords: CO2, structure, seal, fracture, SEM, Crystal Geyser

CCG
ECG

Identification of exceptionally preserved squid and their soft tissue from a new Early Jurassic lagerstätte from Alberta, Canada

selva.marroquin@utexas.edu
Marroquín, S., Jackson School of Geosciences, The University of Texas at Austin, Austin, TX
Martindale, R., Jackson School of Geosciences, The University of Texas at Austin, Austin, TX

The paleontological record is inherently biased towards organisms with hard parts, (eg. shells). It is estimated that the shelly fossil record represents at best 21-33% of marine communities (Allison and Briggs, 1993); opportunities to study a complete ecosystem are rare in marine environments. Lagerstätten are exceptional fossil deposits that preserve soft tissues and, although uncommon, represent a comprehensive snapshot of past life essential for paleontological studies (Allison & Briggs, 1993). The Early Jurassic (201-174 Ma) was a time of intense disturbance for marine communities. Ecosystems were recovering from the end-Triassic mass extinction and were hit by a global anoxic event known as the Toarcian Ocean Anoxic Event (T-OAE, ~183 Ma), which occurred during the Early Jurassic Pliensbachian-Toarcian transition. The T-OAE is known predominantly from Europe and has yet to be studied extensively elsewhere (North or South America). To date, only six Lagerstätten exist globally from the Jurassic, of these only two cover the Early Jurassic, the Posidonia Shale and Osteno, both of which are in Europe. In the summer of 2013 Drs. Martindale and Gill discovered a new Lagerstätte in Alberta, Canada that coincides with the T-OAE interval. This site (Ya Ha Tinda) contains exceptional preservation of numerous taxa including the soft tissues of several squid. After excavation in the summer of 2014, a total of fifteen squid have been found, with at least four preserving internal organs. This site provides a rare opportunity to study a full Early Jurassic marine community from Panthalassa as well as the paleogeographical distribution of squid genera found at this Lagerstätte. Through utilization of novel imaging techniques (CT, SEM and polarized photography) these data can be used to describe the new Jurassic squid fauna discovered at this locality. To date, only two Jurassic squid genera have been studied from North America and the discovery of this site in Alberta has more than doubled the number of Jurassic squid genera from North America.

Keywords: Early Jurassic, T-OAE, Squid, Lagerstätte, Alberta, Paleontology

SHP
ECG

Temporal and Spatial Variation in Bed-material Load and its Connection to Geomorphology of the Backwater Zone on the Trinity River, East TX, USA

jasminemason@utexas.edu
Mason, J., The University of Texas at Austin
Smith, V., The University of Texas at Austin
Mohrig, D., The University of Texas at Austin

Recent observations made in the Trinity River of East Texas reveal that systematic spatial changes in bedform geometry, coverage, and inferred activity correlate with documented shifts in the larger-scale geomorphology of the river. Acoustic imaging data was collected through the transition into the backwater zone, or the reach of river where flow is affected by hydraulic readjustment between quasi-uniform flow further upstream and gradually varying flow (GVF) towards the river mouth. Measurements collected immediately following a minor flood record no significant spatial changes in bedform height, length, or coverage over a ~14 km reach that covers 14 river bends. Over the same reach after a period of extended low river discharge, dune heights decrease from decimeters to centimeters, with dune length decreasing similarly to maintain a relatively constant steepness value before dunes are completely absent. The fraction of the bed that is covered by bedforms decreases drastically from about 80% to around 20%. Accompanying the disappearance of the dune forms is a systematic reduction in the slopes of their lee faces until the bed is completely flat. The location of these shifts in bed-material load coincides nicely with and likely accounts for documented geomorphic changes to the river, including a reduction in point bar surface area and volume and a decrease in channel-bend migration rates (Smith, 2012). Results have obvious implications for understanding coastal fluvial geomorphology and can help elucidate relationships between bedforms, bed-material load, point bars, and river bend kinematics.

Keywords: Geomorphology, Backwater, Bedforms, Sediment transport, Coastal rivers

SETP
ECG

Slip inversion for the Costa Rica 2012 earthquake

kimberly.mccormack@utexas.edu
McCormack, K., Geological Sciences, University of Texas at Austin
Hesse, M., Geological Sciences, University of Texas at Austin
Stadler, G., Courant Institute, New York University

On 5 September 2012, a major megathrust earthquake (Mw=7.6) ruptured the plate interface beneath the Nicoya Peninsula, Costa Rica. This event was centered 12 km offshore of the central Nicoya coast, at a depth of 18 km. The maximum slip exceeded 2 meters, and the rupture spread outward along the plate interface to encompass 3000 km^2 of the Nicoya seismogenic zone. More than 1700 aftershocks were recorded within the first 5 days. These aftershocks outlined two distinct rupture patches; one centered on the central coast and the other beneath the southern tip of the peninsula.

We propose a finite element inversion for coseismic slip on the fault plane based on elastic surface displacement with the goal of imaging the “locked” patch that has been seen using other inversion techniques. We are interested in the elastic response right after the earthquake and thus assume a linear elastic equation for the displacement. This model will serve as the foundation for a time-dependent, poroelastic model for fault slip and fluid migration due to overpressure caused by a megathrust earthquake. Both continuous and campaign GPS stations recorded the coseismic surface displacement associated with the 2012 Nicoya earthquake. Well head pressure measurements and changes in well water levels will be used to determine the initial overpressure caused by the earthquakes and serve as an initial condition for the poroelastic problem. Additionally, since the uncertainty of the solution depends only on the geometry of the problem, this model can be used to carry out geometric optimization of future GPS station deployments in order to best image the locked patch.

Keywords: Inverse model, Earthquake, GPS

PS
U

Characterization of ice sublimation features and their distribution on mid-latitude glaciers of Mars

lizzymckinnon@utexas.edu
McKinnon, L., Institute for Geophysics, The University of Texas at Austin, Austin, TX
Petersen, E., Institute for Geophysics, The University of Texas at Austin, Austin, TX
Levy, J., Institute for Geophysics, The University of Texas at Austin, Austin, TX
Holt, J., Institute for Geophysics, The University of Texas at Austin, Austin, TX

Introduction

Debris covered glaciers in the mid-latitudes of Mars form during periods of high planetary obliquity, in which ice is removed from the polar caps and deposited between 30-60° in both the northern and southern hemisphere of Mars (Head et al., 2003). Crater counts indicate that the glaciers present in the martian mid-latitudes existed by at least 100 Ma but may have been subject to smaller periods of glaciation since their initial emplacement (Levy et al., 2007). Data from the Shallow Radar instrument (SHARAD) aboard the Mars Reconnaissance Orbiter (MRO) reveal that the substrate of the glaciers has a dielectric constant similar to pure water and is insulated by a debris layer of rock and dust ~1-10 m thick (Holt et al., 2008). The low radar attenuation in the data indicates a minimal amount of lithic material present in the ice (Plaut et al., 2009; Holt et al., 2008). Mass wasting of ice in mid-latitude glaciers results in viscous flow of the material, creating features such as lineated valley fill (Levy et al., 2007), concentric crater fill (Levy et al., 2009) and lobate debris aprons (Li et al. 2005).

Little is known about terrestrial debris covered glaciers, which have the potential to be aquifer sources for future generations. Through an examination of martian debris covered glaciers, we can learn a lot about their terrestrial analogs, as well as develop new techniques for studying the features on both planets.

Study area and methodology

This study concentrates on a suite of glaciers present on the dichotomy boundary in the region of Deuteronilus Mensae. High resolution imagery obtained from the CTX and HiRISE camera systems aboard the MRO is used to characterize different geomorphic units present in the LDAs of Deuteronilus Mensae. Each image is divided into 2 km2 bins. These bins are then selected using a random number generator to have their geomorphic units mapped in ArcMap 10.1.

Seven units have been identified in the region based on surface roughness estimates, relative elevations, geomorphology and stratigraphic relationships. The purpose of this study is to establish a relationship between these geomorphic units to better understand the process by which these glaciers evolve.

Keywords: Mars, geomorphology, debris covered glaciers, cryosphere, glaciology

SETP
U

Seamount Arrival into the Franciscan Subduction Complex at 100 ± 2 Ma: Marin Headlands, San Francisco Bay, CA

drewmcpeak@utexas.edu
McPeak, A., Department of Geological Sciences

A seamount fragment composed of basalt and layered radiolarian chert imbricated by thrust faulting is present in the Franciscan Complex rocks exposed in the Marin Headlands. Layered radiolarian chert forms a section about 80 meters thick that includes seven biostratigraphic zones ranging from Pliensbachian (190-183 Ma) to Cenomanian (100-93 Ma). Pillow basalt lava flows and breccias, layered chert, massive to bedded greywacke and shale-matrix mélange are exposed at Rodeo Cove and Blacksand Beach. The radiolarian chert is in depositional contact with basalt at Rodeo Cove and elsewhere in the Marin Headlands. Massive greywacke sandstone is in depositional contact with radiolarian chert at Rodeo Cove and Blacksand Beach. The greywacke includes many angular chert clasts up to 10 cm long. At Rodeo Cove a slab of layered chert a meter long is encased in greywacke near the contact. The layered chert was lithified and exposed at the time of greywacke deposition.

Two samples directly above the depositional contact at Rodeo Cove were collected and analyzed with detrital zircon U/Pb geochronologic techniques (LA-ICP-MS analysis of 120 zircon grains per sample). More than 95% of the zircons are of Mesozoic age and the youngest zircons (n=12) are 100 ± 2 Ma, the maximum and probable age of deposition. A 10-meter wide intrusion of shale-matrix mélange into the basalt and chert sequence is exposed at the southern end of Rodeo Cove; and can be traced uphill roughly 50 meters. The mélange contains boudinaged blocks of greywacke and greenstone. One 50 cm greywacke block encased in the shale-matrix mélange was processed for zircons. Approximately 20% of the zircons in this block are Paleozoic to Precambrian in age, indicating a different provenance than the chert-bearing massive greywacke. The youngest zircons (n=3) in the mélange block are 100 ± 2 Ma, the same as the two greywacke samples.

The simplest explanation for the field and geochronologic relationships is that the basaltic seamount formed far out in the Pacific Ocean basin and was blanketed for about 90 m.y. by radiolarian chert deposition that ended when the seamount entered the Franciscan Trench. At 100 ± 2 Ma sand-rich mass flows sourced from the Sierran magmatic arc were deposited on the seamount as it bulldozed the trench wall. Faulting imbricated the greywacke, radiolarian chert and basalt as the seamount was detached from the Farallon Plate, accreted in the Franciscan accretionary prism and later intruded by the shale-matrix mélange.

Keywords: Subduction,Seamount,San Francisco Bay,Detrital Zircon U/Pb

EG
ECG

Velocity model estimation through velocity continuation of seismic diffraction images

mdm-2006@yandex.ru
Merzlikin, D., Bureau of Economic Geology, The University of Texas at Austin, Austin, TX
Fomel, S., Bureau of Economic Geology, The University of Texas at Austin, Austin, TX

Velocity continuation (VC) describes image transformation under velocity perturbation where the step between different velocities can be infinitely small. In other words, this technique provides the means of image calculation for any specified set of velocities.

There is a special implementation of velocity continuation - oriented velocity continuation (OVC) technique. In that implementation we decompose data into slopes and then apply velocity continuation phase-shift operator to each of the slopes. Stacking over slopes produces the image corresponding to the defined velocity.

Diffractions play a crucial role in velocity estimation by velocity continuation techniques. If migration has been implemented using the correct velocity then the diffraction events will come into focus. Therefore, velocity model estimation can be performed through assessment of diffraction events in images with different migration velocities calculated using VC. When the estimate of the velocity model has been found, the velocity can be applied to the whole image containing both reflections and diffractions as well as to diffraction volume separately. The latter, for example, can provide some insights about fracture orientation.

The goal of this work is to estimate the velocity model for “Barrolka” 3D land dataset. These data have been acquired in the region that contains coal. Fractures in the coal layer are believed to produce diffractions which can be used for velocity estimation.

We use the plane-wave destruction filter to separate diffractions from reflections. VC as well as OVC have been applied for velocity estimation. For the focusing assessment, we used the kurtosis measure for the VC case and semblance for the OVC case. We calculate volumes corresponding to each constant velocity using both methods and then slice through parts which correspond to the highest focusing measure values to acquire the final image.

OVC theoretically is more sensitive to velocity perturbation and therefore is believed to provide more accurate results. However, VC velocity estimate appears to be much more reasonable and better corresponds to normal coal velocities. We make final conclusions comparing the images acquired using both techniques. Diffraction images are considered separately in order to assess imaging of small-scale features.

Keywords: velocity continuation, diffraction, imaging, fracture characterization

SETP
LCPHD

Role of Neogene Exhumation and Sedimentation on Critical-Wedge Kinematics in the Zagros Orogenic Belt, Northeastern Iraq, Kurdistan

renas.i.mohammed@utexas.edu
Koshnaw, R., Department of Geological Sciences, The University of Texas at Austin, Austin, TX
Horton, B., Department of Geological Sciences and Institute for Geophysics, The University of Texas at Austin , Austin, TX
Stockli, D., Department of Geological Sciences, The University of Texas at Austin, Austin, TX
Barber, D., Department of Geological Sciences, The University of Texas at Austin, Austin, TX
Tamar-Agha, M., Department of Earth Sciences, College of Science, University of Baghdad, Jadiriya, Baghdad, Iraq
Kendall, J., ExxonMobil Exploration Company, Houston

The Zagros orogenic belt and foreland basin formed during the Cenozoic Arabia-Eurasia collision, but the precise histories of shortening and sediment accumulation remain ambiguous, especially at the NW extent of the fold-thrust belt in Iraqi Kurdistan. This region is characterized by well-preserved successions of Cenozoic clastic foreland-basin fill and deformed Paleozoic-Mesozoic hinterland bedrock. The study area provides an excellent opportunity to investigate the linkage between orogenic wedge behavior and surface processes of erosion and deposition. The aim of this research is to test whether the Zagros orogenic wedge advanced steadily under critical to supercritical wedge conditions involving in-sequence thrusting with minimal erosion or propagated intermittently under subcritical condition involving out-of-sequence deformation with intense erosion. These endmember modes of mountain building can be assessed by integrating geo/thermochronologic and basin analyses techniques, including apatite (U-Th)/He thermochronology, detrital zircon U-Pb geochronology, stratigraphic synthesis, and seismic interpretations. Preliminary apatite (U-Th)/He data indicate activation of the Main Zagros Fault (MZF) at ~10 Ma with frontal thrusts initiating at ~8 Ma. However, thermochronometric results from the intervening Mountain Front Flexure (MFF), located between the MZF and the frontal thrusts, suggest rapid exhumation at ~5 Ma. These results suggest that the MFF, represented by the thrust-cored Qaradagh anticline, represents a major episode of out-of-sequence deformation. Detrital zircon U-Pb analyses from the Neogene foreland-basin deposits show continuous sediment derivation from sources to the NNE in Iraq and western Iran, suggesting that out-of-sequence thrusting did not significantly alter sedimentary provenance. Rather, intense hinterland erosion and recycling of older foreland-basin fill dominated sediment delivery to the basin. The irregular distribution of thermochronologic ages, hinterland growth, extensive erosion, and recycled sediment in the Neogene foreland basin imply that the Zagros orogenic wedge in the Iraqi Kurdistan region largely developed under subcritical wedge conditions.

Keywords: Zagros, fold thrust belt, out of sequence deformation, exhumation, zircon geochronology, thermochronology

MG
LCMS

Seismic stratigraphy of the Bering Trough, Gulf of Alaska: Late Quaternary history of Bering Glacier dynamics and sedimentation

sashamontelli@utexas.edu
Montelli, A., UTIG

Sedimentary architecture of the cross-shelf Bering Trough is studied using 5 high resolution seismic profiles integrated with the drilling data acquired during Integrated Ocean Drilling Program (IODP) Expedition 341. The objectives of this work are to constrain the number of advance-retreat cycles that have occurred through the Late Quaternary, examine the impact of the Bering Glacier on the continental shelf and slope, and reconstruct Bering Glacier dynamics. By tying these sequences with **δ**18O stratigraphy, we can test the Bering Glacier's relation to global ice sheet evolution and better understand the degree to which the glacial advance-retreat cycles were in phase with global events.
Our results show that: (1) Identification of erosional surfaces and glacigenic landforms that record positions of stillstand events and diagnose the style of retreat allow us to distinguish ten phases of glacial advances and subsequent retreats. (2) Distinctive slope gradient versus sediment supply controlled variability of sedimentation is recognized based on seismic data interpretation. (3) The trough mouth fan started its development during marine isotope stage (MIS) 6, progressively advancing to the position of present shelf edge during the subsequent MIS 4 and MIS 2 and is recognized by evidence of extensive deposition of glacigenic debris flows on the slope. (4) Sedimentation rates in the depocenter are exceptionally high and are estimated to be 1-2 m/k.y. through the middle Pleistocene on the shelf and 4-5 m/k.y. average through MIS 6 on the slope.

Keywords: glacier, high-latitude sedimentation, glacial dynamics, ice stream, ice sheet

MG
LCMS

Use of High Resolution 3D Seismic Data to Evaluate Quaternary Valley Evolution During Transgression and Shallow Fluid Anomalies, Inner Texas Shelf, Gulf of Mexico

mulcahy.francis@gmail.com
Mulcahy, F., The University of Texas at Austin, Austin, TX
Meckel, T., Bureau of Economic Geology, The University of Texas at Austin, Austin, TX

A novel, shallow-investigation, high-resolution 3D (HR3D) seismic acquisition system has been deployed for the first time in the Gulf of Mexico to characterize storage potential and de-risk target reservoirs for CO2 sequestration. HR3D data can image detailed depositional, architectural, and structural features in the shallow subsurface that have previously been below seismic resolution and/or excluded from industry surveys, which are optimized for deeper targets. One 31.5 km2 HR3D survey is located just offshore from San Luis Pass, TX and provides an exceptional 3D example of lowstand to transgressive deposits and the sedimentary architectures that characterize the transition. The dataset images the vertical succession with unprecedented resolution. Peak frequency of approximately 150Hz allows m-scale vertical resolution and twelve 25m cables spaced at 12.5m produce 4-fold data in 6.25m2

Imaged within this dataset at ~100ms TWTT, is a mappable erosional unconformity that is interpreted to be associated with the Brazos River system during the ~130ka glacial-eustatic lowstand and following transgression. Analyses of mapped amplitude horizon geomorphology document system evolution from a lowstand meandering channel system with clear point-bar deposits to a transgressive estuary characterized by dendritic tidal features that is eventually flooded. Detailed seismic descriptions of such transitions are rare and inform understanding of sequence boundaries in updip, basin margin settings.

In addition, we observe a vertical, seismically discontinuous zone within the HR3D volume that is interpreted to be a gas chimney system emanating from a deep, barren (drilled) anticline structure. Within the shallowest stratigraphic interval and at the top of the chimney zone, seismic attribute analysis (NRMS) reveals several high amplitude anomalies suggestive of small shallow gas accumulations. The anomalies accumulate at local fault-bound structural highs within coarser grained deposits and are overlain by finer grained, transgressive deposits.

Interestingly, point-bar deposits as well as channel scour deposits within the same stratigraphic interval show no sign of similar charge, suggesting they may be isolated from the flow system. Current research attempts to core the shallowest of the anomalies to verify the interpretation as derived from a deeper source, which would validate HR3D potential for identifying shallow fluid systems that may relate to deeper systems of economic interest.

Keywords: Seismic Stratigraphy, Seismic Geomorphology, Seismic Fluid Anomaly

CCG
U

Cranial Morphology of Notochelys platynota

ssmuller@utexas.edu
Muller, S., The University of Texas as Austin, Austin, Tx
Burroughs, R., The University of Chicago, Chicago, Illinois
Bell, C., The University of Texas at Austin, Austin, Tx

Notochelys platynota is an endangered, Malayan flat-shelled turtle native to various parts of southeast Asia. Notochelys platynota is reportedly part of the clade Bataguridae (Geoemydidae), a phenotypically diverse and poorly understood clade. Many researchers have attempted to evaluate the phylogenetic relationships of the group, but the large number of species and high morphological disparity among the species, creates numerous problems for elucidation of phylogony based on morphological data. Phylogenies of testudinoid and batagurid turtles reconstructed from molecular data provide conflicting results, suggesting a focus on morphological and molecular characters will be necessary to resolve the phylogeny of this group. Unfortunately, other than limited physical descriptions, there is little information on N. platynota and related batagurid turtles. Previous authors who reviewed N. platynota provided conflicting views about morphological characters that may help resolve phylogenetic issues within this clade. We rendered illustrations from CT data of an adult female specimen of N. platynota to provide a detailed view of the skull and to visualize anatomical features. From examining the skull, we found some character states that deviated from the scoring of the species by previous researchers. This includes the absence of quadratojugals when previously stated to be present, and a keyhole shape of the fissure ethomodalis which was stated to be a broader, oval shape. By providing a detailed description of the cranial anatomy of N. platynota, we help shed some light on the understudied species as well as batagurid relationships.

Keywords: testudines, bataguridae, Notochelys platynota, cranial morphology, CT imaging

PS
ECG

Stratigraphic structures and depositional anomalies in Planum Boreum, Mars, from orbital radar mapping

sn.stefano@gmail.com
Nerozzi, S., Institute for Geophysics, The University of Texas at Austin, Austin, TX
Holt, J., Institute for Geophysics, The University of Texas at Austin, Austin, TX

Planum Boreum is a dome of layered icy material rising ~3 kilometers above the surrounding plains in the northern hemisphere of Mars. It can be divided into two units of differing compositions: a basal accumulation of mostly siliciclastic fine sediment cemented by interstitial water ice (termed “basal unit”, BU), and an overlying thick blanket of almost pure water ice. Previous studies pointed out the different nature of the two deposits and suggested very different deposition ages, rates and styles. However, the reason for such an abrupt change in deposition is still unknown.

Due to exposures in scarps and trough walls, detailed stratigraphy of the uppermost NPLD layers and their evolution have been studied extensively since the first orbital images. However, large portions of Planum Boreum are still unmapped and no detailed studies of the BU-NPLD contact have been performed to date, primarily due to a general lack of outcrops. Correlation of reflectors within radargrams acquired by the Shallow Radar (SHARAD) onboard Mars Reconnaissance Orbiter makes a detailed stratigraphic reconstruction of the NPLD possible. An extensive set of radargrams is available over Planum Boreum and individual reflectors can be traced over hundreds of kilometers with a theoretical vertical resolution of ~9 m in water ice.

In this study, we map the basal unit and the NPLD along this contact, analyze internal stratigraphy, and compare the results with a global ice accumulation model especially tuned for Planum Boreum. The lowermost (oldest) NPLD radar layers are found to be characterized by limited lateral extent, one of them overlying a previously undetected unit adjacent to the basal unit. The two units appear to be contiguous in radar profiles. These results can be explained in terms of nonuniform accumulation resulting from insolation variations and continuous resurfacing by winds. These variations could be induced by both topography and orbital forcing.

Keywords: Mars, radar, stratigraphy, mapping, water ice, resurfacing

EG
ECG

A High-Resolution Chemostratigraphic Record of Cenomanian-Turonian Strata, South Texas, USA

michael.nieto89@gmail.com
Nieto, M., Jackson School of Geoscience
Rowe, H., Bureau of Economic Geology
Phillips II, N., EOG Resources
Ruppel, S., Bureau of Economic Geology

The Eagle Ford Formation of South Texas is classified as a calcareous mudrock that was deposited on the South Texas Shelf during the earliest Late Cretaceous. The sharp contact between the underlying Buda limestone and the Eagle Ford Formation represents a major transgression during the middle Cenomanian. The contact between the Eagle Ford and overlying Austin Chalk can be highly gradational in some locations. Geochemical sampling of a continuous drill core from Atascosa County, Texas, was analyzed using a Bruker Tracer IV-SD handheld XRF (X- ray fluorescence) unit. Elemental data were collected automatically at a 10-mm sampling interval along the entire 90-meter-long core using a MCS-1000, XRF Core Scanner (DeWitt Systems, Inc.). Major (Mg-Fe) and trace (V-U) element analysis was undertaken with no protective window covering the X-ray source, and a steady flow of helium was purged through the nose of the Bruker Tracer IV-SD during major element analysis in order to increase system sensitivity to low energy elements such as Mg and Na.

The Eagle Ford is mineralogically dominated by calcite, and construction of the high resolution chemostratigraphic record was undertaken to better understand the subtle variation in, and stratigraphic significance of, the non-calcite components. Hierarchical cluster analysis (HCA) was undertaken to define how the elemental composition varies within individual samples and how individual samples chemostratigraphically relate. Four elementally-defined clusters (chemical facies) define over 80% of the ~7,600 samples. Clusters enriched in siliciclastically-bound detrital components (Al,Ti, Zr) are defined as having been sourced from outside the basin. Redox-sensitive trace elements (RSTEs) such as Mo, V, and Ni concentrate in strata deposited under oxygen-deprived bottom waters; these clusters are defined as anoxic. Clusters representing samples that are interpreted to be organic-rich (based on %TOC results) are defined as “organic”, and tend to be distinguished by their P, Y, and U enrichments. Clusters enriched in Ca, Sr, and Mn represent stratigraphic intervals that accumulated under predominantly oxygenated bottom waters. Delineation of chemical facies using HCA is integrated with core description to better understand the depositional conditions that persisted across the Cenomanian-Turonian boundary. Recent work suggests that anoxic conditions experienced along the South Texas Shelf during this time were asynchronous with the well-documented Oceanic Anoxic Event 2, implying that local/regional paleoceanographic conditions played a greater role in the occurrence of anoxia.

Keywords: Chemostratigraphy, Eagle Ford, Cenomanian, Turonian, OAE2, X-ray fluorescence, Hierarchical cluster analysis

SETP
ECG

Mechanical modeling of fracturing and collapse along steep-rimmed shelf margin systems

anolting@utexas.edu
Nolting, A., Dept of Geosciences, Jackson School of Geosciences, The University of Texas at Austin
Zahm, C., Bureau of Economic Geology, Jackson School of Geosciences, The University of Texas at Austin
Kerans, C., Bureau of Economic Geology, Jackson School of Geosciences, The University of Texas at Austin

Steep-rimmed carbonate systems represent unique depositional environments with nearly instantaneous lithification of facies creating dramatic heterogeneity of rock mechanical properties within the outer shelf-margin. The variability of facies, especially the presence of older shelf margins, creates a contrast of brittleness that is prone to fracturing and faulting at areas of highest mechanical contrast. Furthermore, areas of high deformation may impact facies deposition, diagenetic fluid movement and commonly creates areas that are prone to subsequent deformation or enhanced subsurface fluid flow. Despite the clear importance of the deformation features to shelf margin evolution, little is known about the conditions, controls or timing of deformation. A variety of mechanisms have been proposed for the development of early-formed fractures including differential compaction adjacent to pre-existing shelf margins and extension by basinalsliding along a dipping shelf margin ramp. In order to investigate the possible mechanisms and expected deformation response, we propose to construct a finite-element model (Elfen) that can accommodate the mechanical changes, including the dynamic updating of rock properties, variable slip surfaces, and overall loading and eventual failure of shelf margin systems.

Excellent outcrop exposure and recent detailed characterization efforts within the Permian Capitan shelf margin located in the Guadalupe Mountains creates an optimal opportunity to test finite-element models of shelf margin systems. For our initial efforts, the Guadalupian 24-26 (i.e., G25 or Hairpin high-frequency sequence) intervals exposed in Slaughter Canyon have been selected. Detailed mapping of stratigraphic facies and chronostratigraphy conducted by Harman (2011) along with fault geometry, stratalgrowth and fault evolution investigated by Mathisen (2014) enable the construction of a detailed finite-element model. We believe that early-formed deformation is critical to the process of fracture development and dictates that stratigraphic layers, including their variable rock properties, be added incrementally to better understand the impact of gravitational loading, slip and slope failure to fracture development. The initial model presented in this poster focuses on the construction of the stratigraphic layers and facies in 2D along a depositional profile. Simplified mechanical facies were developed based on Harman (2011) including facies to represent the shelf, reef, and slope.

After the stratal relationship are modeled, focused efforts on characterization will include: (1) detailed measurement of rock properties of each of the mechanical facies; (2) variations in compaction and porosity reduction by facies; (3) initial and evolving rock properties within the shelf margin complex.

Keywords: Finite-element, Deformation, Carbonate margins, Rock Properties

EG
ECG

Imaging deformation bands in sandstones using argon ion beam milling and scanning electron microscopy

casey.obrien@utexas.edu
O'Brien, C., Bureau of Economic Geology, Jackson School of Geosciences, The University of Texas at Austin, Austin, TX
Elliott, S., Bureau of Economic Geology, Jackson School of Geosciences, The University of Texas at Austin, Austin, TX
Eichhubl, P., Bureau of Economic Geology, Jackson School of Geosciences, The University of Texas at Austin, Austin, TX

Scanning electron microscopy can be used to image microstructures in deformation bands. These microstructures are affected by brittle deformation and chemical diagenetic processes, and control the mechanical and hydraulic properties of deformation bands. However, the ability to use scanning electron microscopy to resolve microstructures is often compromised by surface imperfections created by conventional mechanical polishing techniques. This makes discerning natural mechanical deformation from induced damage difficult. In this study, we prepare samples using argon ion beam milling in order to minimize surface damage during sample preparation. First results using a deformation band from the Entrada Sandstone from the San Rafael Desert in Utah demonstrate that argon ion milling allows imaging of pore space and pore-filling cements at nanometer scale resolution. Pore-filling cement in this deformation band includes crystals of euhedral quartz that precipitated after band formation. These delicate quartz prisms are unlikely to be preserved using conventional mechanical polishing. Cements and other small-scale diagenetic features can control flow through pore throats and thus production from clastic reservoirs that contain deformation bands.

Keywords: scanning electron microscopy, argon ion milling, deformation bands, sandstone, microstructures, diagenesis

SETP
ECG

Recovering continuous thermal histories from single grains by laser ablation 4He /3He and U and Th depth profiling

modlum@utexas.edu
Odlum, M., The Jackson School of Geosciences, The University of Texas at Austin, Austin, TX
Stockli, D., The Jackson School of Geosciences, The University of Texas at Austin, Austin, TX
Patterson, D., The Jackson School of Geosciences, The University of Texas at Austin, Austin, TX
Anfinson, O., The Jackson School of Geosciences, The University of Texas at Austin, Austin, TX
Smye, A., The Jackson School of Geosciences, The University of Texas at Austin, Austin, TX

The spatial concentration profile of the daughter isotope within a mineral is extremely sensitive to a rock's thermal history. In contrast to traditional He dating where analyses of multiple aliquots from different samples are required, a concentration profile of the radiogenic daughter within a single grain provides a mineral's progression through a range of temperatures (dependent on mineral and daughter product) providing a continuous thermal history. The use of laser-ablation depth profiling to spatially constrain the concentration profile of U and Th and their α-particle radioactive decay products (^{4}He) in a single grain is a burgeoning technique, with several advantages over conventional (U-Th)/He thermochronologic techniques. My research involves developing a method to depth profile ^{4}He/^{3}He in proton-irradiated apatite and zircon to determine the radiogenic ^{4}He concentration profile, which can be directly inverted to get a unique and continuous Temperature-time path. The depth profiling method will directly measure parent concentrations, which circumnavigates a major, often flawed, assumption of homogenous parent distribution associated with step-degassing determination of the ^{4}He concentration profile. Laser ablation depth profiling will provide higher resolution thermal histories than conventional step-heating or total degassing techniques that are transportable to a whole array of applications in both industry and academia.

Keywords: 4He/3He, (U-Th)/He, thermochonometry,thermochronology, depth profiling, laser ablation

CCG
LCPHD

New insights into the wind-dust relationship in sandblasting and direct aerodynamic entrainment from wind tunnel experiments

psagar@utexas.edu
Parajuli, S., 1The University of Texas at Austin, Jackson School of Geosciences, 2225 Speedway, Stop C1160, Austin, TX 78712-1692
Zobeck, T., U.S. Department of Agriculture (USDA), Agricultural Research Service (ARS), Lubbock, Texas, USA
Kocurek, G., 1The University of Texas at Austin, Jackson School of Geosciences, 2225 Speedway, Stop C1160, Austin, TX 78712-1692
Stenchikov, G., King Abdullah University of Science and Technology (KAUST), Thuwal, KSA

Numerous parameterizations have been developed for predicting wind erosion, yet the physical mechanism of dust emission is not fully understood. Sandblasting is thought to be the primary mechanism for dust emission but recent studies suggest that dust emission by direct aerodynamic entrainment can be significant. In this work, through carefully designed wind tunnel experiments, we investigate some of the least understood aspects of dust emission in sandblasting and direct aerodynamic entrainment. First, we compare the emitted dust flux and its particle size distribution (PSD) in sandblasting and direct aerodynamic entrainment. Second, we explore the sensitivity of emitted dust PSD to wind friction speed ( ) and soil type during sandblasting and direct aerodynamic entrainment. Finally, we discuss on the differences in physical mechanism of dust emission in these two processes. Results show that dust emission by direct aerodynamic entrainment is a function of surface roughness and it can be comparable to that by sandblasting provided the soil surface has some roughness. We show that dust emission in pure sandblasting may increase or decrease with increasing wind friction speed depending upon the mean jump length function. Our results also indicate that the PSD of emitted dust in sandblasting is sensitive to soil type but not to the friction speed in the range of friction speeds tested. The dust PSD showed sensitivity to soil type in the direct aerodynamic entrainment case as well but the sensitivity to friction speed showed mixed results.

Keywords: Saltation, Sandblasting, Dust Emission, Particle Size Distribution

EG
LCMS

Tracing the effects of fugitive CO2 on dissolved organic carbon at carbon sequestration sites

michael.patson@gmail.com
Larson, T., Jackson School of Geosciences, The University of Texas at Austin, Austin, TX
Havorka, S., Bureau of Economic Geology, The University of Texas at Austin, Austin, TX

Carbon capture and sequestration (CCS) is a proposed solution to mitigate anthropogenic carbon dioxide emissions, yet there are concerns of CO^2 leakage upward to shallower formations. Due to the reactive nature of CO^2 and the complications of measuring an atmospheric gas at surface, other indicators of unintended CO^2 migration into shallow reservoirs, such as changes in dissolved organic carbon (DOC) may provide insights to fluid migration. CO^2 will interact and dissolve into groundwater causing an increase in pCO^2 and a decrease in pH. This change in groundwater chemistry may increase the amount of dissolved organic carbon in solution. The goal of this study is to invesitigate the influence on and sensitivity of CO^2 on DOC through batch experiments.

Batch experiments consist of homogenized and milled rock samples of varying mass, 2mL of DI water and a headspace of pure carbon dioxide or atmosphere. Diffusion of the headspace gas into solution causes samples with pure CO^2 in the headspace have a pH of 4.3 while the atmospheric samples have a pH of 7.5. Two different rock samples were analyzed, Buffalo River Sediment which has a TOC of 3.4% and Illite (Green Shale) which has a TOC of 0.4%. The results indicate a pure CO^2 headspace causes Y mg of C/L= .004*(X mg of Buffalo Sediment) + 2.03 less DOC to desorb than an atmosphere headspace. Both rocks demonstrate this effect of CO^2 with a greater difference between the samples for the Buffalo River Sediment. Additional results show that the effect of CO^2 releasing DOC is reversible.

These results indicate that CO^2 decreases the amount of dissolved organic carbon in solution. Understanding the relationship between CO^2 and DOC may have implications for metal solubility and transport in addition to improving CCS monitoring.

Keywords: Carbon sequestration, Dissolved Organic Carbon, CO2–rock–water reactions, Groundwater monitoring

EG
ECG

Transition from Storm Wave-dominated Outer Shelf to Gullied Upper Slope: The Paleo-Orinoco Shelf Margin (Gros Morne Formation), South Trinidad

ypeng@utexas.edu
Peng, Y., The Department of Geological Sciences, The University of Texas at Austin, Austin, TX
Steel, R., The Department of Geological Sciences, The University of Texas at Austin, Austin, TX
Olariu, C., The Department of Geological Sciences, The University of Texas at Austin, Austin, TX
Clayton, C., The Department of Geological Sciences, The University of Texas at Austin, Austin, TX

Shelf-edge deltas are the key agents for accreting sediment onto clinothems of shelf-margins though the mechanism by which this happens remains understudied. The Gros Morne Formation (the St. Hilaire Siltstone and Trinity Hill Sandstone members), south Trinidad, reveals growth across the earliest Pliocene shelf-break area in front of the paleo-Orinoco Delta and records a transition from the gullied uppermost slope to the storm wave-dominated delta front and outermost shelf.

Analysis of the measured outcrops (240 m thick) demonstrates that: (i) In the outer-shelf areas, multiple coarsening-upward parasequences show increased wave influence upwards. The prodelta is dominated by up to 2 m thick, laminated mudstones with interbedded siltstone (< 10 cm thick). The delta-front deposits are also dominated by laminated mudstones (units up to 1 m) with interbeds of parallel-laminated/wave-ripple laminated, very-fine sandstones (< 50 cm thick) and abruptly changing up to sandstones with amalgamated hummocky and swaley stratification (up to 3 m thick). (ii) On the underlying muddy upper slope, sets of gullies (4 to >10 m deep) filled with interbedded mudstones and gravity flow deposits that include debris-flow conglomerates and sandy turbidite beds. Two types of slope gully underlain by distinctive erosion surface are documented here. Steeply-dipping (up to 50°) deposits are interpreted to represent gully-head morphology and the other, less steeply-dipping (up to 30°) gully-fill strata as the distal parts of a gully. (iii) Further down the slope, the turbiditic deposits are dominantly channels (up to 2.2 m deep) filled with structureless to rippled sandy beds and sheetlike very-fine sandstone units (up to 1.3 m thick) associated with an abundance of soft-sediment-deformed strata.

The observations suggest a setting where upper-slope gullies formed from slump scars near the shelf edge as gradients were locally increased. The key question then is whether much sand bypassed through these gullies to generate sandy submarine fans downslope? Our initial answer on this is NO! Experience from elsewhere suggests that storm-wave dominance at the shelf edge is negative for sand delivery immediately across that boundary. However, if the gullies amalgamate to form a larger conduit, a canyon that extended back onto the shelf and could capture longshore drifting sand, delivery to form fans is possible. In the Gros Morne gullied slope there was little sign of this.

Keywords: paleo-Orinoco Delta, shelf-edge deltas, Gros Morne Formation, slope gully, slump scars, storm wave-dominated deltas

SETP
LCPHD

Punctuated upper-crustal shortening, exhumation, and basin subsidence during flat-slab subduction in southern Peru

nicholas.d.perez@utexas.edu
Perez, N., The University of Texas at Austin, Austin, TX
Horton, B., The University of Texas at Austin, Austin, TX

New geophysical data help define modern flat-slab subduction in the central Andes, but the geologic consequences of slab shallowing in Peru remain poorly resolved. In better-documented regions of North and South America, changes in subduction architecture have been linked to arc migration, orogenic advance, and shifts in deformation style and kinematics. New structural, sedimentary, and geo/thermochronologic results for southern Peru support a reconstruction of Oligocene-Miocene deformation and sedimentation across the Western Cordillera magmatic arc, Altiplano hinterland plateau, Eastern Cordillera fold-thrust belt, and Subandean foreland basin. The spatial and temporal distribution of Andean shortening and basin subsidence in this region encompass a major phase of arc migration that has been attributed to shallowing of the subducting Nazca slab. Detrital zircon U-Pb ages for syndeformational growth strata pinpoint the timing of key forethrust and backthrust systems (Tinajani and Ayaviri faults, respectively) that partitioned the early foreland basin into a smaller, rapidly subsiding hinterland basin (Ayaviri basin) in the Altiplano plateau. A roughly 28 Ma activation of the basement involved Ayaviri backthrust along the Altiplano-Eastern Cordillera boundary matches the mid-Oligocene activation age reported for the entire central Andean backthrust belt, which persists for >500 km along strike southward into Bolivia. The Ayaviri structure potentially represents a reactivated deep-seated Triassic normal fault and/or an inherited crustal-scale boundary. Subsequent Miocene activation of the Tinajani forethrust and coeval thrust-related exhumation within the Eastern Cordillera are suggestive of distributed regional shortening during flat-slab subduction. Available data suggest a spatiotemporal coincidence of shallow subduction in southern Peru with inboard arc migration, basement-involved shortening, and focused rapid subsidence in the Altiplano plateau.

Keywords: Central Andes, tectonics, fold-thrust belt, foreland basin, geodynamics

PS
ECG

An ice flow modeling approach to understanding regional and aspect-dependent differences between debris-covered glacier lobes in Deuteronilus and Protonilus Mensae, Mars

eric_petersen@utexas.edu
Petersen, E., Institute for Geophysics, The University of Texas at Austin
Holt, J., Institute for Geophysics, The University of Texas at Austin
Parsons, R., Fitchburg State University, Fitchburg MA
Levy, J., Institute for Geophysics, The University of Texas at Austin

Debris-covered glacier (DCG) complexes are known to be abundant in the northern and southern mid-latitudes of Mars, where they are found filling valleys and craters or as coalescing lobes surrounding high mesas and massifs. Climate modeling supports the hypothesis that these features are the remnants of past high obliquity-induced ice ages in the mid latitudes of Mars. In addition, ice flow models developed for the physical conditions relevant to lobate DCGs on the Martian surface have been able to replicate their observed topography.

We apply the ice flow model developed by Reid Parsons to lobate DCGs in the northern mid-latitude regions of Deuteronilus and Protonilus Mensae (DPM). DCGs in this region exhibit varied properties in SHAllow RADar (SHARAD) sounding results and surface geomorphology. SHARAD soundings reveal clear, low angle basal reflectors under DCGs in western DPM, while generally no basal reflectors are observed under DCGs in eastern DPM. Despite this fact, similar large-scale gross morphology is observed between DCGs across the region.

The application of the Parsons flow model to these DCGs provides tough constraints on the basal slope required to replicate surface topography. The slope called for by the model is reconciled with the slope observed by SHARAD where available and provides a first-order estimate where SHARAD does not observe the base. Preliminary results show similar basal slopes required for lobes in east and west DPM, suggesting that differing radar results do not correlate with basal geometry.

In addition, the Parsons model provides an estimate for flow timescales given certain assumptions about rheology and climate. A comparison of results from DCGs across DPM provides clues as to the relative timing of glacial events, as well as the possibility of varied degrees of post-emplacement ice loss and debris layer interaction. These results shed light on the interpretation of radar results in DPM and in turn upon the glacial history of the region.

Keywords: glaciology, planetary, modeling, ice, flow, climate, radar, geophysics

SETP
U

Understanding the role of strike-slip faulting as oceans close, north central Turkey

bridgetpettit@utexas.edu
Pettit, B., Jackson School of Geosciences, The University of Texas at Austin, Austin, TX
Catlos, E., Jackson School of Geosciences, The University of Texas at Austin, Austin, TX
Elliot, B., Bureau of Economic Geology, The University of Texas at Austin, Austin, TX

The goal of this project is to compile and interpret remotely sensed imagery and produce maps intended to lessen hazards associated with Turkey's North Anatolian Shear Zone (NASZ). These hazards include landslides and rock falls due to seismic activity. The NASZ contains the North Anatolian Fault, a right lateral strike slip fault extending approximately 1200 km in length. The NASZ is speculated to have accommodated from 25 to 110 km of displacement, depending on location. In the proposed field area, the shear zone is comprised of five major strands: Erbaa, Tosya-Ladik, Niksar-Kalekoy, Erzincan, and Tasova-Tekke faults with a combined estimated displacement of ~80 km. These strands, although named after villages and towns along the NASZ, do not have consistent names in the geological literature. The range of names highlights the fact that many details of these structures are unknown. By looking at surface expressions, it is possible to identify the extent of each fault and their relationship to one another; the resulting maps help to understand the tectonic history and identify geohazards of the region. To produce these maps, aerial photographs, Digital Elevation Models (DEMs), geological maps, and strike and dip data of the field area are compiled. Locations, extent, and type of faulting are proposed based on data visible in the maps. The final step is to visit the proposed locations in outcrop and update the map according to the results. As an outcome, a series of maps have been produced that focus in the region around the town of Amasya.

Keywords: North Anatolian Shear Zone (NASZ), Turkey, geohazards

EG
ECG

A Combined Stratigraphic, Architectural, and Ichnologic Analysis of the Loyd Sandstone (Late Cretaceous) Near Rangely, Colorado

timothy.h.prather@utexas.edu
Prather, T., Bureau of Economic Geology, University of Texas at Austin, Austin, TX
Flaig, P., Bureau of Economic Geology, University of Texas at Austin, Austin, TX
Burton, D., Anadarko Petroleum Corporation, Denver, Colorado
Hasiotis, S., University of Kansas, Lawrence, Kansas

The type locality of the Loyd Sandstone member of the Buck Tongue of the Mancos Shale (Loyd) is located 100 km northeast of Rangely, CO near Hamilton. Subsurface correlations indicate that Loyd-equivalent strata are exposed in outcrops near Rangely. We describe the facies, ichnology, and architecture of the Loyd near Rangley to determine the paleodepositional environment represented in outcrop. This approach reveals that abundant foresets built by traction-dominated underflows (hyperpycnal flows) indicate that the Loyd delta should be classified as river-dominated. However, a high abundance and high diversity trace fossil assemblage, deeply penetrating burrows, and flaser-wavy-lenticular bedded mud between foresets is evidence that the delta front experienced recurring, extended periods of slow sedimentation and oxygen-rich marine water influx during which marine fauna flourished and tidal and wave forces dominated.

North of Rangley, the Loyd thickens laterally from a sub-meter scale sand bed to a 20+ m-thick succession. The basal contact of the Loyd is gradational with the underlying Buck Tongue of the Mancos, displaying a classic upward-coarsening succession typical of deltas. Facies include: muddy-siltstones, low-angle planar laminated sandstones interbedded with flaser-wavy-lenticular bedded muds, and gradational to erosively-based trough cross-stratified sands. Interpreted depositional environments include prodelta, delta front, distributary mouth bars, and distributary channels. Low angle planar lamination in delta foresets is the dominant sedimentary structure and mirrors the sequences documented from other described river-dominated deltas. Trough cross-stratified sands the top of the Loyd are interpreted as mouth bars and subaqueous to subaerial distributary channels. The trace fossil assemblage that includes Ophiomorpha, Thalassinoides, Planolites, Schaubcylindrichnus, Palaeophycus, Diplocraterion, Helminthopsis, and Bergaueria is uncharacteristically high in diversity for a delta that sedimentary structures and architectures indicate to be river-dominated.

Although the Loyd has many characteristics typical of a river-dominated delta, care should be taken when assigning this classification. Closer inspection may reveal that much time is recorded by relative quiescence on the delta front, a characteristic not typically associated with river dominance.

Keywords: Delta, Loyd, Ichnology, Cretaceous, Transitional Environments

SETP
LCPHD

Influence of structural complexities on low-angle normal fault slip rates

mprior@utexas.edu
Prior, M., Department of Geological Sciences, The University of Texas at Austin, Austin, TX
Stockli, D., Department of Geological Sciences, The University of Texas at Austin, Austin, TX

Calculating fault slip rates with thermochronometry is an often-applied method in both contractional and extensional tectonics. Within extensional settings the timing, magnitude and rates of extension can be determined using thermochronometry, but several structural processes can significantly complicate the interpretation of these data. Many key ideas about continental extension and the structural evolution of low-angle normal faults were formulated in the Colorado River extensional corridor (CREC) of eastern California and western Arizona where continental crust is extended along regional low-angle normal fault systems that accommodated up to 40-50 km of displacement. The timing, magnitude, and rates of extension along low-angle normal faults are predominantly constrained with thermochronometry in the absence of unambiguous offset marker units; therefore understanding how low-angle normal fault systems evolve and accommodate exhumation of mid-crustal rocks relies on accurate thermochronometric measurements.

Previous authors have interpreted very rapid slip rates of up to ~30 km/Myr from apatite (U-Th)/He dating in the Harcuvar Mountains core complex, but whether these estimates are reasonable or accurately measure fault slip rates is questionable. The Harquahala Mountains core complex is directly south of the Harcuvar Mountains and the southernmost exposure of Tertiary mylonites exhumed along a regional low-angle normal fault system that connects the lower plate of the Chemehuevi, Whipple, Buckskin-Rawhide, and the Harcuvar Mountains. The regional setting of the Harquahala Mountains makes it a key location to test the validity of rapid slip estimates and understand the pattern of extension within the CREC as a complete system. An ~45 km transect of samples for zircon and apatite (U-Th)/He dating (n=23) was collected from the Harquahala footwall along the regional extension direction of ~060° to determine the cooling history associated with core complex exhumation and slip along the Eagle Eye detachment (EED). Zircon (U-Th)/He ages (ZHe) plotted versus distance from the EED display three key characteristics: **1)** samples furthest from the EED record older, pre-extension cooling ages of ~40-50 Ma, **2)** a decrease in ZHe ages through a fossil partial retention zone (PRZ), and **3)** ten nearly invariant ages that decrease from 17.6 ± 0.3 to ~15-16 Ma over the last 22 km and record cooling due to slip on the EED. The inflection point between the PRZ and ZHe ages recording fault slip indicates extension began at ~17-18 Ma in the Harquahala Mountains and that the Eagle Eye detachment accommodated ~22 km of displacement. An inflection point in cooling ages is rarely observed in core complexes and indicates extension starts later in the Harquahala Mountains and the EED accommodates less displacement than structurally lower core complexes (e.g. Buckskin-Rawhide Mountains).

Standard linear regression of the nearly invariant ZHe ages yields slip rates of up to ~50 km/Myr which are interpreted as geologically unreasonable, whereas rates of ~10-16 km/Myr are calculated by simply taking the 22 km distance over the ZHe age difference. Apatite (U-Th)/He ages along the same transect distance show one slope that yields a slip rates of 4.3 +1.6, −1.0 km/Myr. Several structural possibilities that could cause invariant age profiles in thermochronometric studies are investigated to better interpret scenarios where a simple regression is not valid. The most probable scenarios include isostatic rebound, pervasive hanging wall thinning during fault slip, and repetition or perturbation of cooling profiles along high or low-angle faults. An inherent assumption when calculating slip rates is that the hanging wall behaves as a rigid block; therefore structural thinning of the hanging wall will cause an overestimation of slip rates. Hanging wall extension can also cause isostatic rebound of the footwall and may contribute a significant component of vertical exhumation. Coeval or subsequent low and high-angle faulting can also alter otherwise linear age versus distance relationships and are most pronounced in under sampled transects that can overestimate slip rates. Geometric and thermal modeling may provide new constraints on the relative importance of the aforementioned processes and give new insights into the structural evolution of low-angle normal fault systems.

Keywords: Harquahala Mountains, core complex, (U-Th)/He, low-angle normal faults, slip rates

SETP
LCPHD

(U-Th)/He and U-Pb double dating constraints on the interplay between thrust deformation and basin development, Sevier foreland basin, Utah

edgardopujols@utexas.edu
Pujols, E., Jackson School of Geosciences, The University of Texas at Austin, Austin, TX
Stockli, D., Jackson School of Geosciences, The University of Texas at Austin, Au
Horton, B., Jackson School of Geosciences, The University of Texas at Austin, Au
Steel, R., Jackson School of Geosciences, The University of Texas at Austin, Au
Constenius, K., Independent researcher

The degree of connectivity between thrust-belt deformation and foreland basin evolution has been a matter of debate for decades. This is in part due to the lack of chronological constraints on thrust-belt deformation and depositional ages. Moreover, hiatus in the stratigraphic record, limited exposures, scarce fossils and constant sediment recycling obscure our ability to make basin-wide chronostratigraphic correlations. This research is employing zircon (U-Th)-(Pb-He) double dating on pre- and syn-tectonic sediments along the Sevier thrust front and basin to provide an unprecedented geochemical framework, which will be used to temporally and spatially link the Sevier foreland basin stratigraphy to nearby sources. These new data shed light on the in-depth connectivity and feedback relationships between foreland basin and thrust belt dynamics, the temporal aspect of thrusting and clastic progradation, sediment sources, basin subsidence, and stratigraphic architecture. Preliminary results from samples in the hinterland and foreland basin substantially improve current constraints on the timing and magnitude of deformational events and sediment dispersal. The hinterland (U-Th)/He zircon (zHe) ages from the Charlestone-Nebo Salient (CNS) and Canyon Range (CR) preserve two different exhumation phases. The CNS records a fast cooling event at 93 ± 4Ma, whereas the CR records a zHe partial retention zone with ages as young as Santonian. These hinterland ages additionally constrain the youngest possible detrital populations derived from these two provinces. The most proximal deposits along the CR- and CNS- strike synchronously record short zHe depositional lag-times associated with fast exhumation (>1km/my) during the late Albian and Coniacian-Santonian times. However, during periods of slow exhumation, the zHe depositional lag-times in those stratigraphic sections substantially increase in scatter, which can be explained by heterogeneous unroofing, changes in drainage patterns and basin compartmentalization. In the Book Cliff section the youngest detrital zHe ages appear to be sourced from an area with a different cooling history than the Sevier thrust front. Nonetheless, the overall cooling history recorded in the Book Cliff sedimentary succession is linked to exhumational pulses during orogenic construction in the hinterland. Analyzing the youngest detrital zHe ages from time-equivalent strata, in the Book Cliff, we identified three third-order orogenic cycles. Their timing and magnitude seem to correlate with fast clastic progradational cycles. These results substantiate the role played by hinterland deformation on foreland basin architectural changes.

Keywords: Foreland basin evolution, thrusting, (U-Th)/(He-Pb) double dating

EG
ECG

An Integration of Core Description, Petrography, and Geochemistry to Define Stratal Architecture and Paleoceanographic Conditions of the Mississippian Barnett Formation in the Southern Fort Worth Basin of North-Central Texas

lauren.redmond@utexas.edu
Redmond, L., Bureau of Economic Geology, The University of Texas at Austin, TX
Loucks, R., Bureau of Economic Geology, The University of Texas at Austin, TX
Rowe, H., Bureau of Economic Geology, The University of Texas at Austin, TX

The Mississippian Barnett Formation is a shale-gas system located in north-central Texas that was deposited over a 25-m.y. period in the Fort Worth Basin, a foreland basin resulting from the collision of Laurasia and Gondwana. The basin is bounded to the west by the Bend Arch, to the south by the Llano Uplift, to the east by the Ouachita fold and thrust belt, and to the north by the Red River and Muenster Arches. The main producing area is the Newark East field located in the northern Fort Worth Basin. This area has been extensively studied since initial production began in the 1980s, other areas of the basin however are far less studied. The objective of this study is to unravel the stratigraphic architecture, depositional setting, and lithofacies of the thermally-immature Barnett Formation in the southern Fort Worth Basin.

To conduct this investigation, a suite of 30 cores were described, thin-sections were analyzed, and energy dispersive x-ray fluorescence (XRF) analysis for major and trace element concentrations were completed on several cores at a 2-inch scanning interval using the core face. Currently, geochemical and thin-section petrologic data has been obtained for the Houston Oil and Minerals No. D-6-1 Petty core in Brown County. In addition to these methods, x-ray diffraction for bulk mineralogical composition, total organic carbon, and total inorganic carbon are being analyzed. Data from this investigation will be used to: 1.) Integrate core descriptions and geochemistry to define facies, 2.) Correlate these facies regionally to construct the stratal architecture, and 3.) Interpret the paleoceanographic conditions during the deposition of the Barnett Formation.

The Barnett Formation is a siliceous mudstone unit; via thin-section inspection three lithofacies and one diagenetic facies were observed: peloidal argillaceous siliceous mudstone, skeletal packstone, phosphatic packstone, and pseudosparite. Preliminary XRF data shows Si concentrations varying around 30% throughout the formation, there are also Ca excursions where the concentration approaches 40%. Covarying enrichments in redox-sensitive trace elements U, Ni, V, and Mo are present at various depths. This indicates that these Barnett strata were deposited in oxygen-poor or anoxic conditions. Phosphorus enrichments were also observed at these intervals, further evidence of anoxia. Some biota evidence consisting of transported brachiopod, crinoid, and benthic foraminifera fragments suggests that some sediments were supplied from a shallower water carbonate setting on a slope. These allochems were not noted in studies of the deeper, more restricted Barnett mudstones. Therefore, the Barnett in the southern Fort Worth Basin was deposited in an anoxic setting but it was not as restricted as the northern Fort Worth Basin.

Keywords: Barnett Formation, Mississippian, stratal architecture, paleoceanographic conditions, XRF

EG
ECG

Signal Recovery Beyond the Nyquist

kregimbal@utexas.edu
Regimbal, K., Bureau of Economic Geology, The University of Texas at Austin, Austin, TX
Fomel, S., Bureau of Economic Geology, The University of Texas at Austin, Austin, TX

The digital sampling interval of seismic signals is associated with the maximum recoverable frequency in the signal, which is known as the Nyquist frequency. Aliasing occurs if frequencies above the Nyquist exist in the input signal prior to sampling. The higher frequencies will be irretrievably mixed with low frequencies below the Nyquist. This paper provides a strategy that recovers frequencies above the Nyquist without immensely increasing the data volume. In conventional processing, the Nyquist frequency places an upper limit on recoverable, unaliased signal. I introduce a new application of shaping regularization to demonstrate that it is possible to accurately recover frequency beyond the Nyquist and overcome aliasing. The proposed method uses shaping regularization to recover frequencies beyond the Nyquist in the context of NMO and stack. Regularization methods are used in ill-posed geophysical estimation problems. The main idea of regularization is to impose additional constraints on the estimated model. Shaping regularization implies a mapping of the input model to the space of acceptable functions. This type of regularization is integrated in a conjugate-gradient algorithm for iterative least-squares convergence. Shaping regularization is applied to synthetic and real data from the North Sea. The results suggest that temporal aliasing is eliminated and the resolution of the final image is improved.

Keywords: Nyquist, shaping regularization, NMO

CCG
LCMS

Variability in methane production from Texas coastal wetland systems

aresovsk@gmail.com
Resovsky, A., The University of Texas at Austin, Austin, TX

Methane is an important greenhouse gas, and the predominant source of natural methane globally is its production in wetland soils. Subtropical wetlands compise over six million acres of land in coastal Texas and thus may represent a significant component of the global climate system. Despite the importance of these areas, high spatial and temporal variability in emissions and a lack of reliable in-situ measurements makes their precise contribution to the global carbon budget uncertain.

This M.S. research aims to describe the environmental factors that influence methane emissions from natural wetlands in Texas at seasonal and interannual timescales. It furthermore explores the applications of GIS-based data assimilation in the development of a process-based regional emissions model. Such a framework could aid in predicting the response of Texas wetlands under future climate projections.

Keywords: Climate, methane, wetlands, subtropical, Texas, hydrology

SETP
U

Dating the Menghai Batholith, Southern China

enrique.reyes@utexas.edu
Reyes, E., Jackson School of Geosciences, The University of Texas, Austin TX
Catlos, E., Jackson School of Geosciences, The University of Texas, Austin TX
Brookfield, M., School for the Environment, University of Massachusetts at Boston, Boston MA
Shin, T., Jackson School of Geosciences, The University of Texas, Austin TX
Stockli, D., Jackson School of Geosciences, The University of Texas, Austin TX

Paleogeographic reconstructions are used to determine the evolution and migration of Earth's continents, identify important economic resources that formed during specific times in Earth's history, and assess geological hazards that result due to reactivation of older faults or mass movement of rocks. The goal of this study is to improve our understanding of the complex tectonic history of southern China by constraining the timing of crystallization and uplift of the Menghai batholith, a suite of metaluminous and peraluminous granodiorites on the Shan Plateau. We aim to obtain U-Pb zircon ages from 8 samples of the batholith to decipher its tectonic and magmatic history and relationship to surrounding areas. The batholith is part of the Lancangjiang belt, a principle boundary between Gondwana and Eurasia, on the eastern side of China's Shan Plateau, an encompasses the southern extension of the Lincang Granite group. A few U-Pb zircon ages have been reported for the Lincang granite, timing emplacement during the Upper Triassic. Prior to this study, no U-Pb ages exist for the Menghai batholith. Zircon grains were separated from rock samples from the study area and have been dated using Laser Ablation-Inductively Coupled Plasma-Mass Spectrometry. From LA-ICP-MS data, zircon rim ages are from 207.6 +/- 8.9 Ma and 254.1+/- 4.7 Ma, constraining crystallization to throughout most the Triassic period, starting as early as the end of the Permian. Core ages for some zircons range from 434.8+/- 6.0 Ma to 3187.0+/- 23.0 Ma. In addition to the ages, petrographical work will be done to assess microstructures. Overall, reliable age data from the Menghai batholith will aid in determining the tectonic and magmatic history of the region, including understanding the dynamics of ancient Tethyan ocean closure in southern China.

Keywords: granitoids, exhumation, thermochronology, zircon, batholith,

EG
LCMS

Hierarchical Cluster Analysis of a High-Resolution XRF Dataset from the Cline Shale, Midland Basin, TX

reedroush@gmail.com
Roush, R., Bureau of Economic Geology, The University of Texas at Austin, Austin, TX
Hamlin, S., Bureau of Economic Geology, The University of Texas at Austin, Austin, TX
Rowe, H., Bureau of Economic Geology, The University of Texas at Austin, Austin, TX

The Cline Shale is an organic-rich mudrock deposited in the Midland Basin during the Upper Pennsylvanian. X-ray Fluorescence (XRF) data were collected at 2-inch intervals from four cores of the Cline. The XRF dataset consists of the weight % of 28 elements at more than 1900 data points. The XRF dataset was statistically analyzed using an agglomerative hierarchical cluster analysis method with Tibco Spotfire. Hierarchical cluster analysis is a statistical method that groups like data points into clusters based upon their entire elemental signature simultaneously; this method is a comprehensive tool that statistically separates the data using all of the information available. For this cluster analysis, Ward's method was used, and the elemental percentages were normalized from 0-1.

Facies were delineated by evaluating empirical relationships of elements to determine both mineralogy and organic matter content of each facies. Concentrations of Si, Al, and Ca were compared to quartz and feldspars, clays, and carbonates respectively from XRD to determine the mineralogy of each cluster. Ni, Cr, and Zn were plotted vs TOC to find empirical cutoffs of organic matter content. From these relationships, we can assign geologic names to statistically derived geochemical clusters.

Keywords: Cline Shale, Midland Basin, XRF, Cluster Analysis, Geochemistry

CCG
ECG

Investigating Rainfall Changes in the SPCZ using Cave Deposits from the Solomon Islands in the Western Tropical Pacific

nsekhon@utexas.edu
Sekhon, N., University of Texas Institute for Geophysics, The University of Texas at Austin, Austin, TX
Quinn, T., University of Texas Institute for Geophysics, The University of Texas at Austin, Austin, TX
Partin, J., University of Texas Institute for Geophysics, The University of Texas at Austin, Austin, TX

The South Pacific Convergence Zone (SPCZ) is the largest band of rainfall in the Southern Hemisphere that provides the majority of the perennial precipitation for the South Pacific Island nations. Rainfall associated with SPCZ varies on different timescales from seasonal to interannual; recent studies provide strong evidence that it fluctuates on decadal and multidecadal scales as well. This study will investigate multidecadal rainfall oscillations that can dramatically affect climate on human life span timescales by altering water resources and fisheries in regions throughout the Pacific Ocean. To better understand multidecadal climate variability in the region, we will use carbonate $\delta^{18}O$ (proxy of rainfall variability) in speleothems from caves in the Solomon Islands, a location where rainfall is strongly associated wit the SPCZ . Well-preserved stalagmites collected in 2012 from Munda, Western Solomons (8.3° S, 157.3° E) and Florida Islands, Central Solomons (9.8° S, 160.2° E) are the archives that we use in this study. The Munda stalagmite dates between 1825 A.D. and 1937 A.D, and the Florida Islands stalagmite dates between 1637/1517 A.D and 1437 A.D, allowing us to generate sub-annually resolved reconstructions of rainfall over different time periods from the last several centuries. Future work from this research will focus on using multiple stalagmites from the western, tropical Pacific to study the spatial relationships in the changes of rainfall on multidecadal timescales. Hopefully, the results of this research will help to understand the mechanisms behind multidecadal climate variability, which may allow for better predictions of future climate change.

Keywords: Paleoclimatology, Stalagmites, Stable Isotopes, SPCZ, Decadal Variability

SETP
LCPHD

Garnet (U-Th)/He thermochronometry and its application to exhumed high-pressure low-temperature metamorphic rocks

spencer.seman@utexas.edu
Seman, S., Department of Geological Sciences, The University of Texas at Austin, Austin, TX
Stockli, D., Department of Geological Sciences, The University of Texas at Austin, Austin, TX
Smye, A., Department of Geological Sciences, The University of Texas at Austin, Austin, TX
Hernandez-Goldstein, E., Department of Geological Sciences, The University of Texas at Austin, Austin, TX

The timing of cooling and exhumation of HP-LT metamorphic terranes has traditionally been constrained by a combination of white-mica $^{40}Ar/^{39}Ar$ and lower temperature (U-Th)/He techniques (e.g. apatite and zircon). However, the interpretation of $^{40}Ar/^{39}Ar$ data from phengite is often clouded by complex multi-stage growth histories and extraneous Ar contamination. This leaves a significant 'gap' between 200-400°C for which there are no well-characterized thermochronometers. In the depressed geothermal gradient which characterizes subduction zone settings, cooling through this thermal window should be coincident with exhumation from mantle depths. Several newly developed (U-Th)/He thermochronometers, magnetite, rutile, and specifically garnet are sensitive to cooling through this temperature interval. Garnet is a common, rock-forming phase in HP-LT assemblages across a variety of bulk compositions, making it a particularly attractive thermochronometric tool. We present new age determinations and diffusion data from 'ideal' case skarn derived grossular-andradite as well as HP-LT almandine from the Cycladic Blueschist Unit of Syros Island, Greece. Grossular-andradite compositions sourced from skarns are particularly tractable to the (U-Th)/He method due to their relatively high U concentrations (1-100's ppm). Diffusion experiments on a range of grossular-andradite compositions from various localities yield closure temperatures from 180 – 300 °C, with no strong correlation to garnet composition. Unlike skarn derived garnet, the concentrations of alpha producing U, Th, and Sm in HP-LT garnet are inherently low (<< 1 ppm). Therefore, the vast majority of measured parent and daughter are sourced from inclusions, specifically allanite, zircon, and apatite in this locality. The relatively 'slow' diffusion kinetics of garnet relative to inclusions allows the host garnet to act effectively as a helium 'bottle'. Samples yield reproducible ages which trend older than ZHe and AHe from Syros and are consistent with experimentally determined diffusion kinetics. Furthermore, diffusion experiments on varying size fractions of garnet yield appropriate shifts in the D_0/a^2 term, confirming that the diffusion domain is hosted within the garnet grain and not simply the inclusions. Lastly, we combine garnet (U-Th)/He data with rutile U-Pb, ZHe, and AHe data in order to inverse model the retrograde time-temperature history of the CBU of Syros Island.

Keywords: (U-Th)/He, thermochronometry, garnet, high-pressure low-temperature, blueschist, eclogite, Cyclades

SETP
LCMS

Apatite U-Pb thermochronometry applied to a fossil hyperextended rift margin in Corsica

nikki.m.seymour@utexas.edu
Seymour, N., The University of Texas at Austin, Austin, TX
Smye, A., The University of Texas at Austin, Austin, TX
Stockli, D., The University of Texas at Austin, Austin, TX

Present thermal evolution models of magma-poor continental rifting are based on pure-shear extension (McKenzie, 1978), in which crustal and mantle strain is co-located and all rocks experience continuous cooling throughout rifting. Conversely, the multi-phase rift model of Lavier and Manatschal (2006) accommodates lithospheric extension via spatially offset crustal and mantle strain, producing depth-dependent thinning and exhumation of lithospheric mantle. Significant reheating of the upper plate is a predicted consequence of mantle exhumation. This study will constrain the time-temperature (t-T) history of the upper-plate Tethyan margin via application of apatite U-Pb thermochronometry to discriminate between contrasting thermal models.

Modern magma-poor margins are not accessible for direct study, as they are located in deep water. Corsica preserves the hyperextended upper-plate distal margin of the Jurassic Tethys Ocean, a fossil analogue for modern margins. An exposed suite of upper crustal tonalites and lower crustal gabbronorites are juxtaposed by the Belli Piani Shear Zone, recently suggested to be active during Jurassic rifting (Beltrando et al, 2013). Greenschist-facies metamorphism during Alpine Orogeny reset zircon (U-Th)/He and zircon fission track thermochronometers, creating a need for higher-temperature methods. Apatite is the only mineral abundant throughout both upper and lower crustal units, making it uniquely suited to capture the thermal history of the entire crustal section. When coupled with rutile U-Pb and zircon U-Pb thermochronometry, apatite U-Pb provides a new opportunity to examine thermal histories in regions that experienced amphibolite and granulite conditions, such as the lower crust of hyperextended rift margins. Differences in apatite (T_C = 400-450°C) and zircon U-Pb (T_C = >800°C) ages in metamorphosed terranes reflect cooling and crystallization ages, respectively, and provide the necessary test for reheating of the Corsican margin. Inversion of rounded [Pb] profiles produced by thermally-activated volume diffusion of Pb from the apatite lattice permits modeling of t-T histories (e.g. Smye and Stockli, 2014). Initial results show 200 Ma cores with 150 Ma rims, consistent with zircon U-Pb metemorphic rims and rutile U-Pb (T_C = 400-500°C) concentration profiles. Together these data point to a rift-coeval reheating event in the upper plate, as predicted by the Lavier and Manatschal model.

Keywords: apatite U-Pb, thermochronology, tectonics, rifting, Corsica

EG
LCMS

Architecture of Coarse Grained (Conglomeratic) Deep Water Lobes at the Base of a Sandstone Dominated Fan, Jurassic Los Molles Formation, Neuquén Basin, Argentina

mshin@utexas.edu
Shin, M., Jackson School of Geosciences, The University of Texas at Austin, Austin, TX
Olariu, C., Jackson School of Geosciences, The University of Texas at Austin, Austin, TX
Steel, R., Jackson School of Geosciences, The University of Texas at Austin, Austin, TX

The complex structural and stratigraphic framework of the Neuquén Basin affected by Triassic-Jurassic extensional processes formed a deep basin and accumulated coarse-grained gravity flow deposits on the lower slope and basin floor. Lower Los Molles Formation exposes the succession of turbidites from conglomerates to mudstones over a 9 km outcrop belt. The Los Molles Fm. is over 1000 meters thick and its base is ~100 meters consisting of 3 units capped by 1-3m thick conglomerates. This initial deep water fan units start with unusual pebble- and cobble-rich conglomerate beds at its base. To characterize the conglomerate lobes and their link with the other basin-floor lobe complexes, satellite images, DEM (Digital Elevation Model), photomosaics (a few km), and about 20 measured sections have been collected and interpreted. In all units measured, each lobe contains, from bottom to top, very coarse, poorly sorted, and erosional-based conglomerates (1-3m) overlain by amalgamated, normal graded turbidite sandstones (20-30m), and silty mudstones (up to 10m). Each of these 3 facies forms a succession (about 30-40 m thick) of lobe complexes with an overall fining upward trend. The conglomerate thickness and lateral extent decreases upwards as the third (uppermost) conglomerate layer demonstrates rather discontinuous, lenticular bodies. In contrast, the sandstone increases upward in thickness and has finer grain size and better sorting. The conglomerates are interpreted as debris flow deposits based on their structureless and poorly sorted texture. However, few conglomerate deposits are at times erosional at the base, poorly sorted throughout, but some capped by normal grading for up to a third of their thickness. Normal grading suggests debris flow transforms into turbidity flow vertically. Flute marks associated with conglomerate beds indicate paleoflow toward the east, in contrast to the younger sandy fans that prograded dominantly north-northeastwards. The Var River system in southern France is a modern analog with pebbles and cobbles transported to deep water via steep gradient slope. Similarly, coarse sediments in the Los Molles Fm. bypass the shelf and steep slope to build the initial conglomerate base of the fan. In summary, the earliest Los Molles conglomeratic fans are linked with high relief of the basin margin that later decreased and formed sandstone dominated fans.

Keywords: Lobe, Architecture, Facies, Conglomerate, Deep water, Jurassic, Los Molles Formation, Neuquén, Argentina

PS
ECG

Compiling the evidence for an ancient Martian ocean: the spatial distribution of terrestrial deep-water analogs on Mars

katherineshover@gmail.com
Shover, K., Bureau of Economic Geology, The University of Texas at Austin, Austin, TX
Moscardelli, L., Bureau of Economic Geology, Jackson School of Geosciences, The University of Texas at Austin; now at Statoil North America–Research, Development and Innovation in Austin, TX
Wood, L., Bureau of Economic Geology, Jackson School of Geosciences, The University of Texas at Austin, TX; now at Colorado School of Mines, Golden, CO

The controversial hypothesis of an ancient ocean on Mars has prompted researchers to explore lines of evidence that support this idea by connecting Martian features to potential terrestrial analogs, from large-scale polygonal terrains to massive boulders that may have been transported through underwater mass-transport events. Mapping the distribution of such features provides another avenue for exploring these potential indicators of a hypothetical ocean on Mars. Systemic mapping of features in the Northern Plains of Mars that have been linked to terrestrial deep-water analogs, in addition to other deposits and geomorphologic elements associated on Earth with oceans, will be pursued to establish their spatial distribution within the context of a hypothetically Late Hesperian-Early Amazonian ocean.

Keywords: Mars, geomorphology, deep-water deposits, spatial mapping

SETP
ECG

Evaluating the consistency of experimental paleopiezometers using naturally deformed rocks

pamela.speciale@utexas.edu
Speciale, P., Jackson School of Geosciences, The University of Texas at Austin
Behr, W., Jackson School of Geosciences, The University of Texas at Austin

The magnitude of stress in the continental lithosphere, particularly the lithospheric mantle, is highly uncertain and frequently debated, but is critical to understanding continental mechanics. Differential stress can be estimated using paleopiezometry, which is an inverse relationship between the recrystallized grain size formed during dislocation creep and the flow stress. This relationship has been quantified experimentally for a wide range of earth materials, including olivine, orthopyroxene (OPX), quartz and feldspar.

We examine quartz + feldspar (mid-crustal rocks) and olivine + OPX (upper mantle rocks) recrystallized grain sizes to determine how consistent the experimental piezometers for these mineral pairs are with one another. Measurements focus on regions within each sample that a) show no significant grain growth, b) do not exhibit phase mixing, and c) represent isoviscous deformation. Our sample suite includes rocks from exhumed shear zones, metamorphic core complexes, and mantle xenoliths that represent a variety of pressure and temperature conditions. We establish stress (σ)–grain size (d) relationships for naturally deformed feldspar ($\sigma=177d^{-.66}$) and OPX ($\sigma=397d^{-.52}$), based on the well-established experimental piezometers for quartz and olivine, respectively.

The existing quartz and feldspar piezometers predict similar stress magnitudes (within ~15-25 MPa), especially for grain sizes near those of the experimental calibrations. The OPX piezometers predict OPX grain sizes to be larger than olivine at high stresses. Our observations of natural rocks, however, show the opposite relationship: OPX grain sizes are smaller than olivine at stresses above ~25 MPa. Comparison of the OPX piezometer with olivine indicates that stress estimates correlate best for grain sizes near those of the experimental calibrations, but do not correlate well at high stresses, with stress differences >60 MPa.

Our naturally constrained piezometers can be used to estimate stress magnitudes in rocks such as granulites and pyroxenites wherein feldspar or OPX are the primary recrystallized phases and quartz or olivine are unsuitable. More experimental work, as well as additional analyses of naturally deformed rocks, would help to better constrain the stress–grain size relationships in middle to lower crustal and upper mantle rocks

Keywords: paleopiezometer, dynamic recrystallization, olivine, orthopyroxene, quartz, feldspar

EG
ECG

Elastic wave-vector decomposition in orthorhombic media

sripanichy@utexas.edu
Sripanich, Y., Bureau of Economic Geology, The University of Texas at Austin, Austin, TX
Fomel, S., Bureau of Economic Geology, The University of Texas at Austin, Austin, TX
Sun, J., Bureau of Economic Geology, The University of Texas at Austin, Austin, TX

The problem of wave-mode separation and vector decomposition aim to separate full elastic wavefield into three wavefields with each corresponding to each wave mode in anisotropic media. This process is of great significance because geo- physicists tend to handle each wave mode independently when applying imaging techniques. Several of previously proposed methods to accomplish this task are based on the knowledge of the polarization vectors of all three wave modes in a given anisotropic medium. In this study, I consider only the wave-vector de- composition method where the wavefield is separated in the wavenumber domain via the analytical decomposition operator. To extend the elastic vector decomposition method to orthorhombic media, I first show that the most appropriate way to define the two shear modes is to sort them based on phase velocity, which is equivalent to dividing the shear-wave phase-slowness surfaces along the point singularity. I subsequently show that we can locate point singularity using an analytical condition derived from the exact phase-velocity expressions for shear waves. This condition will allow us to approximate the proximity to a point singularity and to define the area in which we will apply a smoothing operator to reduce the planar artifacts cause by the local discontinuity of polarization vectors at the singularity. The proposed method leads to an effective decomposition of the two shear modes in the wavenumber domain with reduced planar artifacts.

Keywords: elastic, anisotropy, orthorhombic, shear waves

CCG
LCMS

Morphological data for 'Cryptagama aurita' Yield New insights into the endemic Australian agamid lizard radiation

stilson@utexas.edu
Stilson, K., Jackson School of Geosciences, The University of Texas at Austin, TX
Maisano, J., Jackson School of Geosciences, The University of Texas at Austin, TX
Mead, J., Department of Geosciences, East Tennessee State University, TN
Bell, C., Jackson School of Geosciences, The University of Texas at Austin, TX

The endemic Australian agamid lizard fauna represents a diverse and biogeographically interesting radiation that remains poorly understood. Phylogenetic analyses of both morphological and molecular data yield alternative hypotheses for relationships within the endemic radiation. Numerous fossil deposits across the continent contain fossilized remains of agamid lizards, but those materials remain unpublished and poorly studied. Adequate understanding of the fossil record and holistic perspectives on phylogenetic relationships within the group require detailed knowledge of skeletal morphology. Morphological data are deficient for the majority of Australian agamids and are completely absent for several taxa. One of those is the rare and enigmatic *Cryptagama aurita*. The species is known from only four specimens; a fifth individual recently was photographed, but not collected nor tissued. There are no tissues available, and no skeletal preparations exist. We CT scanned two specimens of *Cryptagama aurita*, including a relatively large individual, and an obviously juvenile specimen. *Cryptagama aurita* shares several features of the skull and mandible only with the bizarre thorny devil, *Moloch horridus*. Those characters include a lingual process of the coronoid bone that does not extend ventrally to the lower margin of the mandible, lack of caniniform teeth (also possibly absent in *Chelosania*), a reduced nasal that weakly meets the facial process of the maxilla, a weakly developed ventrolateral process of the basioccipital, and a flattened quadrate process of the pterygoid. Those features are not shared by any other endemic Australian Agamids, are absent in the outgroups to that clade (e.g., *Physignathus*, *Agama*), and represent a derived condition within the Australian clade. These data provide the first hard evidence for a close relationship between *Cryptagama* and *Moloch*.

Keywords: morphology, osteology, phylogenetics, agamidae, Australia

SETP
U

Investigating tectonically-driven fluid flow through fractured carbonates from the Erbaa-Niksar pull-apart basin, Turkey

colinsturrock@gmail.com
Sturrock, C., Department of Geological Sciences, University of Texas at Austin, Austin, TX
Catlos, E., Department of Geological Sciences, University of Texas at Austin, Austin, TX

This study investigates fluid flow through fractured carbonate rocks collected along strands of the North Anatolian Fault (NAF) in north central Turkey. The research objectives for this study are to: (1) describe the number and types of fracture generations in these rocks and their relationship to each other, (2) determine the source of fluids that worked to precipitate minerals filling in fractures, and (3) determine the number and extent of geochemically distinct fluid flows throughout the sampled region. Samples from the NAF have been petrographically analyzed using transmitted light and cathodoluminescence (CL) imaging to determine the range of potential mineral generations within individual veins, and fracture relationships. I am now focusing on a few (2-3) ideal specimens for geochemical analysis. Fluid inclusion analysis is underway on two samples in which fluid inclusions have been found, to determine entrapment conditions and temperature of vein mineralization. Preliminary isotope data attained through conventional methods for whole, individual veins have shown variation in δ13C from -7.4 to 0.02 +/- 0.05 per mil (v. PDB), while δ18O v. PDB ranges varied from -8.12 to -8.79 +/- 0.05. The δ13C variation is interpreted as variability of fluid/host rock interaction, while the low variability in δ18O is indicative of similar fluid source for veins in the sampled region. SIMS stable isotope analysis of oxygen and carbon in calcite fills will be performed at UCLA in February to discern if differences exist across fluid generations seen in petrographic and CL analyses. In addition, trace element analysis via LA-ICP-MS has been performed for REE and Mn on line scans traversing the width of the veins. The line scans have shown compositionally distinct mineral generations, and REE diagrams plotted from the line scans show differing patterns for distinct areas. We hypothesize that (1) these rocks served as conduits for volatile rich fluid flow driven by tectonic events and (2) a range of fluids (including meteoric and deep-seated crustal fluids) are trapped within the carbonates that shed light into the evolution of the fracture network in this part of the NAF as the fault continues to move. These hypotheses are based on CL work already performed, that shows distinct zones of luminescence and quenching between separate mineral generations within a single vein. These differences in luminescence most likely represent differences in concentrations of REE's and/or Mn in the vein calcite, suggesting a change in fluid source during the mineralization of the vein. Source will be investigated through δ18O analysis via SIMS, and δ18O variations within veins will be compared between different samples to show fracture network connectivity laterally along the fault zone, and extent into the crust. Connectivity between lateral areas along the fault would show similar compositions in later fracture/mineral generations, while a propagation of the fracture network into deeper crustal levels would show in δ18O and REE patterns consistent with deeper crustal fluid reservoirs. The overall goal of this project is to determine how the fluid chemistry apparent within the calcite veins changes as later generations of minerals are crystallized, and to use this characterize the fracture network evolution within carbonates in this highly fractured region.

Keywords: fluid flow, calcite veins, stable isotopes, Turkey, strike slip fault

EG
LCPHD

Lowrank Elastic Modeling and Imaging Using Pure Wave Modes in Isotropic Media

junzhesun@utexas.edu
Sun, J., The University of Texas at Austin, Austin, TX
Fomel, S., The University of Texas at Austin, Austin, TX

Reverse-time migration (RTM) is a depth-imaging algorithm in which wavefields are extrapolated in time. Wavefield extrapolation, the numerical propagation of wavefield in time, is thus the kernel of RTM. A lowrank algorithm is an emerging technique that can be applied to wavefield modeling, which leads to highly accurate seismic imaging methods. I implemented 2D elastic reverse-time migration in isotropic media based on wavefield vector decomposition. I employ lowrank approximation to tackle the mixed-domain problems arise in wavefield propagation and wave mode separation, reducing the computational cost. Application of the lowrank elastic RTM to the Marmousi 2 data set demonstrates the advantages of performing imaging condition separately for different wave modes using multi-component data.

Keywords: seismic, elastic, modeling, imaging, migration

EG
LCMS

Analysis of the separation of diffractions and noise

ryan.swindeman@utexas.edu
Swindeman, R., The University of Texas at Austin, Austin, TX
Fomel, S., The University of Texas at Austin, Austin, TX

One of the largest benefits of using seismic diffractions is the ability to gather information from below seismic resolution. By separating the coherent reflectors, the process associated with diffraction imaging leaves behind a mixture of diffractions and noise. Unfortunately, this noise can be detrimental to the focusing process in velocity continuation which establishes time migration velocities. We seek to develop a new strategy to separate noise from the diffractions to produce a cleaner and more accurate image. Our method is applied before velocity continuation to the P-cable high-resolution, marine dataset to overcome some of the challenges with its noise and fault detection. We design a program in the Madagascar software package to create a parallel implementation of this workflow for cluster-based computation.

Keywords: geophysics, diffractions, noise, velocity, processing, data, reflectors, resolution

SETP
ECG

Natural and artificial radiation damage effect on confined track lengths

tamer@jsg.utexas.edu
Tamer, M., UT Austin, Technische Universitaet Bergakademie Freiberg
Jonckheere, R., Technische Universitaet Bergakademie Freiberg
Ketcham, R., UT Austin

The common assumption that the annealing and etching behaviours of fission tracks induced to form in pre-annealed apatites and spontaneous fission tracks that form in non-pre-annealed apatites are equivalent has led to neglect of the possible influences of the background radiation damage that accumulates over geological time. From step-etched prismatic sections of a Durango apatite it was reported that the rate of increase of the mean induced track length in a pre-annealed section is low (0.008±0.003 μm/s) whereas the rate for the mean spontaneous track length is significantly higher (0.025±0.003 μm/s) under the same etching conditions (4.0 M HNO3 at 25 °C) [1].

This investigation looks into the possible effects of natural radiation damage on spontaneous and induced confined track lengths in three different prismatic step-etched Durango apatite sections: 1- non-pre-annealed neutron irradiated; 2- natural; and 3- pre-annealed neutron irradiated. For this study step-etch experiments were performed from 20s to 60s at 10s intervals using more widely-used etching conditions (5.5 M HNO3 at 21 °C). Using the assumption that the induced and spontaneous confined track length populations are normal distributions, the induced track data in the first Durango section were deconvoluted by fitting a pair of Gaussian curves, where the spontaneous track length distribution is adopted from the second section. We also observe that the fossil tracks become more anisotropic with etching time, whereas the induced tracks become more isotropic.
It has been reported that the mean track length can decrease in a step etch experiment [2] if the track length measurements are performed on different tracks for each etching step and recently-appeared tracks in the late etching steps are considered together with early-appearing tracks which had longer track etching times. In this work, in order to eliminate the difference between the track etching time and bulk crystal etching time, the track length data of recently-appeared confined tracks after 20s etching step were migrated to the 20s crystal etching time since their effective track etching time was lower than 20s.

In our and most other similar experiments to date, the rates of increase of the mean track length of fossil and induced tracks in natural apatite during step etching are indistinguishable from each other but faster than that of induced tracks in pre-annealed apatite. We infer that this difference is caused by radiation damage, principally from alpha recoil, accumulated over geological time in natural apatite. Further experiments planned to be completed by the meeting will elucidate whether the few observations that do not corroborate this trend may be due to poorly thermalized neutrons being used for irradiation. Clarifying the effect of background radiation damage on track etching will improve our ability to derive meaningful information from and concerning etch figures and initial track length, and ultimately address its role in annealing.

References
1. Jonckheere, R., Enkelmann, E., Min, M., Trautmann, C., Ratschbacher, L., 2007. Confined fission tracks in ion-irradiated and step-etched prismatic sections of Durango apatite. *Chemical Geology* 242, 202-217.
2. Green, P.F., Duddy, I.R. Gleadow, A.J.W., Tingate, P.R. Laslett, G.M., 1986. Thermal annealing on fission tracks in apatite 1. A qualitative description. *Chemical Geology* 59, 237-253.

Keywords: Fission Tracks, Modelling

SETP
ECG

Insights into sedimentary drainage evolution using detrital zircon U-Pb and (U-Th)/He double dating, Ainsa Basin, South Central Pyrenees, Spain

kellydthomson@gmail.com
Thomson, K., Jackson School of Geosciences, The University of Texas, Austin, Tx
Stockli, D., Jackson School of Geosciences, The University of Texas, Austin, Tx
Clark, J., Statoil Research Center, Austin, Tx

Well preserved deposits of the South Central Pyrenees foreland basin provide a sedimentary record of the tectonic and thermal history of the Pyrenean orogeny. Late Cretaceous to Oligocene deposits of the Ainsa Basin preserve an example of drainage network evolution in response to an actively deforming hinterland. The Ainsa Basin in the southern Pyrenees is an ideal field site to apply double dating techniques due to the well-constrained depositional ages throughout the basin, and age constraints on thrust fault displacement in the hinterland. Detrital zircon geochronologic and thermochronologic analyses of 40 sandstone samples taken throughout the Ainsa Basin were used to identify multiple distinct sedimentary sources. U-Pb analysis is used to determine sedimentary sources while (U-Th)/He analyses provide insights into erosional and tectonic processes in the source area. When both analysis are conducted on distinct source populations and examined over a stratigraphic sequence the results can reveal the evolution of drainage networks in an active orogen.

Preliminary U-Pb data indicate two main source areas, a dominant U-Pb peak in age distributions of 270-360 million year old grains sourced from the axial zone Hercynian granitic plutons, and a 550-650 million year old peak in grain distributions sourced in the eastern Pyrenees from the Cadomian orogeny. Two distinct suites of samples are identified from U-Pb age distributions, one suite showing a mixture of the two sources and a second suite of more recent depositional ages with an overwhelming Hercynian signature assumed to represent localized erosion of axial zone plutons.
(U-Th)/He results are anticipated to show variable thermal histories among the different source area populations, possibly indicating a tectonically driven mechanism for switching sediment source locations. Given the structural and stratigraphic context of the study area, our data seeks to refine the drainage network evolution during the Eocene - Oligocene in the Southern Pyrenees.

Keywords: Foreland Basin, Tectonics, Thermochronology, Basin analysis, Pyrenees

SHP
LCMS

Characterizing transitional flow deposits in the Brushy Canyon Formation, Texas

ustipak@utexas.edu
Ustipak, K., Department of Geological Sciences, The University of Texas at Austin, Austin, TX
Mohrig, D., Department of Geology Sciences, The University of Texas at Austin

Transitional flow deposits appear to be connected to progradation of channels in basin floor deposits of the Brushy Canyon Formation, Texas. Transitional flow deposits are highly variable in their sedimentology and have characteristics of turbulent deposition near the base that grade upward into more laminar depositional styles, ideally resulting in a fining upward bed that becomes enriched in clay or mudclasts near the top. A detailed study of a famous roadcut near the Guadalupe Mountains National Park is here presented to illustrate the complexity of depositional processes in the deepwater environment. Initial findings suggest that a prograding channel has a predictable series of beds that appear in a vertical stack: organic-rich siltstone, interbedded siltstone and fine sandstone, transitional flow deposits, tabular turbidites and finally channel turbidites. The progression from siltstone to turbidite suggests a complex evolution of sedimentary processes that build the seascape. This is the first attempt to define the context of transitional flow deposits in the Brushy Canyon Formation, significantly impacting interpretations that have been held in the deepwater community for decades.

Keywords: Brushy Canyon Formation, Transitional Flow Deposits, Deepwater, Turbidite

SETP
ECG

Magmatism and Hydrothermal Fluid Flow in the Ertsberg-Grasberg Mining District, Papua, Indonesia: Insights from Zircon U/Pb and Trace Element Analysis

swafforn@utexas.edu
Wafforn, S., Department of Geological Sciences, The University of Texas at Austin, Austin, TX
Cloos, M., Department of Geological Sciences, The University of Texas at Austin, Austin, TX
Stockli, D., Department of Geological Sciences, The University of Texas at Austin, Austin, TX

The Ertsberg-Grasberg mining district, located in Papua, Indonesia, contains one of the single largest recoverable resources of copper and gold in the world. The district is built on four spatially and temporally distinct ore deposits: the supergiant Grasberg porphyry copper deposit, the giant multi-level Ertsberg East Skarn System, the large Big Gossan skarn the giant Kucing Liar Skarn. These deposits are associated with Pliocene quartz diorite to quartz monzonite intrusions emplaced into sedimentary strata of the Cretaceous and Tertiary Kembelangan and New Guinea Groups. Some of the outstanding questions in the district include how long was magmatism and hydrothermal fluid flow active in order to form these world-class deposits? What controls the mineralizing potential of the hydrothermal fluids?

Isotopic dating of intrusions and hydrothermal alteration from porphyry copper deposits worldwide often suggests that ore formation is the result of multiple hydrothermal pulses that occur over several million years; however the duration and cooling history of ore-forming hydrothermal systems are rarely constrained with a resolution better than one million years. The Erstberg-Grasberg district has the advantage of being sufficiently young that high resolution zircon U/Pb dating of intrusions that host and cross-cut ore grade mineralization provides a constraint on the maximum duration of hydrothermal fluid flow. New zircon U/Pb ages (n=58; 23 in Grasberg, 11 in Ertsberg, and 24 other) show that the oldest intrusion is the Dalam at 3.33±0.04 Ma and the youngest is the Erstberg Dike at 2.71±0.07 Ma. The best characterized deposit is Grasberg, where the main ore stage post-dates the MGI (3.08±0.06 Ma, n=4) and pre-dates the Kali Phase (3.03±0.04, n=4). The second minor ore stage post-dates the Kali Phase and pre-dates the Post Kali Dikes (2.97±0.06 Ma). Based on these ages the Grasberg deposit formed in less than 230 kyr, and perhaps less than 50 kyr. Magmatism in Grasberg and Ertsberg occurred over a maximum 730 kyr time window. The world-class Ertsberg-Grasberg mining district formed in less than a million years; a remarkably short time frame given the huge metal endowment in the district.

The zircon trace elements in the Grasberg magmatic suite indicate a relatively small europium anomaly (Eu/Eu* = 0.4 to 0.6) that decreases as the mineralizing system evolves. These small, decreasing europium anomalies are interpreted to indicate an oxidized magma that becomes more oxidizing with time. This trend may be explained by the conversion of SO_4^{-2} in the melt to SO_2 that exsolves into the hydrothermal fluid. The ability to detect evolving redox conditions of a mineralizing magmatic system through time based on trace element analysis and U/Pb dating of zircon has the potential to delineate magmatic evolution trends that are favorable for the formation of porphyry copper systems.

Keywords: Grasberg, Porphyry Copper Deposit, Zircon U/Pb Dating, Zircon Trace Elements

CCG
LCPHD

Examining cloud feedback-based emergent constraints in a single model ensemble

wagmanbe@gmail.com
Wagman, B., Institute for Geophysics, The University of Texas at Austin
Jackson, C., Institute for Geophysics, The University of Texas at Austin

As global climate models have improved at simulating the observational record, the inter-model spread in predicted climate sensitivity (the increase in global average surface temperature after a doubling of CO_2) has not decreased. Because climate models are a key component to predicting climate change, understanding and reducing this spread is of high priority. To constrain climate sensitivity, modelers need to know what processes to focus their efforts, and observationalists need know what data to collect to improve prediction--besides “everything.” Targeted metrics are needed that connect an observable measure of model performance to the prediction of interest, i.e. prediction of global temperature change. Recent “emergent constraints” purport to do just that by constraining global cloud feedback with present day observations of water vapor in the tropics and subtropics.

Although these emergent constraints hold across large ensembles of models, we present evidence that they do not effectively predict climate sensitivity in a single model ensemble derived from the NCAR Community Atmosphere Model (CAM). The reason appears to be the different spatial patterns of cloud feedback in CAM and the degree to which types of cloud feedback are linked together. In CAM, the storm track feedback is positive and of much larger magnitude than the stratocumulus and trade cumulus feedbacks in the tropics and subtropics, and the storm track feedback does not appear to be linked to the published tropical water vapor constraints. Furthermore, because the single model ensemble contains otherwise acceptable models, the results suggest that the emergent constraints may not necessarily apply in nature. Successful emergent constraints on global cloud feedback may have to treat independent types of cloud feedback separately.

Keywords: clouds, cloud feedback, climate change

MG
LCPHD

Updated mapping and seismic reflection data processing along the Queen Charlotte fault system, southeast Alaska

maureenlwalton@utexas.edu
Walton, M., Institute for Geophysics, The University of Texas at Austin, Austin, TX
Gulick, S., Institute for Geophysics, The University of Texas at Austin, Austin, TX
Haeussler, P., U.S. Geological Survey, Anchorage, Alaska
Rohr, K., Kristin Rohr Consulting, British Columbia, Canada
Roland, E., The University of Washington, Seattle, Washington
Tréhu, A., Oregon State University, Corvallis, Oregon

The Queen Charlotte Fault (QCF) is an obliquely convergent strike-slip system that accommodates offset between the Pacific and North America plates in southeast Alaska and western Canada. Two recent earthquakes, including a M7.7 thrust event near Haida Gwaii on 28 October 2012, have sparked renewed interest in the margin and led to further study of how convergent stress is accommodated along the fault. Convergence along the QCF is highest south of 53.2°N due to a restraining bend in the fault, near where the Haida Gwaii thrust event occurred. The Haida Gwaii event is thought to have been caused by incipient underthrusting of the Pacific Plate related to the oblique convergence along the QCF in that region; however, the fault structure near the earthquake is poorly understood and the interface that slipped to cause the earthquake has yet to be explicitly imaged.

Through updated seismic reflection processing, fault mapping, and seismic interpretation, we are able to better image and map the QCF along-strike and observe that strain manifestation could be related to fault geometry. We observe downwarping of oceanic basement crust north of the Haida Gwaii event and suggest that this crust was once located in a more convergent regime, translated north along the QCF to its current position with its flexure "preserved" by sedimentary loading. Additionally, we provide updated fault mapping and seismic imaging to supplement and support the idea that a change in strike of the QCF at ~53.2 degrees north has led to significant differences in stress and the style of strain accommodation along-strike. One of the highest-quality seismic reflection surveys along the Queen Charlotte system to date, EW9412, was last processed to post-stack time migration for a 1999 publication. Due to heightened interest in high-quality imaging along the fault, we have completed updated processing of line 1250 of the EW9412 survey and provide a prestack migration with water-bottom multiple reduction. Our new imaging better resolves faults, folds, basement surfaces, and the highly deformed sediments within the slope deposits of the Queen Charlotte Terrace.

Keywords: marine geophysics, strike-slip, tectonics, seismic reflection, oblique, earthquake, Haida Gwaii, Craig, Queen Charlotte Fault, Alaska

SHP
LCPHD

Nature of non-Fickian transport through tortuous and rough fractures

wlc309@gmail.com
Wang, L., Department of Geological Sciences, The University of Texas at Austin, Austin, TX

Non-Fickian transport is a well-known process across all scales within fractured and porous geological media. Fundamental understanding and appropriate characterization of non-Fickian transport through fractures is critical to predict the fate of solutes and other scalars of interest. We used either theoretical derivation or numerical simulations, including direct simulation and particle tracking random walk, to investigate the origin of non-Fickian transport through either homogeneous or heterogeneous fractures.

For the simplest homogenous fracture case, i.e., parallel plates, we theoretically derived a formula of dynamic longitudinal dispersion (D) within Poiseuille flow. The theoretical D implies that preasymptotic and asymptotic dispersive transport are separated by a given time (T) and length (L) scales, with T and L proportional to the second and fourth order of b, where b is the aperture of parallel plates.

As to heterogeneous fractures, the fracture roughness, correlation length and variation of b field are closely associated to the T and L, and thus constituting the origin of non-Fickian transport. The fracture roughness contributes the important aspect of asymptotic non-Fickian transport as revealed by our direct simulations through 2D rough fractures. Furthermore, the degree of non-Fickian deviating from Fickian transport in the frame of continuous time random walk with truncated power law, is proportional to the fracture roughness.

Moreover, we found that transport transitions from non-Fickian to Fickian with increasing the length of correlation length of b field through simulating particle tracking random walk through 3D fractures. As expected, the estimated L is much greater than the theoretically-derived L as if through parallel plates with the same b. This reveals the L is highly dependent on the correlation length and variation of b field. Therefore, a precaution should be taken into account when applying formulations either derived from non-Fickian or Fickian transport theories across different length scales.

Keywords: Non-Fickian, Fickian, Fractures, Dispersion, Solute transport

EG
ECG

Bedding-Parallel Fracturesin Shales: Characterization, Prediction and Importance

wangqiqi@utexas.edu
Wang, Q., Jackson School of Geosciences, The University of Texas at Austin, Austin, TX
Gale, J., Bureau of Economic Geology, The University of Texas at Austin, Austin, TX

Natural fracture systems are important for production in shale gas reservoirs as they may contribute to permeability of the reservoir or they may reactivate during hydraulic fracture treatment. This project examines sealed bedding-parallel fractures, a subset of the natural fracture system that has so far received little attention. Impacts on hydraulic fracture growth might include height growth inhibition and horizontal propagation. Natural, sealed bedding-parallel fractures may facilitate horizontal growth of hydraulic fractures by acting as planes of weakness that enhance the already marked strength anisotropy due to bedding-parallel laminae and planar fabric. The project goals are to characterize:1) Intensity and morphology of bedding-parallel fractures in several shale using outcrops and core; 2) Cement fill mineralogy and texture; 3) Fracture porosity, porosity related to cement texture (interfiber porosity), or cement mineralogy (for example, Celestine intergrowth in calcite 'beef' creates porosity); 4) Scaling of opening-mode bedding-parallel fractures, to see if their aperture-size populations follow power-law distributions, as do vertical/sub-vertical fractures; 5) Stable isotope geochemistry and fluid inclusions. These will be used to constrain conditions and timing of formation. Once the fractures are characterized I will investigate the mechanisms that may be responsible for fracture generation, and the factors influencing fracture development and distribution in shales. Non-tectonic factors to consider are: lithology and mineral composition, rock mechanics, local overpressure, shale thickness, dehydration, abundance and mechanical properties of TOC and clay minerals, compaction and pressure solution during diagenesis. Tectonic factors: local or regional stress vs. shale strength. An understanding of these factors is necessary for fracture prediction.

Keywords: Bedding-Parallel Fractures, Shale, Fracture Characterization, Mineralogy, Geomechanics

SHP
ECG

Delineation of Two Karst Springsheds in the Middle Trinity Aquifer, Western Hays County, Texas.

jefficus@gmail.com
Watson, A., Jackson School of Geosciences, The University of Texas at Austin, Austin, TX
Hunt, B., Barton Springs/Edwards Aquifer Conservation District
Gary, M., Jackson School of Geosciences, University of Texas at Austin, Austin,TX
Wierman, D., Independent Geologist

Jacob's Well Spring (JWS) and the recently documented Pleasant Valley Spring (PVS) are large karst springs discharging from the Trinity Aquifer which provide perennial base flow to the Blanco River upstream of Wimberley, Texas. In order to better understand groundwater flow and sources of recharge to these springs (springsheds), we conducted a potentiometric surface investigation of the Middle Trinity Aquifer in July 2013. Using 59 water level measurements from the vicinity of the two springs we constructed a potentiometric map of the Middle Trinity Aquifer. Nine spring discharge measurements of PVS were taken using an acoustic doppler velocimeter (ADV) from Dec. 2012-Aug. 2013. Results indicate that groundwater flow is NW to SE in the study area, parallel to the direction of structural dip of Middle Trinity strata. Potentiometric gradients increase from 2.84 m/km in recharge areas to 11.37 m/km in the confined zone SE of the springs and major faults in the Balcones Fault Zone (BFZ). Potentiometric data suggest the Blanco River watershed, including an area of exposed Cow Creek Fm in the river, is a source of recharge for PVS. Potentiometric data suggest the source area for JWS could be limited to the Cypress Creek watershed, although contributions under differing hydrologic conditions could also include the Blanco River. We interpret a potentiometric trough, which represents a preferential flow path, surrounding the mapped JWS cave passage extending NW along Cypress Creek. A small potentiometric ridge is present between the Blanco River and Cypress Creek watersheds, suggesting a localized hydraulic separation between PVS and JWS. This trough is coincident with a structural anticline in Middle Trinity strata that may be controlling groundwater flow paths locally. Additional evidence for hydrologic separation of the JWS and PVS springsheds was demonstrated by the differential springflow response to a large storm on May 25-26, 2013. PVS flow increased significantly in response to increased Blanco River flows, while JWS did not respond. These data help to define the source areas for PVS and JWS and suggest under drought conditions they may have independent springsheds. These data have implications for groundwater management and the preservation of springflows.

Keywords: Karst, Spring, Springshed, Potentiometric

MG
LCPHD

Unusual Tidal Sandbodies in the Transgressive Phase of the Brent Group

250498582@qq.com
Wei, X., Jackson School of Geoscience, The University of Texas at Austin, Austin, TX
Steel, R., Jackson School of Geoscience, The University of Texas at Austin, Austin, TX
Olariu, C., Jackson School of Geoscience, The University of Texas at Austin, Austin, TX
Ravnas, R., A/S Norske Shell

The Middle Jurassic Brent Group in the Northern North Sea wasrecently shown to include unusually thick (15-60m) sandy deposits in the Ness and Tarbert formations that are shown to have been strongly influenced by tidal currents and are also high quality reservoirs. However, their origin and depositional environments are still unclear and controversial. Using data from some 18 wells and well correlations along landward (S) to seaward (N) fairways in the North Viking Graben system three types of these thick sandbodies are suggested. Type1 sandbodies were developed in the lower Ness Formation in some of the more northerly areas. With 40-60 m thick marine sandstone units showing bi-directional cross bedding and *Ophiomorpha* traces they are likely to be stacked tidal bars composed of single and compound dunes. The overall upward-fining succession suggests that the bars fill channels in an open estuary-mouth setting that was transgressing. The clean nature, good sorting, and coarse grain size suggest that these estuarine tidal bars received active sediment supply at the estuary mouth by strong flood tidal currents. Type2 sandbodies, also in the Ness formation but farther south in the graben system, are ca. 15-30 m thick, and possess both abundant bi-directional cross-bedding and pervasive double mud drapes. However, these sandbodies tidal bars coarsen upwards, bioturbation is centralized at the base, and wave generated structures decrease upwards, suggesting possible mixed-energy, wave and tide-influenced delta mouth bars. Type3 sandbodies are fairly widespread in the graben and occur within Tarbert formation. They reach 30-40 m in thickness, show well-sorted fine-grained sand, ubiquitous mud drapes and vague bi-directional cross bedding, contain marine or brackish trace fossils *Chondrites, Planolites and Diplocraterion,* and they have an overall upward-fining tendency. These bodies are interpreted in terms of tidal dunes and bars within an estuary, but in the middle to inner estuarine reaches.
The thick, well- sorted estuarine units likely accumulated during overall transgression due to increased rates of subsidence in the Viking Graben and may be better reservoirs than the deltaic parts of the Brent Group. The tide-dominated estuaries evolved into mixed-energy estuaries, reflecting a reshaping of coastline during transgression.

Keywords: Middle Jurassic, Brent Group, thick tidal deposits, deltaic tidal bar, estuarine tidal bar

SHP
ECG

Imaging of Deepwater Channel Architectural Elements of the Jackfork Formation, Arkansas, Using Ground Penetrating Radar and Application to Reservoir Modeling

logan.m.west@utexas.edu
West, L., Jackson School Geosciences/Bureau of Economic Geology-QCL, UT-Austin
Wood, L., BEG-QCL, UT-Austin & Colorado School of Mines

Deepwater channel sands are common targets for offshore hydrocarbon exploration. High net-to-gross systems are desirable as reservoirs but difficult to map in conventional seismic due to the lack of differentiation of their sandy lithologies from their often silty shales that exert an important influence on fluid flow. This study uses ground penetrating radar (GPR) to image outcrops and near-outcrop subcrops of the Jackfork Formation in Pulaski County, Arkansas. The Jackfork Formation is interpreted as a middle-Pennsylvanian deepwater slope and basinfloor depositional system along the margins of an oblique foreland basin that formed in front of the encroaching Ouachita accretionary prism.

In this study, GPR data are collected for the top 3-5 meters (m) of subcrops of deepwater features of the Jackfork system using a 200 megahertz (MHz) antenna. The data are processed and corrected for variations in surface topography. Where possible, GPR data are constrained with adjacent outcrops. At several data collection areas, GPR lines were taken in grids to visualize the 3-D internal architecture of the deposits.

The sites from which GPR data are collected are interpreted to represent a variety of local environments and relative stages of large slope channel infill from pre-channel muddy slope deposits through amalgamated channels to meandering leveed channels. GPR data capture a variety of architectural elements included in this channel system. These elements include individual channel stories, slope mud troughs, crevasse splays, sand sheets, and debris material. Fully imaged channels extend up to at least 50 meters wide and 5 meters deep. Gridded GPR data show the spatial continuity of crevasse deposits 3-5 meters thick over up to one square kilometer.

With the collected data, this work aims to use associated outcrops and GPR data qualities to identify mud-rich lenses within the high net-to-gross system to provide an example of the two- and three-dimensionality of baffling facies within the channel. With the sub-meter resolution of the GPR data, this should inform fluid flow property variability within channels at a higher resolution than conventional seismic and, where grids were taken, in added dimensionality to outcrop studies.

From the analysis, this work provides valuable insight into the nature of high net-to-gross deepwater channel deposits and can assist in identifying potential baffles and barriers to flow prior to full-scale, deepwater subsurface developments in similar deposits around the world.

Keywords: Deepwater channel architecture, 3-D, GPR, Jackfork, Arkansas, channel system, crevasse splay

EG
ECG

Nanoscale Flow Pathways in Shale Fracture Cements

erick.wright@utexas.edu
Wright, E., Bureau of Economic Geology, The University of Texas at Austin, Austin,TX
Eichhubl, P., Bureau of Economic Geology, The University of Texas at Austin, Austin,TX
Landry, C., Bureau of Economic Geology, The University of Texas at Austin, Austin,TX

Natural fractures are considered to be a major contribution to fluid flow within hydrocarbon bearing shale formations, and may aid in production of hydrocarbon through reactivation caused by interaction with hydraulic fracturing. Most natural fractures in shale are filled with fracture fill mineral cements. These mineral cements are thought to be impermeable, with no previous studies or evidence to suggest otherwise, nor have the effects of their reactivation been taken into consideration in shale reservoir production models. We propose that these cements can actually act as flow pathways, inhibiting fluid flow at a lesser degree than previously thought and allowing migration of hydrocarbons from the host rock matrix into the hydraulic fracture network.

Preliminary studies using a combination of broad ion beam milling sample preparation and SEM imaging of barite cement from the Barnett Shale in the Delaware Basin demonstrate the presence of flow pathways similar to features seen previously in calcite cement of the Eagle Ford Shale. These structures are on the scale of a few hundred nanometers to several micrometers in aperture. While some of these structures are likely to be induced during core handling, many show the presence of healing structures within the cements that can only form as a result of opening during in situ conditions. Although these microscale fluid pathways have been identified in core from the Eagle Ford Shale, it is unknown how prevalent they are amongst all fracture cements, and what effect they may have during production of oil and gas from ultra-low permeable reservoirs. This study will combine broad ion beam sample preparation, high magnification SEM backscatter imaging and numerical flow modeling to investigate the frequency of micro-to-nanoscale flow pathways in fracture cements and their effect on the production of oil and gas during hydraulic fracturing

Keywords: Fracture, Fluid Flow, Petroleum, FRAC

SETP
LCPHD

Modes of continental extension in a lithospheric wedge

glwu@utexas.edu
Wu, G., Jackson School of Geosciences, The University of Texas at Austin, Austin, TX
Lavier, L., Jackson School of Geosciences, The University of Texas at Austin, Austin, TX
Choi, E., Center for Earthquake Research and Information, The University of Memphis, Memphis, TN

We studied extension of a lithospheric wedge as an approximation to an orogenic belt or a continental margin. We ran a series of numerical models to quantify the effects of the strength of the lower crust and a mid-crustal shear zone (MCSZ) on the extension processes. When the MCSZ is present, we found that the regional lower crustal flow plays a critical role in controlling the modes of extension. The compensation is long-wavelength when the lower crust flows from the highest to the lowest elevation in order to compensate upper crustal thinning. In response to this motion, the mantle flows towards the highest elevation in order to balance for the lower crust leaving the area under the highest topography. For weak (wet quartz regime with partial melting) or intermediate (wet quartz regime), or strong (dry quartz regime) lower crust, we recognized three predominantly decoupled modes of extension characterized by 1) significant lower crustal exhumation exemplified as a large massif, 2) formation of core complexes and detachment faults, and 3) distributive domino faulting, respectively. Without the MCSZ, however, the lower crustal flow is essentially subdued with predominantly coupled extension. For weak or intermediate, or strong lower crust, we recognized three coupled modes characterized by 1) localized generally symmetric crustal exhumation, 2) distributed grabens and narrow rifts, and 3) wide continental margins, respectively. The MCSZ controls the degree of decoupling of the lower crustal flow such that a frictionally stronger MCSZ does not change the behaviors of the models but results in a more distributed extension. Due to the long-wavelength compensation, subhorizontal Moho is achieved where intensive extension occurred for all the decoupled models with a MCSZ. Natural counterparts for each mode may be easily identified, for instance, in the Basin and Range or the Aegean.

Keywords: Contiental extension, core complexes, detachment fault, lower crust, shear zone, decoupling

MG
LCPHD

Sediment input pathways from North American highlands to the Gulf of Mexico in Lower Miocene interval: based on detrital zircon U-Pb and U-Th/He dating

jiexu@utexas.edu
Xu, J., Department of Geological Sciences, Jackson School of Geosciences, The University of Texas at Austin, Austin, TX
Snedden, J., Institute for Geophysics, Jackson School of Geosciences, The University of Texas at Austin, Austin, TX
Fulthorpe, C., Institute for Geophysics, Jackson School of Geosciences, The University of Texas at Austin, Austin, TX
Stockli, D., Department of Geological Sciences, Jackson School of Geosciences, The University of Texas at Austin, Austin, TX

The lower Miocene is a period of significant sediment input to the Gulf of Mexico (GOM) Basin that accompanied tectonic and climatic changes in North America. However, the resulting sediment pathways from continental upland sources to basinal sink remain poorly constrained. We employ detrital zircon (DZ) U-Pb and (U-Th)/He double dating to define both basement provenance and the exhumation histories of detrital source regions.

We have collected samples from outcrops across the northern Gulf, from Texas to Florida, in order to discriminate sediment pathways. Most of our data show a mixture of source terranes, including Oligocene volcanic centers, Cordilleran Arc, Laramide uplifts, Grenville, Mid-Continent, Yavapai-Mazatzal, and Appalachian-Ouachita as major provinces and Wyoming and Superior regions as minor provinces. However, major DZ age peaks vary greatly between different samples, providing a means to differentia drainage systems. Five major sediment input pathways are defined: the Paleo-Rio Grande, Paleo-Red, Paleo-Mississippi and Paleo-Tennessee rivers and a local river system in Florida draining from Appalachians. The Paleo-Rio Grande and Paleo-Red rivers show a significant sediment input from Oligocene volcanic centers, Laramide uplift regions and the Cordilleran Arc, whereas the Paleo-Tennessee River received most of its sediments from Appalachian-Ouachita and Grenville basement. The Paleo-Mississippi River lies within a transitional zone between western and eastern North American drainage systems.

By integrating (U-Th)/He ages we can further distinguish first order volcanic zircons from recycled zircons. This can increase the ability to discriminate different drainage systems because the recycled zircons come from source terranes that are different from the original basement in which they formed. For example, two different Grenville-age zircon sources are differentiated by our U-Pb and (U-Th)/He ages. Sediments in Texas show a mixed zircon source from both local Grenville basement (Llano uplift) and eastern Appalachian Grenville basement, recycled via the Colorado Plateau. In contrast, sediment in Louisiana lacks sediment sourced directly from Llano uplift, indicating a well-defined drainage system divide between Texas and Louisiana boundary.

Keywords: Lower Miocene, Gulf of Mexico Basin, Provenance, U-Pb and U-Th/He

EG
ECG

3D frequency-domain full-waveform inversion with sparsity constraint

zhiguangxue@gmail.com
Xue, Z., Bureau of Economic Geology, The University of Texas at Austin
Zhu, H., Bureau of Economic Geology, The University of Texas at Austin
Fomel, S., Bureau of Economic Geology, The University of Texas at Austin

Full-waveform inversion (FWI) is a challenging data-fitting procedure based on full-wavefield modeling to extract quantitative information from seismograms. We propose to incorporate sparsity constraint in FWI to increase its robustness in the presence of random noise and interference in seismic data. The sparsity is conducted by having a threshold on the model in seislet domain, where the transformed data has a really good compactness and sparsity pattern. Furthermore, we apply parallel sweeping preconditioner, a 3D Helmholz solver, in modeling process of the inversion, which makes our algorithm efficient and applicable. Numerical tests on 3D SEG/EAGE overthrust model show that sparsity constraint can greatly improve the robustness of FWI and provide a high-quality velocity model when the seismic data is severely contaminated by random noise and interference caused by simultaneous-source data.

Keywords: Full-waveform inversion, 3D, frequency domain, sparsity constraint, seislet transform, parallel sweeping preconditioner

CCG
LCPHD

The effect of stem water storage on Amazon rainforest response to seasonal dryness

byan@utexas.edu
Yan, B., Jackson School of Geosciences, the University of Texas at Austin, Austin, TX
Dickinson, R., Jackson School of Geosciences, the University of Texas at Austin, Austin, TX

An increase in dry season length over the Amazon basin has been detected and projected for the future by IPCC report, which will inevitably modify vegetation distributions there. In order to improve our ability to predict vegetation dynamics and its influence on surface energy and water balances, we need to improve the simulation of vegetation response to drought by incorporating strategies of vegetation to cope with water shortages. In this work, we add the tree trunk water storage pool, which has been proved to be vital for tropical forests to resist droughts, in the Community Land Model 4.0. The trunk water pool is directly connected with each soil layer via roots and the flux between two layers is described by Darcy's law. The hydraulic properties of plant parts are adopted from previous researches. Allometric relationships of trees are used to estimate the capacity of tree trunk to store water. The modified and default model was run at a LBA site (the BR-Sa3 site) that is located in the middle of the Amazon basin and mainly covered by the evergreen broadleaf forest with canopy top up to 35 m. The average daily precipitation is 12 mm with dry season from August to October. Results show an increase in vegetation water availability and a consequently higher latent heat flux during the dry season for the modified model compared with the default one, which is more consistent with observations. A diurnal fluctuation of trunk water content is also seen in response to the diurnal evolution of two processes, namely water extraction from tree trunks for daytime transpiration and water refill from soil to tree trunks.

Keywords: Amazon, trunk water storage, community land model

SHP
LCPHD

Controls on the dynamics of the subterranean estuary and hyporheic zone of a river estuary determined from hydraulic, thermal and geophysical monitoring

pbzamora@utexas.edu
Zamora, P., Department of Geological Sciences, The University of Texas at Austin, Austin, TX
Cardenas, M., Department of Geological Sciences, The University of Texas at Austin, Austin, TX
Cook, P., Water Studies Centre, School of Chemistry, Monash University, Clayton, Victoria, Australia

The subterranean estuary is broadly defined as the subsurface zone of mixing of saline and fresh groundwater in coastal areas. The seldom studied flow and transport processes in subterranean estuaries mediate biogeochemical and thermal processes. We investigated groundwater flow and salinity dynamics at nested spatial and multi-temporal scales of the subterranean estuary underlying a small river estuary. We conducted subsurface electrical resistivity (ER) surveying at the river-estuary transition zone through the tidal cycle and also across the entire estuary to map porewater salinity variation. Groundwater hydraulic measurements and vertical temperature profiling were also conducted within the sediment. Time-lapse ER across the channel at the river-estuary transition zone revealed a static resistive zone on the side of the channel with a pronounced thalweg/cut bank. At the shallow portion of the opposite bank, zones that became less resistive with increasing estuary water level were observed. Groundwater head gradients indicating strong upward flux and pronounced vertical temperature gradients with colder temperatures deeper within the sediment indicate a stable zone of fresh groundwater discharge along the cut bank. Subsurface temperatures closer to that of surface water, head distributions indicating both groundwater efflux and influx, and higher porewater salinity indicate that the shallow water areas were dominated by hyporheic circulation. The high ER near the cut bank was persistent in the estuary-wide ER profiles, which showed similar patterns in thalwegs/cut banks of sinuous portions of the estuary and low ER values in shallower areas mainly in straighter estuarine reaches. A decrease in estuary-wide ER in highly resistive zones when the regional water table is lower, indicate infiltration of surface water into the sediment. Our study highlights the importance of channel morphology and surface water-groundwater interaction on porewater salinity dynamics of the subterranean estuary underneath a river estuary. Understanding porewater salinity dynamics at different scales in subterranean estuaries can improve our understanding of material transformations and their contributions to measured chemical fluxes from coastal streams.

Keywords: Subterranean estuary, porewater salinity, coastal groundwater

CCG
LCPHD

Diurnal cycle of warm season rainfall over West Africa: Observations and regional high-resolution simulation

gz@utexas.edu
Zhang, G., Department of Geological Sciences, Jackson School of Geosciences, The University of Texas at Austin, Austin, TX
Cook, K., Department of Geological Sciences, Jackson School of Geosciences, The University of Texas at Austin, Austin, TX

The diurnal cycle is a fundamental mode of tropical rainfall variability, and its accurate portrayal remains a challenging issue for numerical weather and climate prediction. The purpose of this study is to better understand the diurnal cycle of warm season (June-September) rainfall over West Africa and its underlying physical processes. We use rainfall data from the Tropical Rainfall Measuring Mission (TRMM) and atmospheric dynamics fields from reanalyses to explore the rainfall diurnal cycle in the climatology (1998-2013) and a case study of 2006. In addition, a simulation with the Weather Research and Forecasting (WRF) model at a convection-permitting resolution of 3 km resolution is analyzed to evaluate the model's ability to capture the rainfall diurnal cycle in the warm season of 2006.

The rainfall in the warm season of 2006 shows a mixture of afternoon and nocturnal peaks over West Africa, which is similar to the climatology. Further examination of the 2006 case is focused on three domains: (1) the AF domain (3°W-0°W, 9°N-11.5°N) with late afternoon peaks (2) the SN domain (2°E-5°E, 9°N-11.5°N) with nocturnal peaks, and (3) the NN domain (2°E-5°E, 13.5°N-16.5°N) with nocturnal peaks. For each domain, the rainfall diurnal cycle is more related to the diurnal cycle of rainfall frequency than of the intensity, and it is largely shaped by the diurnal cycle of the frequency of extreme rainfall events. The afternoon rainfall peaks over the AF domain are associated with unstable atmospheric profiles below 850 hPa. The nocturnal rainfall peaks over the NN and SN domains are associated with westward-propagating rainfall systems initiated on the previous afternoon around the complex topography to the east (about 5-15°E).

The rainfall produced by the convection-permitting simulation shows similar westward-propagating features. The model realistically captures the nocturnal rainfall peaks over the SN domain, because it reproduces the westward-propagating rainfall systems originated from the Jos Plateau located just east of the domain. However, the model fails to simulate the rainfall peaks over the northern part of the NN domain due to a dry bias, and over the AF domain due to an overestimation of nocturnal peaks.

Keywords: West African rainfall, diurnal cycle, propagation, WRF, cloud-permitting simulation

SHP
ECG

Decreased channel dimensions and sediment flux through the Paleocene Raton-Wilcox rivers: implications for Wilcox shelf margin

jinyu.zhang@utexas.edu
Zhang, J., Jackson School of Geoscience
Ron, S., Jackson School of Geoscience
William, A., Jackson School of Geoscience
William, F., Jackson School of Geoscience

The Paleocene-Eocene Wilcox Group of onshore South Texas reaches a thickness of 1300 m, and contains a linked facies succession passing from coastal plain to shoreline to shelf and out to deepwater slope deposits. This spectrum of facies associations across Texas were the very deposits giving rise to the original concepts of 'depositional systems' (Fisher and McGowen, 1967).
A re-visit of some 500 wells and 1500 feet of cores through the Wilcox succession in South Texas shows that the fundamental organization of the linked facies tracts was one of some 24 transgressive(T) to regressive(R) units, thickening from av. 25 m on inner shelf to av. 75 m on outer shelf. Cores show that the transgressive part of units or sequences formed mainly from mixed energy, tidally-influenced estuaries, whereas the regressive part represents mainly river- and wave-dominated deltas. These fundamental sequences reflect the fact that the Wilcox shelf-margin prism was constructed by the repeated T-R transits of shorelines across the widening shelf, driven ultimately by northerly rivers. As successive T-R sequences accumulated, the shelf break of the clinoform system migrated up to 8 km basinward per sequence.
To further evaluate the feeder river systems that drove the Wilcox shoreline, the Paleocene, Raton and Poison Canyon formations of the Laramide Raton Basin were examined, as these represent coeval fluvial systems that flowed southwards across New Mexico and Texas. The fluvial channels of the older Raton Formation are up to 6 times wider and up to 5 times deeper than the younger Poison Canyon channels. In addition, the former were more interconnected and sometimes sheet-like in their amalgamation, compared to the more isolate, lower net-to-gross channels of the Poison Canyon Formation. It is likely that the decreased sediment discharge through time in the Raton Basin reflects the change from coarser-grained Lower Wilcox to finer-grained Middle Wilcox on the GOM shelf-margin prism, and is also consistent with the recorded decrease in rates of shelf-margin progradation from Lower Wilcox (20-30 km/My) to Middle and Upper Wilcox (4-8 km/My) (Carvajal et al., 2009). Although the large Raton channels and Wilcox distributary channels indicate Paleocene high sediment discharges to the coeval Gulf coast, the decreasing sediment discharge in late Paleocene and Eocene suggests lower Laramide relief generation and possibly northward diversion of some of the Laramide rivers.

Keywords: Wilcox, Raton, Source-to-sink, Sediment supply

CCG
LCPHD

What controls stratospheric water vapor variations in extratropics?

kzkaizhang@gmail.com
Zhang, K., Jackson School of Geosciences, The University of Texas at Austin, Austin,TX

A comprehensive study of how water vapor varies in the extratropical stratosphere and what controls stratospheric water vapor variations will be shown in my poster. I will present preferred pathways of water vapor tranport into the stratosphere and the role of temperatures in controlling stratospheric water vapor variations.

Keywords: water vapor, stratosphere, temperature

CCG
LCPHD

The Influence of Meteorological Forcing Biases on Land Snow Data Assimilation

yfzhang.nju@gmail.com
Zhang, Y., Department of Geological Sciences, The University of Texas at Austin, Austin, TX
Yang, Z., Department of Geological Sciences, The University of Texas at Austin, Austin, TX

A land data assimilation system (LDAS) is an important means by which an accurate high-resolution dataset of terrestrial water and energy balance can be developed. However, the quality of the LDAS dataset depends on many factors such as the realism of land surface models that produce the water and energy balance, the accuracy of the meteorological forcing fields (e.g., precipitation and radiation) that drive the models, and the quality of satellite datasets to be assimilated. This study focuses on a diagnosis of biases in meteorological forcing and their influence on the snowpack water storage in the Northern Hemisphere.

An ensemble of global meteorological forcing, produced by the coupled Community Atmosphere Model version 4 (CAM4) and Data Assimilation Research Testbed (DART), is used in a newly developed land data assimilation system based on the coupled Community Land Model version 4 (CLM4) and DART. CAM4/DART exhibits large negative precipitation biases over western Eurasia and the eastern United States and large positive precipitation biases over eastern Eurasia, Canada, and the western United States. Large negative biases of radiation are found over the western United States and eastern Eurasia, which is consistent with the positive biases in precipitation over these regions. Pentad precipitation data from the Global Precipitation Climatology Project (GPCP) and monthly radiation data from the Clouds and Earth's Radiation Energy System (CERES) are used to correct the biases in CAM4/DART. The influence of the forcing bias correction on snow data assimilation is quantified by comparing the CLM4/DART output with independent data. The forcing bias correction leads to improved accuracy of snow water storage estimates, which is in the same range as that brought by assimilating the Moderate-resolution Imaging Spectroradiometer (*MODIS*) snow cover fraction.

Keywords: Forcing bias, Precipitation, Radiation, Snow, Data Assimilation

EG
ECG

Analysis of Impact of Reservoir Heterogeneity on Hydrocarbon Accumulation – Used Donghe Sandstone in Tarim Basin as an example

zhy921125@gmail.com
Zheng, H., Bureau of Economic Geology, The University of Texas at Austin, Austin, TX

Donghe sandstone, a set of thick marine sandstone underlied by an uncomformity, is a key horizon for exploration and development in Tarim basin. Heterogeneity is the main factor influencing the reservoir characteristics. Based on the outcrops, drill cores, and wireline logs in Bachu formation, this thesis proposes a new methodology for heterogeneity classification, the physical property heterogeneity consisting of vertical formation rhythm, and structural heterogeneity formed by interlayer distribution. Various reservoir numerical simulations have been conducted in terms of the introduction of Ant Colony Algorithm. The simulation results turn out that the physical property heterogeneity can affect the migration route of petroleum, while structural heterogeneity not only influences vertical migration, but also intensifies petroleum loss. Based on the numerical simulations in Hadexun Oildfield both vertically and planarly, the favorable accumulation regions have been regarded as areas with high permeability and porosity, which match the actual geological condition.

Keywords: Reservoir Numerical Simulation, Physical Property Heterogeneity, Structural Heterogeneity, Donghe Sandstone, Hadexun Oilfield

SHP
LCPHD

Diurnal temperature effect on nitrate removal and production efficiency in bedform-induced hyporheic zones

lizhizheng@utexas.edu
Zheng, L., Department of Geological Sciences, The University of Texas at Austin, Austin, TX
Cardenas, M., Department of Geological Sciences, The University of Texas at Austin, Austin, TX

Rivers and aquifers are connected through the hyporheic zone (HZ). Pore water in the subsurface sediments is continuously exchanged with the overlying surface water. The exchange of water, mass and energy occurring along the surface-subsurface interface or within the HZ exerts a strong influence on the quality of both surface and subsurface waters, and fluvial ecology. Moreover, the HZ is rich in biologically active sediment, creating a favorable condition for microbially facilitated reactions to occur, including organic carbon oxidation (aerobic respiration), nitrification, and denitrification. Inorganic N, especially NO_3^-, is of concern as a drinking water pollutant and as a cause for eutrophication that threatens ecosystems. The biogeochemical reactions in the HZ could produce or consume NO_3^- and thus the HZ could function as nitrate source or sink role in the fluvial system. In addition, because of the river's diel thermal signal and hyporheic exchange at the sediment-water interface (SWI), a diel temperature pattern would penetrate and result in a dynamic temperature pattern which would affect the biogeochemical reactions in the HZ. However, there have been few studies focused on coupling and integrating fluid flow, heat transport, and reactive solute transport to understand the complex links and feedbacks between hydrodynamic and biogeochemical processes in the HZ. Therefore, the main objective of this study is to integrate all the processes that occur along the SWI to understand how diurnal temperature variations affect the biogeochemical function of the HZ. We conducted numerical simulations of coupled turbulent open-channel fluid flow, porous fluid flow, porous heat transport and reactive solute transport to study feedbacks and coupling between these processes. We assumed the diurnal temperature follow the sinusoidal variations. We studied different average temperatures and different amplitudes of the diurnal temperature variations effect on nitrate removal or production efficiency in the HZ, respectively. The simulation results show that the average temperature effect on the HZ nitrate source-sink functionality and its associated efficiency has strong dependence on the $[NO_3^-]/[NH_4^+]$ ratio in the river. While, the amplitude of temperature variations has minimal effect on the nitrate removal and production efficiency in diurnal periodic.

Keywords: hyporheic zone, denitrification, diurnal temperature variations, reactive transport, bedform